AVIATION SAFETY
INVESTIGATION REPORT

Enclosures

6th Aviation Regiment – NHIndustries MRH-90 Taipan A40-040, Spatial Disorientation leading to Controlled Flight Into Terrain (CFIT), Whitsunday Islands, QLD, 28 July 2023.

INTENTIONALLY BLANK

Defence acknowledges the Traditional Custodians of Country throughout Australia. Defence recognises their continuing connection to traditional lands and waters and would like to pay respect to their Elders both past and present.

Defence would also like to pay respect to the Aboriginal and Torres Strait Islander people who have contributed to the defence of Australia in times of peace and war.

Defence has authorised the release of this Aviation Safety Investigation Report with certain personal, commercial-in-confidence, international partner and operationally sensitive information removed from the body of the report due to its security classification. Additionally, four enclosures are not available to the public due to sensitive material related to medical-in-confidence information and personal privacy.

ISBN: 978-0-9874958-2-2 (print)

ISBN: 978-0-9874958-3-9 (online)

TABLE OF CONTENTS

ENCLOSURE 1

DFSB Biomathematical Fatigue Modelling

ENCLOSURE 1 TO
BP44206784

BIOMATHEMATICAL FATIGUE MODELLING

This enclosure provides an overview of Biomathematical Fatigue Modelling (BFM) conducted as a part of the investigation. Biomathematical models are tools for predicting crewmember fatigue levels based on a scientific understanding of the factors that contribute to fatigue. BFM is widely used by investigative agencies to analyse a person's expected fatigue level at a specific time based on analysis of their prior sleep.

The Australian Civil Aviation Safety Authority (CASA) released the *Biomathematical Fatigue Models Guidance Document* in 2014, as well as supplementary guidance related to the use of BFM in 2021. These documents provide a comprehensive overview of the science of BFM, usage limitations and a summary of select commercially available models, including SAFTE-FAST provided by the Institutes for Behavioural Resources.

SAFTE-FAST is a desktop and web-based software application that utilises the validated Sleep, Activity, Fatigue and Task Effectiveness (SAFTE) model. The SAFTE model derived from research conducted by the US Walter Reed Army Institute of Research has been used extensively throughout military and civilian aviation settings. The *Review of ADF Aviation Workforce Fatigue Management* released in 2013 recommended SAFTE-FAST as the preferred BFM for use in the Defence Aviation context.

SAFTE-FAST, like all BFM software applications, has limitations that must be considered, including:

a. The model assumes that personnel are fully rested at the beginning of the schedule.
b. The model predicts risk probabilities for a population average rather than fatigue levels of a specific individual.
c. The model does not account for the impact of workload or personal and work-related stressors that may affect fatigue levels.
d. The model does not consider the influence of all components of environmental stress or workload on predicted alertness.

Accordingly, the use of SAFTE-FAST to model whether an individual was likely to have been fatigued at the time of a safety event must be undertaken with caution.

SAFTE-FAST Input Data. The SAFTE-FAST models for the AC and CP were generated using sleep estimate data as detailed in Table 1 and Table 2. The sleep estimates were based on interviews and sleep data from other aircrew. All times are expressed in local (K) for context. While the use of sleep estimate data is considered appropriate in this context, the results must be interpreted with the acknowledgement of this limitation. The quality of sleep specified within SAFTE-FAST was adjusted based on the environment and in accordance with guidance from the RAAF Institute of Aviation Medicine[1].

[1] IA-2024-014-AG – Use of Tools and Strategies to Assess and Manage Fatigue, Annex E.

Table 1: BSMN 83 AC Sleep and Wake Times (5 Days)

Date	*Wake*	*Sleep*
24 Jul 23	0500K	0005K (Tues 25th)
25 Jul 23	0700K	2330K
26 Jul 23	0900K	0200K (Thurs 27th)
27 Jul 23	0700K 0930K[2]	0200K (Fri 28th)
28 Jul 23	0700K	---

Table 2: BSMN 83 CP Sleep and Wake Times (5 days)

Date	*Wake*	*Sleep*
24 Jul 23	0600K	2230K
25 Jul 23	0730K	2230K
26 Jul 23	0730K	0330K (Thurs 27th)
27 Jul 23	0815K	0100K (Fri 28th)
28 Jul 23	0830K	---

Interpreting SAFTE-FAST Output Metrics. SAFTE-FAST models the ability of the average person to perform effectively as determined by time of day, biological rhythms, time spent awake, amount of prior sleep, and sleep quality. SAFTE-FAST produces a number of performance and fatigue-related metrics.

The primary metric used to estimate cognitive performance in SAFTE-FAST is called Effectiveness. Effectiveness scores are based on predicted reaction time speed on the Psychomotor Vigilance Task and is displayed as a percentage of individual optimum performance. Lower Effectiveness scores indicate slower cognitive reaction times and speed of cognitive processing. As shown in Table 3,

[2] After waking at 0700, the AC had an additional window of sleep opportunity (via an intended nap)

Effectiveness scores correlate with other variables that are known to effect performance such as continuous wakefulness, reaction time and blood alcohol level.

Table 3: Relationship between SAFET-FAST Effectiveness Scores and Other Fatigue Metrics

Effectiveness (% of baseline)	Continuous hours of wakefulness	Reaction time (% increase from baseline)	Blood alcohol level equivalent
80%	18	+25%	
77%	18.5	+30%	0.05%
75%	19	+33%	
70%	21	+43%	0.08%
65%	40	+54%	

The US Federal Aviation Administration (FAA) consider Effectiveness scores below 77% to constitute a fatigue risk[3]. An Effectiveness score of 77% is equivalent to being awake for 18.5 hours continuously, a 30% increase in reaction time and a blood alcohol level of 0.05%. The *Defence Aviation Fatigue Management Guidebook* provides guidance to support the interpretation of Effectiveness scores (see Table 4). Consistent with the FAA, the Guidebook defines 77% as the Effectiveness threshold for exercising 'caution'. The Guidebook notes that Effectiveness scores at or below 77% constitute a fatigue risk and require active management.

Table 4: Guidance on SAFTE-FAST Effectiveness Scores

Effectiveness score	Fatigue risk management recommendations	
Green (above 90%)	Proceed	The work schedule is unlikely to contribute to fatigue.
Yellow (90-77%)	Monitor	The work schedule may contribute to low levels of fatigue. Tactical fatigue-management strategies should be utilised to minimise fatigue arising from the schedule.
Amber (77-65%)	Caution	The work schedule is likely to contribute to heightened levels of fatigue. Caution is advised for personnel conducting duty or tasks in safety critical areas. Consider adjusting duty and rest periods to increase the schedule's effectiveness score above 77 per cent. If the schedule cannot be amended, minimise risk by applying available and authorised treatments/controls.
Red (below 65%)	Re-evaluate	The work schedule is highly likely to contribute to heightened levels of fatigue. Duty or conduct of tasks in safety-critical areas should not be conducted if predicted fatigue risk falls in this zone. Re-evaluate duty and rest periods to increase the schedule's effectiveness score. If duty must be conducted, the decision to proceed should be supported using local deliberate risk-management processes.

[3] FAA, 2012. Flightcrew member duty and rest requirements. In: F.A. Administration. US Department of Transportation, Washington DC.

SAFTE-FAST Graph for AC. The SAFTE-FAST graph for AC is shown in Figure 1.

SAFTE-FAST estimated that the AC had an Effectiveness score of 73% at the time of the accident (2230hrs). An Effectiveness score of 73% is equivalent to 19-21 hours of wakefulness, a 37% increase in reaction time and a blood alcohol level above 0.05%. SAFTE-FAST estimated that, at the time of the accident, the AC was 4.5 times more likely to experience a lapse in attention than would be expected during an average day in a well-rested person. Effectiveness scores below 77% are considered to constitute a fatigue risk.

SAFTE-FAST estimated that the AC's Effectiveness score would have continued to progressively fall to approximately 49% should the duty period have continued to its maximum scheduled limit of 0300hrs.

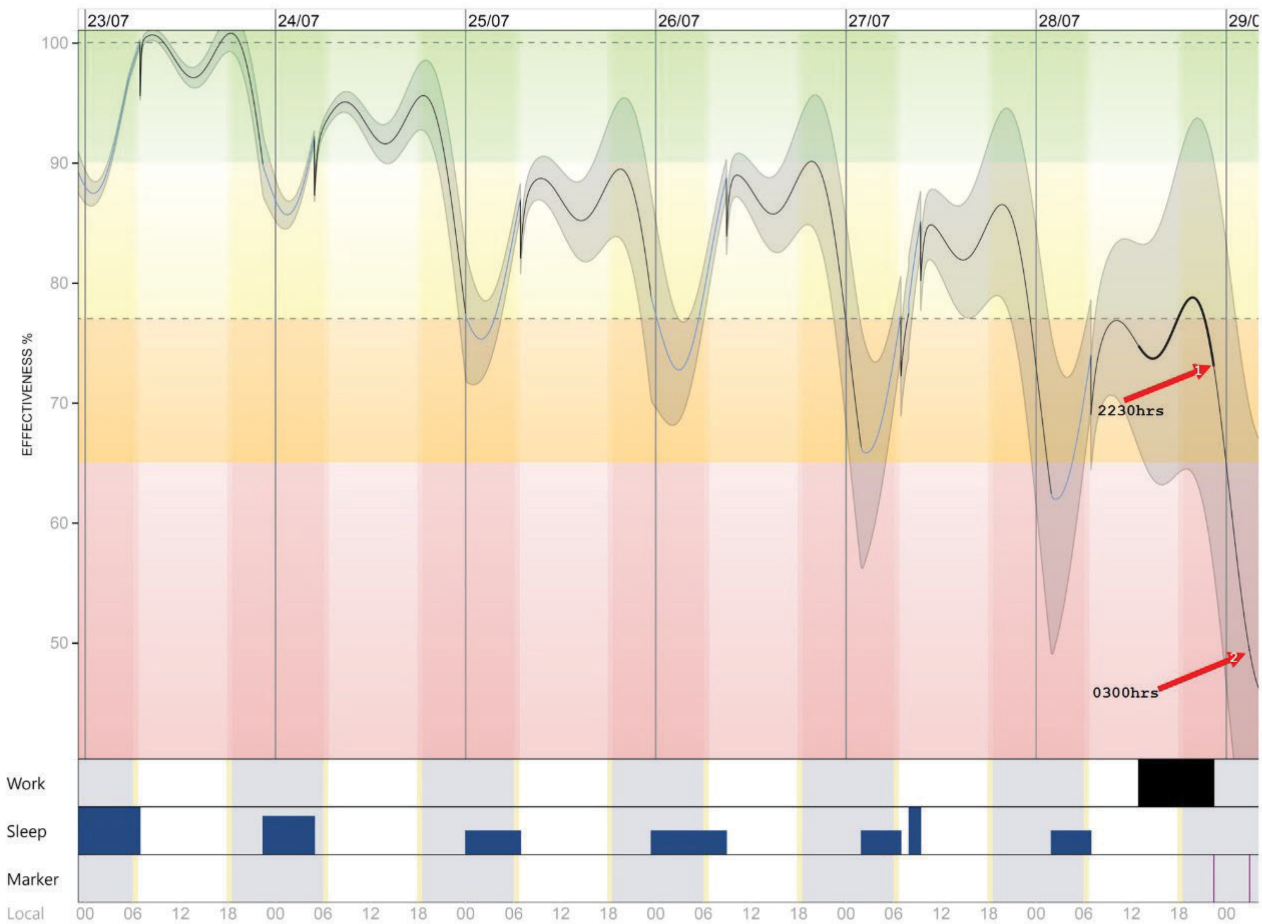

Figure 1: SAFTE-FAST Graph for AC

SAFTE-FAST Graph for CP. The SAFTE-FAST graph for CP is shown in Figure 2.

SAFTE-FAST estimated that the CP had an Effectiveness score of 77.5% at the time of the accident. An Effectiveness score of 77.5% is equivalent to approximately 18.5 hours of wakefulness, a 29% increase in reaction time and a blood alcohol level below 0.05%. SAFTE-FAST estimated that, at the time of the accident, the CP was 3.6 times more likely to experience a lapse in attention than would be expected during an average day in a well-rested person. For the purposes of SAFTE-FAST modelling, Effectiveness scores above the 77% are considered to not constitute a safety risk.

SAFTE-FAST estimated that the CP's Effectiveness score would have continued to progressively fall to approximately 54% should the duty period have continued to its maximum scheduled limit of 0300hrs.

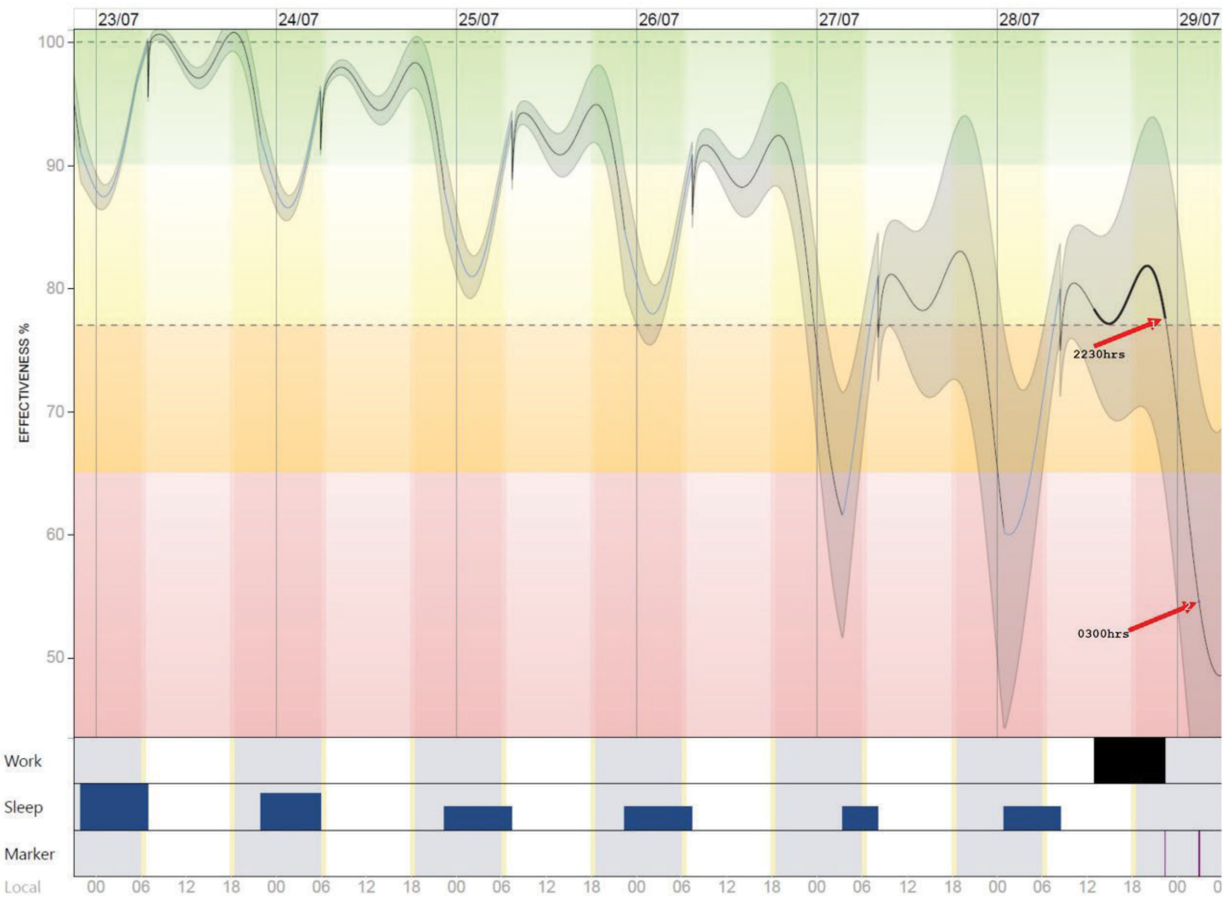

Figure 2: SAFTE-FAST Graph for CP

Summary. The analysis of sleep history data using BFM indicated that, at the time of the accident, it is likely the AC was experiencing a level of fatigue sufficient to impede their performance. Effectiveness scores below 77% are considered to constitute a fatigue risk. At the time of the accident, the predicted Effectiveness score for the was 73% for the AC and 77.5% for the CP. Effectiveness scores for the pilots would have continued to progressively fall should the duty period have continued as scheduled. Noting the general limitations of BFM, these results cannot be interpreted in isolation and require consideration in combination with other available sources of information and the circumstances of the event.

5

ENCLOSURE 2

Aviation Safety Investigation Technical Report – 6th Aviation Regiment – NHIndustries MRH-90 Taipan A40-040, Spatial Disorientation leading to Controlled Flight Into Terrain (CFIT), Whitsunday Islands, QLD, 28 July 2023

BP44116922

ENCLOSURE 2 TO BP44206784

Aviation Safety Investigation Technical Report

6th Aviation Regiment – NHIndustries MRH-90 Taipan A40-040, Spatial Disorientation leading to Controlled Flight Into Terrain (CFIT), Whitsunday Islands, QLD, 28 July 2023

EXECUTIVE SUMMARY

1. Examination of the wreckage of MRH-90 Taipan A40-040 did not identify any existing damage to the airframe and major systems nor any malfunctions of major systems throughout the flight or prior to impact with water. The degree of aircraft damage is indicative of the last flight data recordings of 135 KIAS and a 5200 ft/min descent rate, suggesting the aircraft impacted the water at high speed. Damage to the main rotor components revealed that the rotor blades were turning at high speed, with the engines operational and driving the rotors at the time of impact. The Aviation Safety Investigation Team (ASIT) could find no evidence of fatigue damage or pre-impact failure of the airframe or major aircraft systems within the scope of the investigation.

2. Analysis of data acquired from the Voice and Flight Data Recorder (VFDR) confirmed there were no discrepancies between the pilot's physical control inputs and aircraft's Flight Control System outputs.

3. The technical investigation concluded that the aircraft impacted the water on the front left-hand side of the airframe in a nose down and left-wing-low attitude. This was drawn from evidence related to the presence of cockpit components in the rear fuselage and associated impact damage to the airframe and major systems. Of note, the Preliminary Report indicated that the aircraft might have impacted the water at an angle of bank to the right. Since the last data reading was 1 to 2 seconds prior to impact, it would not have picked up the attitude change from right back to left bank.

4. The ASIT concluded that the aircraft's major systems such as engines, gearboxes, main and tail rotor transmissions, and flight controls were operating normally and were serviceable throughout the flight and at impact with the water. Within the scope of the investigation, the ASIT could not find any evidence of an aircraft unserviceability during the technical Lines of Enquiry (LOE).

List of figures

INTRODUCTION

5. On 28 Jul 23, an MRH-90 Taipan A40-040 from 6 Aviation Regiment (6 AVN REGT), call-sign ‘Bushman 83’, collided with water during Exercise TALISMAN SABRE 23 (EX TS23). An Aviation Safety Report (ASR) DEFEV2371190 was raised (Reference A). On 29 Jul 23, Commander Aviation Command (COMD AVNCOMD) appointed the Defence Flight Safety Bureau (DFSB) to form an Aviation Safety Investigation Team (ASIT) to investigate this Class A event (Reference B). DFSB provided a Preliminary Report (Reference C), on 29 Aug 23. It detailed the key sequence of events and preliminary operational and technical information acquired by the ASIT. This report is an enclosure to the Aviation Safety Investigation Report (ASIR) and represents the detailed analysis and findings associated with the technical investigation Lines of Enquiry (LOE).

6. The ASIT completed the Technical LOE through visual examination, disassembly and borescope inspection of both engines, and forensic examination of aircraft components retrieved from the accident site. Voice and Flight Data Recorder (VFDR) data from the aircraft’s Crash Survivable Memory Unit (CSMU) was analysed and compared to the results gained from the examination of aircraft wreckage. DFSB also tasked the Defence Science and Technology Group (DSTG), Airbus Australia Pacific (AAP) and NHIndustries (NHI) to conduct independent visual and forensic examination of the wreckage and analysis of VFDR data in support of the investigation, with respective reports provided at References C through F.

FACTUAL INFORMATION

Aviation platform

7. Details of the incident MRH-90 Taipan are contained in the Factual Information section of the ASIR (OBJ: BP44206784).

Weight and balance

8. A40-040 Chart A – Kit checklist (OBJ: BQ49699667) and Chart C – Basic weight and balance record (OBJ: BQ29955789) were last updated on 25 Jul 23. Weight and balance were within limits and there was no discrepancies between Chart A and Chart C.

Fuel

9. Fuel samples could not be recovered due to the state of A40-040's wreckage. Samples were taken from the other three formation aircraft and the original aircraft that subsequently became unserviceable before flight. All four aircraft were replenished from the same fuel source as A40-040. Samples were taken from various fuel cells from each aircraft to ensure widespread sampling range and sent to DSTG for analysis. Subsequent results from DSTG (BP43392110) found that samples from all aircraft were clear of any anomalies and fit for purpose at the time of the event.

Technical information

10. **Structure.** The MRH-90 structure (**Figure 1**) comprises four separately manufactured main sections which are joined at interface Frames 4, 11 and 14:

a. forward (FWD) fuselage (Frames 1 to 4)

b. centre fuselage (Frames 4 to 11) including upper deck fairings and sponsons

c. rear fuselage (Frames 11 to 14) including Tail Rotor Drive Shaft (TRDS) fairings

d. tail pylon (aft of Frame 14) including tail pylon fairings.

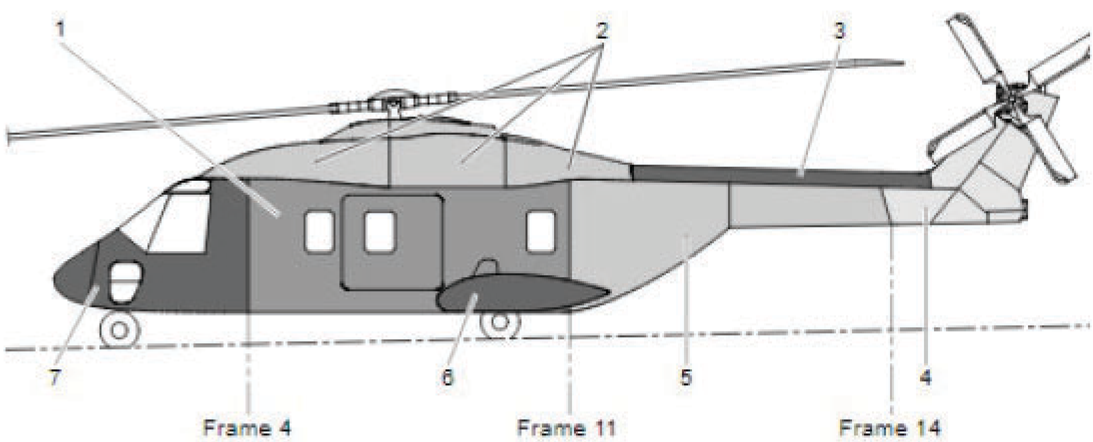

Figure 1: MRH-90 fuselage structure

11. The MRH-90 structure is primarily made of composite materials (**Figure 2**) manufactured in a monocoque construction. The use of composite materials gives weight saving/strength advantages over conventionally monocoque constructed (aluminium) helicopter designs.

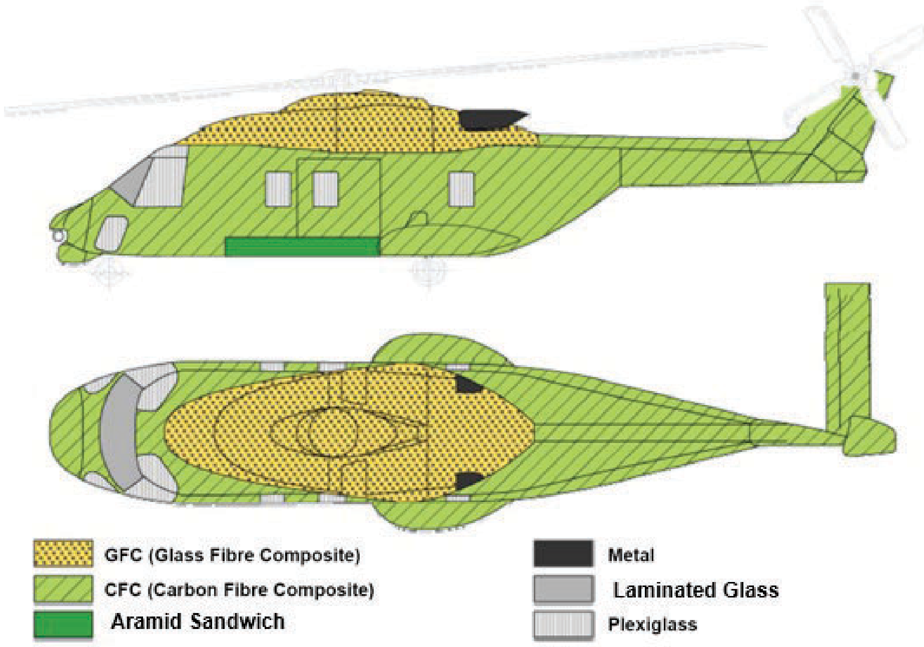

Figure 2: MRH-90 fuselage construction

12. **Flight Control System (FCS).** The FCS utilises a full Fly-by-Wire (FBS) system, with electrical wires transmitting control signals to actuators, replacing the conventional control rods, bell cranks, pullies and cabling used in other helicopters. The FCS is based on a multi-redundant architecture comprising a Primary Flight Control System (PFCS) supporting basic functions and the Automatic Flight Control System (AFCS), which controls mission task functions. The aircraft also has a low-mounted, non-moving horizontal stabiliser on its starboard side.

13. The Cyclic Control **(Figure 3)** comprises a cyclic stick, with an electro-mechanical trim servo that assists with inputs to the channel. Both the left- and right-hand cyclic control assemblies are interlinked via a coupler shaft located under the cockpit floor that runs between the two cyclic stick inputs.

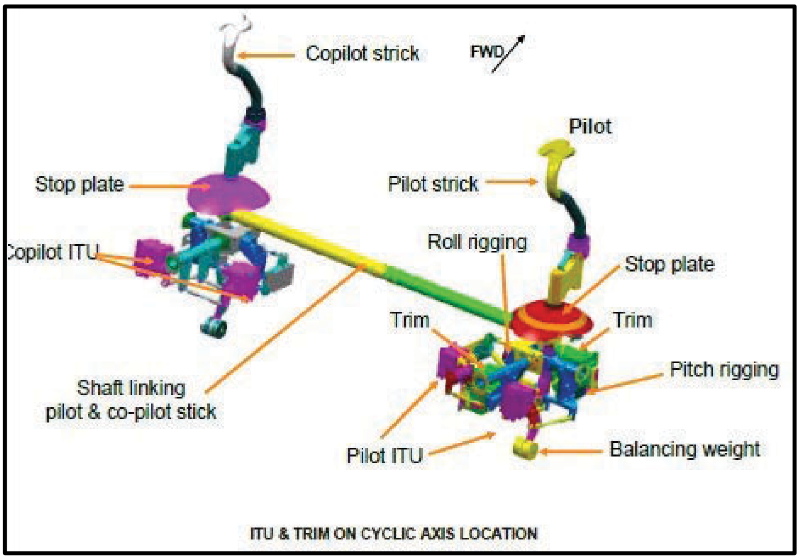

Figure 3: Cyclic system

14. The collective inputs are similar in construct with a collective stick, Inceptor and Transducer Units (ITUs) and a trim servo. Both collective inputs are connected via a coupler shaft under the cockpit floor. These inputs are then transmitted via the ITUs and the trim servos to the Flight Control Computer (FCC), which provides appropriate inputs to the three hydraulic servos.

15. The hydraulic servos change the angle of the swashplates; the swashplates are connected to the main rotor Pitch Change Rod (PCR) and subsequently connected to the main rotor blade. As the angle of the swashplate is altered, so is the angle of the main rotor blade, thereby providing directional changes.

16. The yaw control system (**Figure 4**) contains two sets of mechanically linked pedals, electrically connected to the FCC via ITUs. Electrical signals are subsequently sent from the FCCs to the tail rotor for directional input.

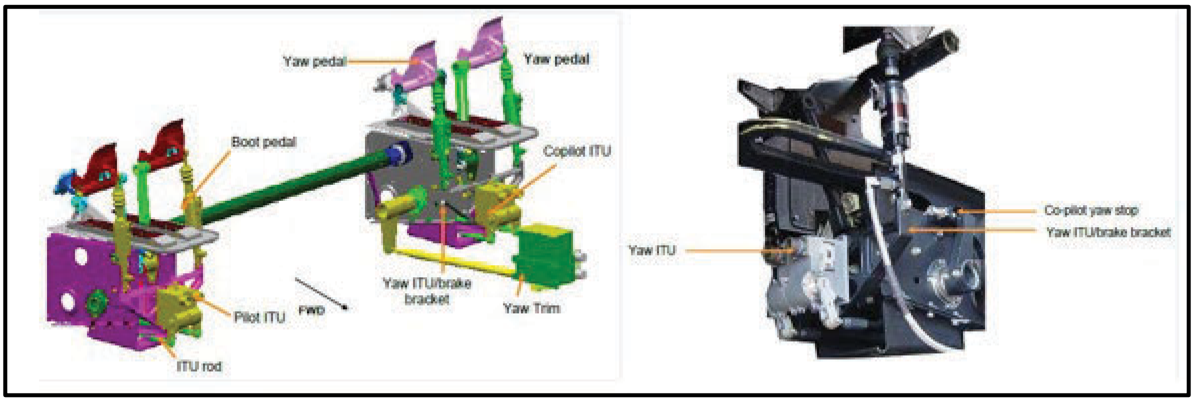

Figure 4: Yaw control system

17. **Main rotor system.** The main rotor has four main rotor blades, with yellow, blue, black and red identifying markings as they progress through their rotation. The blades are attached to the rotor hub via a sleeve and a spherical bearing and are linked to each other with lead-lag dampers. Lead and lag stops limit the contact between the blade and the rotor head, with pitch control transmitted from the swashplate to each blade through the PCRs. **Figure 5** shows the MRH-90 main rotor components.

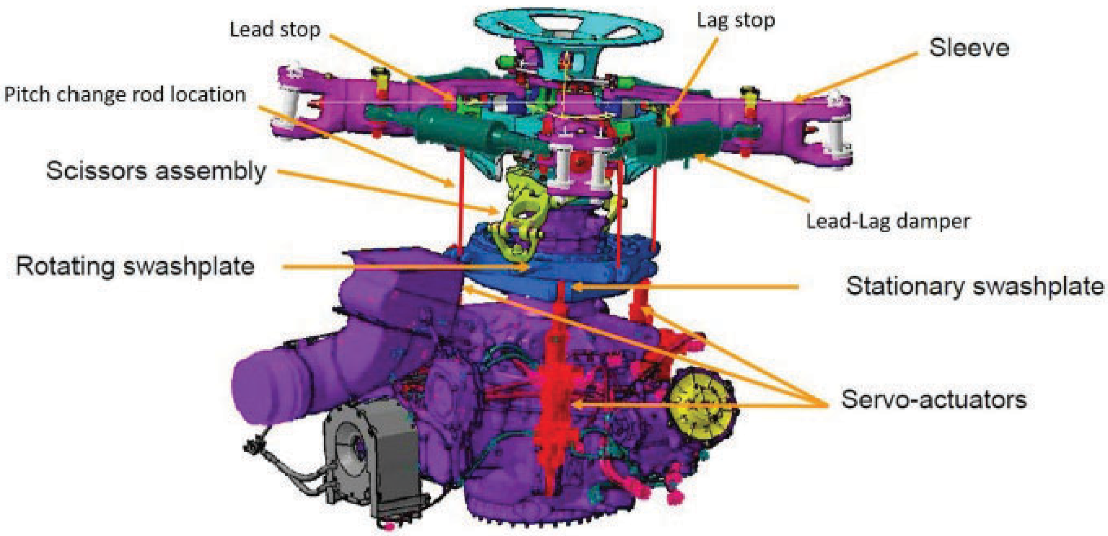

Figure 5: MRH-90 main rotor components diagram

18. **Main Rotor Gearbox (MRGB).** Part of the MRGB attachment is the Système Anti-Résonnance Intégré à Barres (SARIB) system, **Figure 6**. The SARIB allows transmission of loads from the main rotor to the aircraft, reduces dynamic loading, assists in system alignment and can absorb some loads from the main rotor and MRGB in the event of a crash.

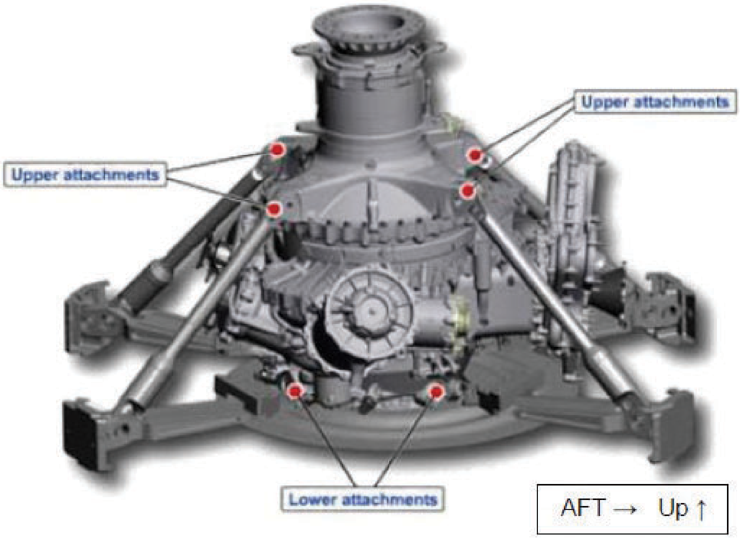

Figure 6: SARIB system diagram

19. **Tail rotor system.** The tail rotor drive (**Figure 7**) comprises four connected drive shafts originating from the rear side of the MRGB. These shafts are connected to the Intermediate Gearbox (IGB), which feeds up to the Tail Rotor Gearbox (TRGB) to turn the tail rotors.

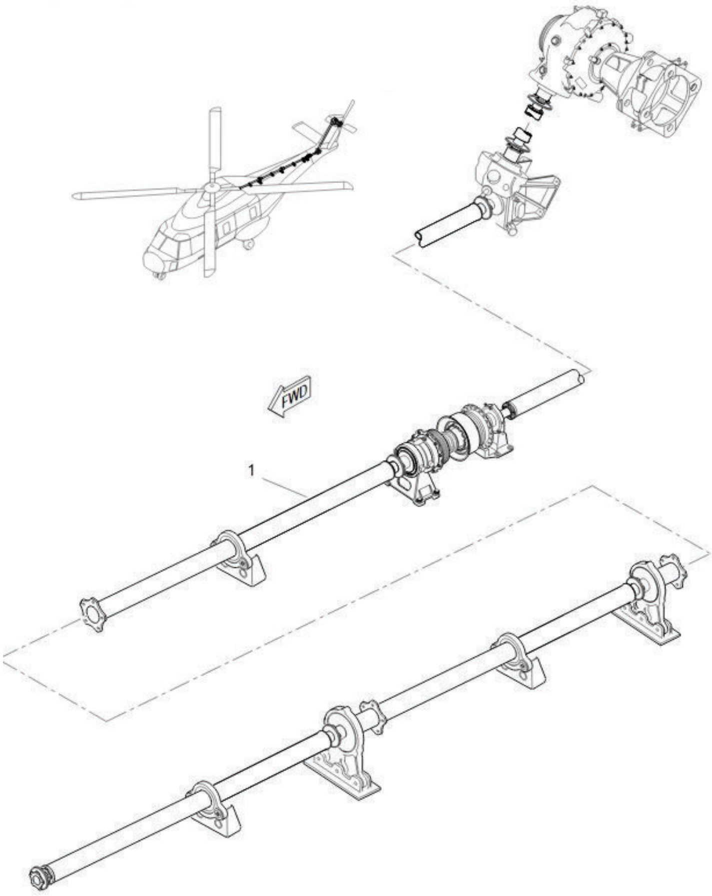

Figure 7: Tail rotor drive

20. **Horizontal Stabiliser.** The Horizontal Stabiliser assembly (**Figure 8)** is located below the tail rotor and provides the down-force necessary to keep the helicopter stable in flight. On the ground, it acts as a work platform for one member during tail rotor maintenance.

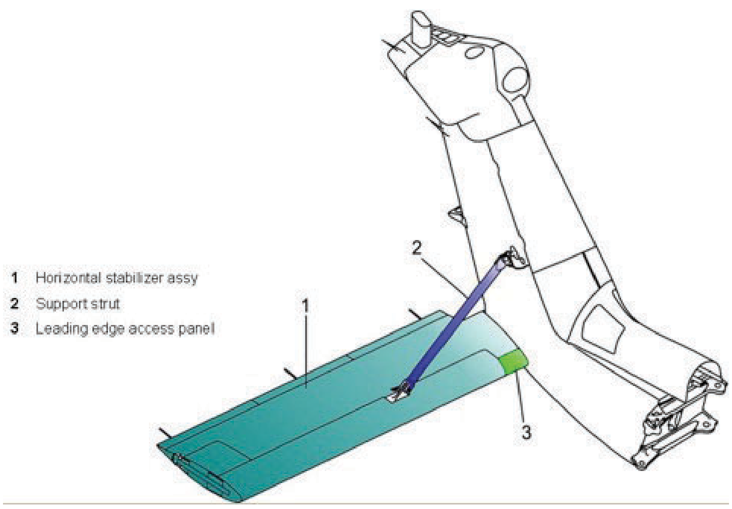

Figure 8: Stabiliser assembly

21. **Engines**. The MRH-90 is fitted with two RTM-322.01/9 engines, manufactured by Safran. **Figure 9** shows a cross-section of the MRH-90 RTM-322.01/9 engine with the major engine component assemblies. A40-040 was fitted with the following engines:

a. Left-hand (LH) engine 1: ESN 6514, with a total of 1431.3 engine hours (ENHR). ESN 6514 had undergone HP1 Blades Modification (MOD 7210.023-392) on 4 Apr 23.

b. Right-hand (RH) engine 2: ESN 6556, with a total of 803.5 ENHR. ESN 6556 had undergone HP1 Blades Modification (MOD 7210.023-392) on 7 Jun 21.

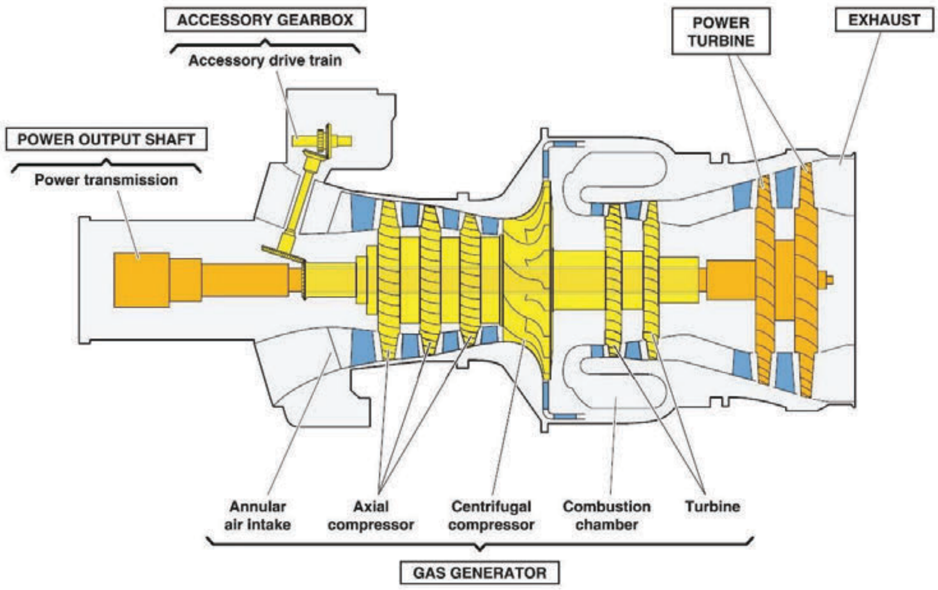

Figure 9: Cross-section of the RTM-322.01/9 engine

Damage to aircraft

22. **Evidence of fire.** There was no evidence of fire.

23. **Aircraft Damage Level (ADL).** A40-040 sustained Class A ADL in accordance with the DFSB Classification of Flight Operations Aviation Safety Events[1]. The definition of Class A is:

a. the aircraft has either been destroyed, missing, unrecoverable or

b. has sustained damage to such an extent that it is unrepairable or uneconomical to repair.

24. **Impact site. Figure 10** shows the initial impact site south of Hamilton Island and the resulting debris field. Aircraft debris was spread approximately 304 m across the seabed due to the tidal flow in the Whitsunday Passage as detailed in the environmental section of the main report.

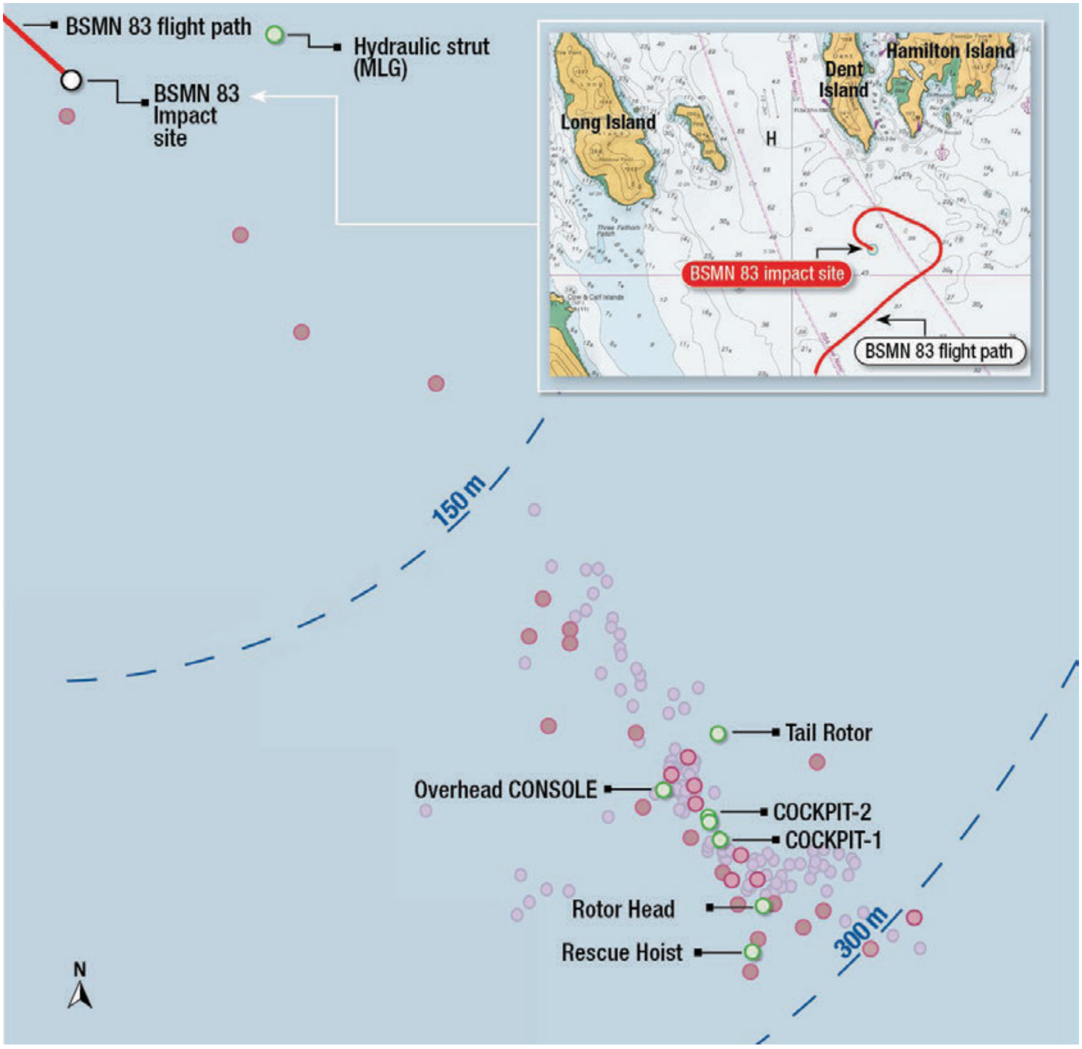

Figure 10: Aircraft impact site and debris field

[1] Latest ASR classification information is available on the DFSB website WEF 21 Apr 2023. [Pages - ASR Support and Resources]

25. **Recovered wreckage.** The recovered wreckage was transported to HMAS *Harman* by air and road for detailed examination. The wreckage included the following large items:

a. LH and RH engines

b. main rotor head, main gearbox and upper structural sections of the fuselage

c. tail pylon section from the start of the rear ramp to the aft end of the tail boom

d. tail rotor section aft from the IGB.

26. Small items recovered included, but were not limited to, composite skin sections, instruments, tail rotor drive shaft sections, avionic boxes and flight control components.

27. The ASIT completed on-site evidence recovery operations on 15 Oct 23, having recovered all essential wreckage required to complete the technical LOE. The site was handed over to AVNCOMD to continue recovery operations using the contracted civilian company and assets. Further recovered evidence was delivered to HMAS *Harman* by the end of November 2023.

Figure 11: Initial debris consolidation

28. **Structure.** Multiple pieces of aircraft debris were recovered, including substantial fractured pieces of the composite fuselage. **Figure 11** displays the debris recovered and consolidated at the Queensland Police Service (QPS) station in Airlie Beach. The ASIT estimated that approximately 70% of the aircraft fuselage was recovered from the seabed and impact site.

29. The intact rear fuselage and tail pylon section, aft of Frame 11, was recovered and included the structure from the rear crew ramp to the aft end of the tail boom (**Figure 12**). There were several areas of structural damage to the rear fuselage and tail pylon section including cracking due to a downward deflection of the tail at Frame 13. The aft tail section, which includes the tail rotor assembly, was found to have separated from the tail pylon at the aft end of the tail boom. The TRDS cowling exhibited rubbing damage with some paint missing. The rear cabin interior suffered structural damage and contained displaced wiring and some cockpit instruments that were propelled from the forward fuselage.

Figure 12: Aft fuselage

30. A laser-level was used to confirm alignment of three distinct locations of damage to the crew ramp. These included impact damage to the cabin floor and frame, a piece of composite wedged in the ramp access hatch, and damage to the crew escape hatch opening, which was missing the crew escape hatch (**Figure 13**). The damage deflected outwards from front to rear direction (**Figure 14**). The hole found in the crew ramp (**Figure 15**) is approximately 90 x 60 mm, similar in size to the cabin crew seat upright support (**Figure 16**).

Figure 13: Damage progression from start of foot ramp to rear edge (arrowed) with laser level

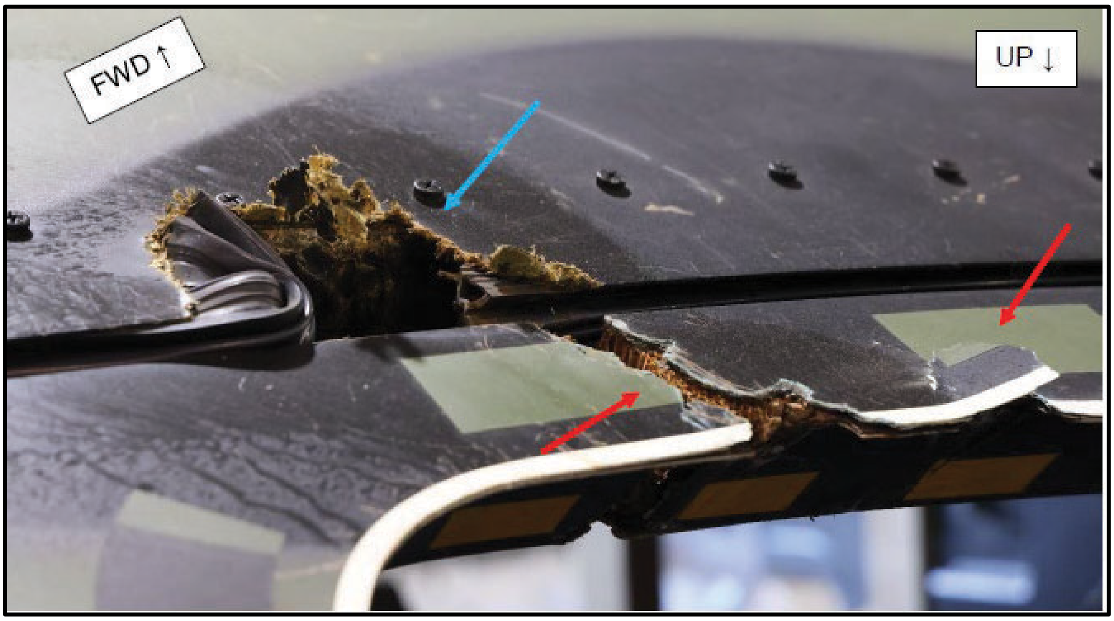

Figure 14: Damage of the lower face of the crew ramp splaying outwards

Figure 15: Lower edge crew ramp

Figure 16: Rear cabin crew seat with the upright supports arrowed

31. There was extensive cracking to the tail boom composite skin at the aft end on the RH side (**Figure 17**), whereas the LH side showed comparatively small skin cracking (**Figure 18**). Additional damage identified on the RH side of the tail boom structure (**Figure 19**) is consistent with a deflection from an external component. The witness mark on the horizontal stabiliser at approximately 0.85 m from the outboard leading edge is consistent with the exposed tail boom bolt located at approximately 0.85 m aft of the RH side damage (**Figure 19**). **Figure 20** is an Australian Transport Safety Bureau (ATSB) laser-scanned reproduction of an MRH-90 that shows the stabiliser path on impact and breakup.

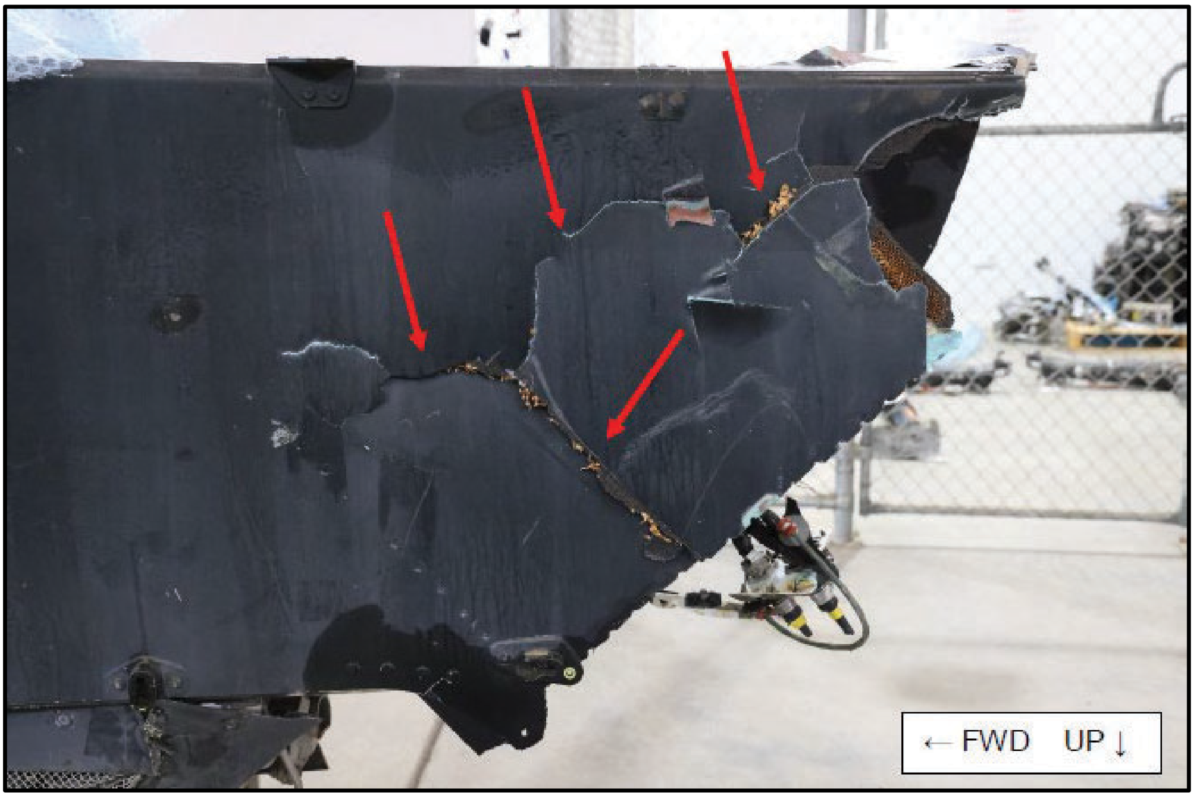

Figure 17: Extensive cracking on the RH-side of the tail boom

Figure 18: Minor damage on the LH-side of the tail boom

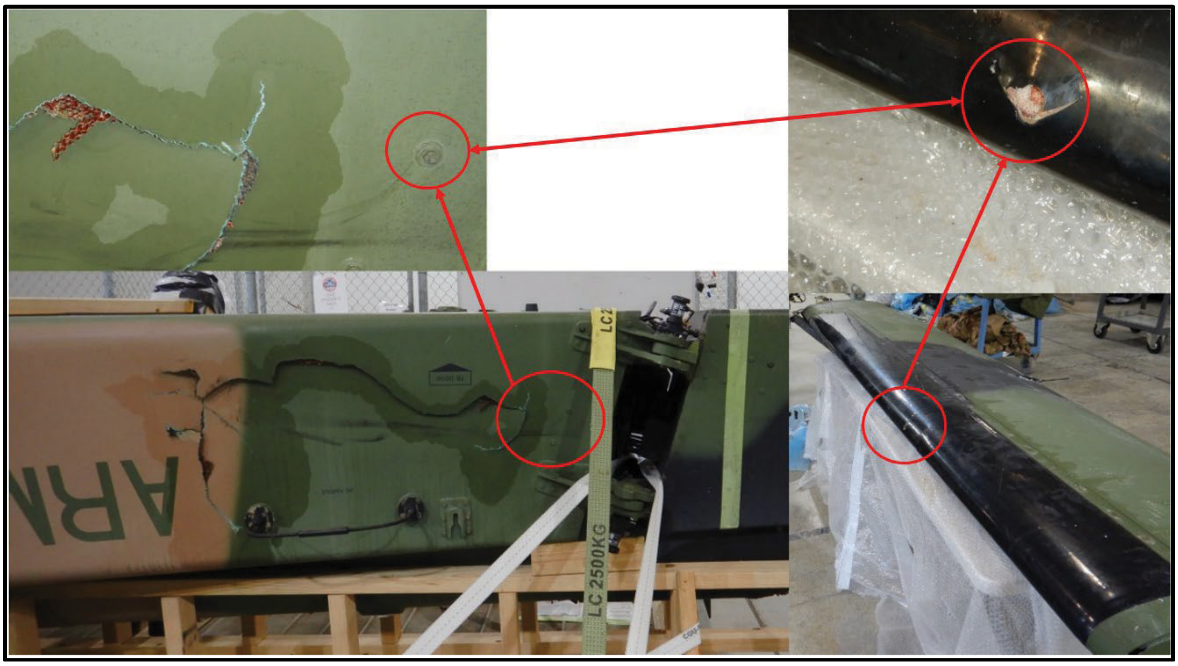

Figure 19: Stabiliser/aft fuselage impact damage

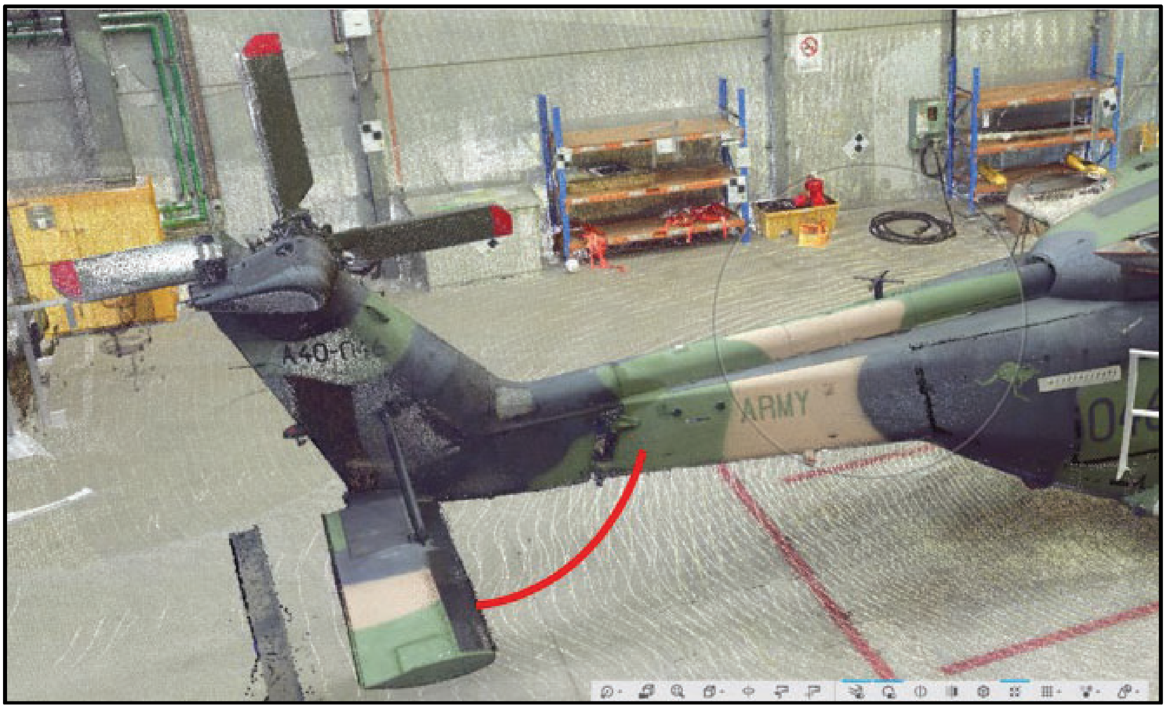

Figure 20: Stabiliser path upon impact and separation

32. **Flight Control Runs**. Approximately 60% of the cyclic system was recovered. **Figure 21** shows the cyclic stick assembly recovered items. The recovered cyclic assemblies comprised the majority of the LH cyclic stick system but only RH Cyclic Grip. Damage identified on the cyclic and collective flight control runs are consistent with high-energy impact damage. There is no evidence of material fatigue on the broken surfaces of the recovered components. A significant amount of corrosion was present on the recovered components due to salt-water exposure, which was expected.

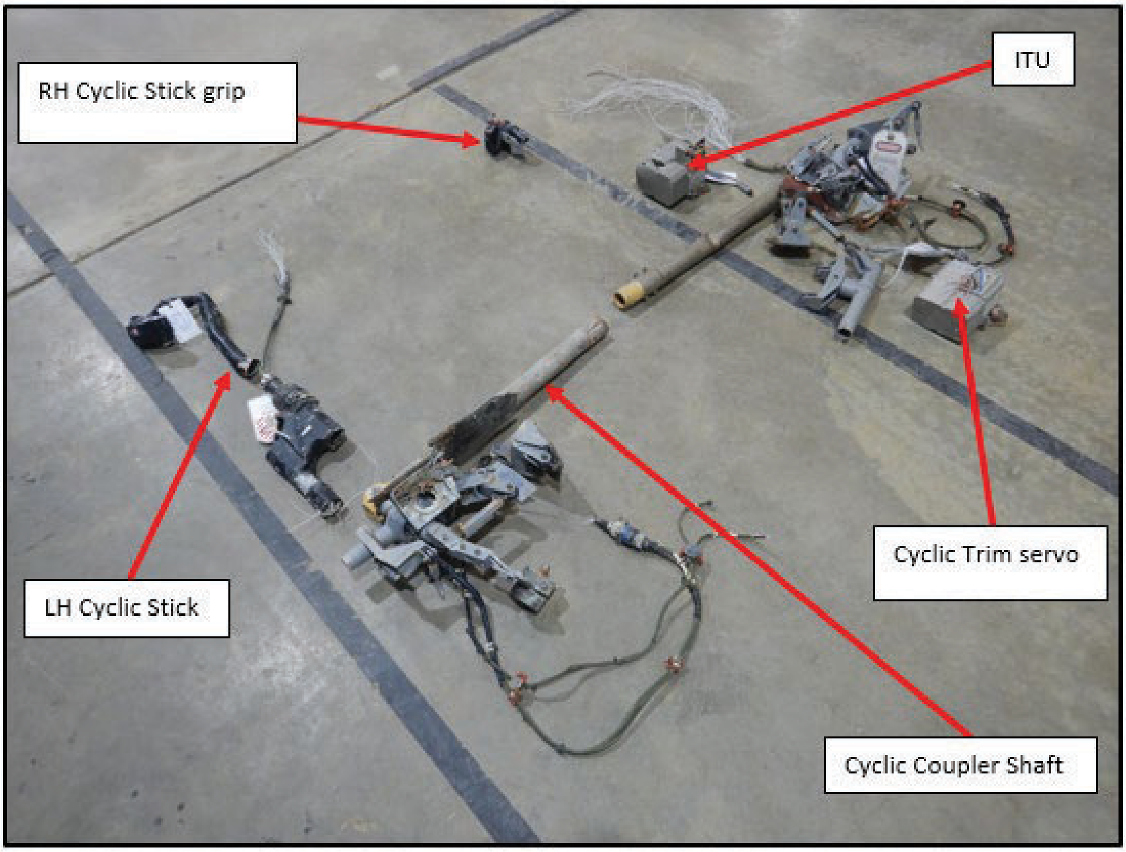

Figure 21: Recovered cyclic and coupler assembly

33. **Figure 22** provides an indication of the recovered portions of the collective system. The majority of the RH collective stick and assembly were recovered. Only a portion of components of the LH-side collective system were recovered. This includes a portion of the Coupler and the LH Collective Stick Grip. Both the pilot stick grips had separated from the LH and RH collective control sticks and were recovered with buttons missing.

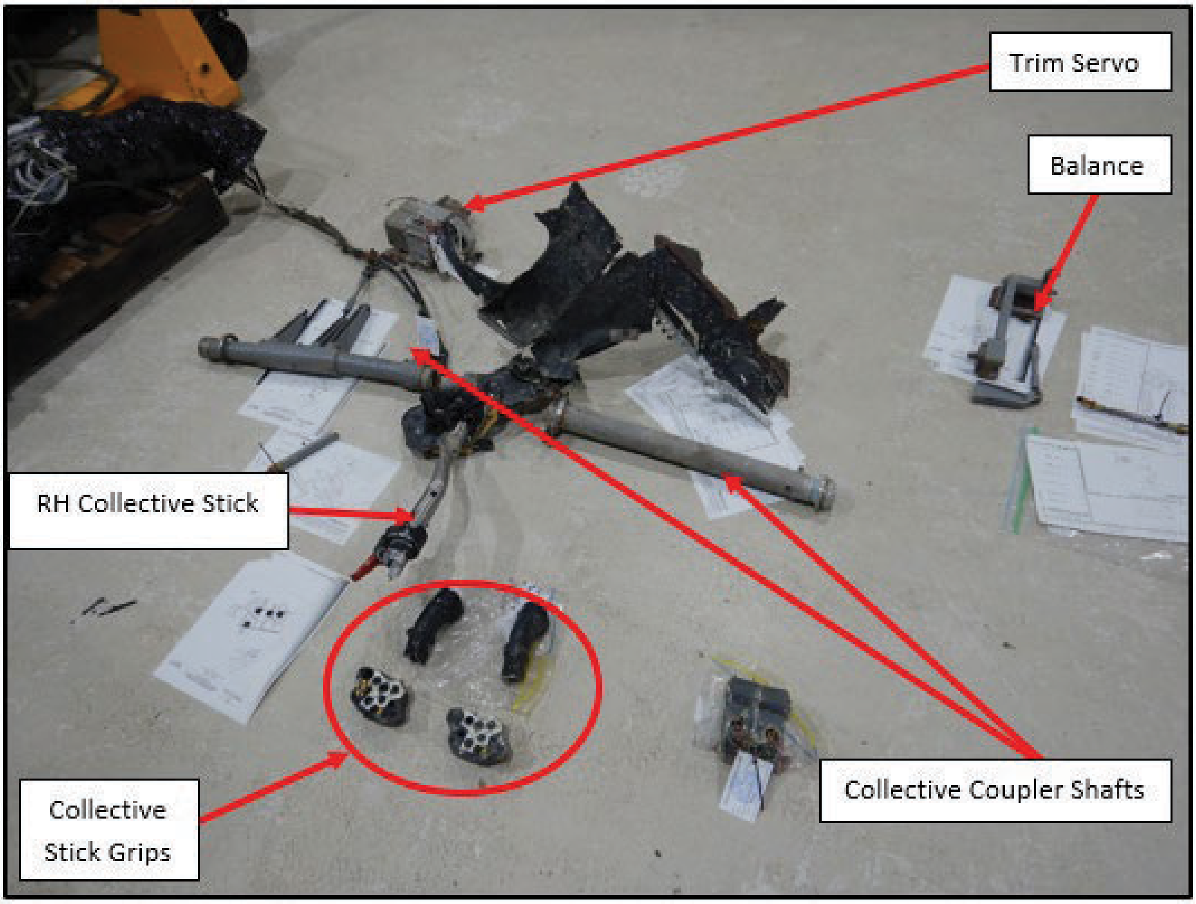

Figure 22: Recovered Collective System Components

34. **Yaw control system.** Approximately 90% of the yaw control system was recovered. Both the pedal assemblies suffered significant damage (**Figure 23**). The components were deformed and sheared off from the airframe. There was no indication of material fatigue on the recovered components.

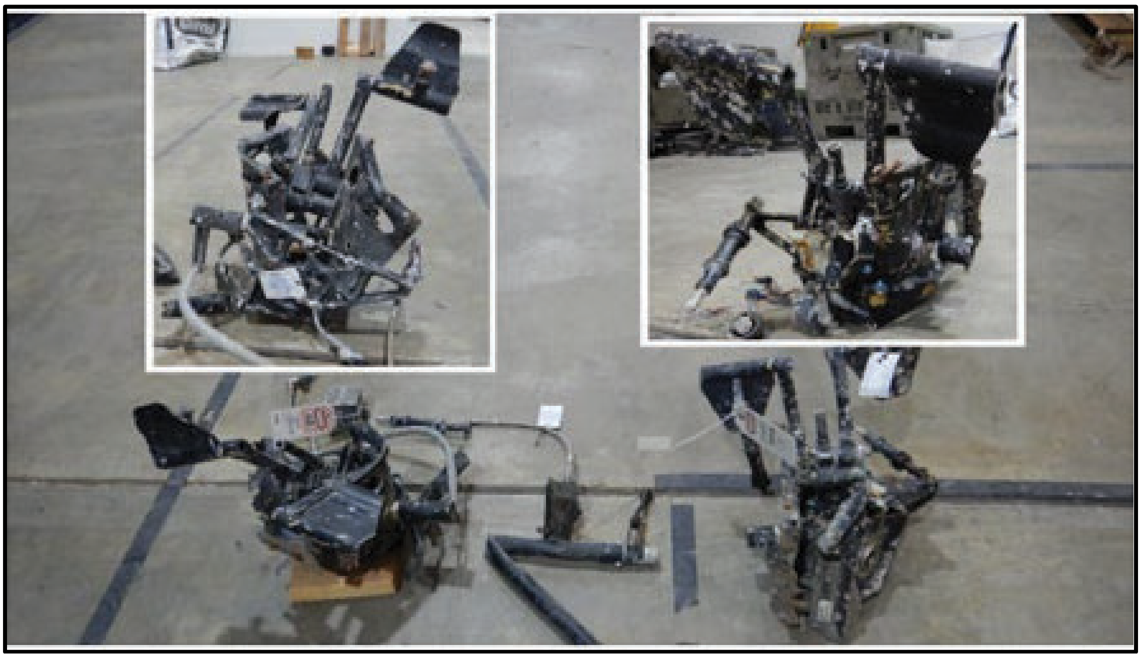

Figure 23: Recovered yaw control components

35. **Main rotor system.** A majority of the MRGB assembly and sub-assemblies were recovered from the seabed (**Figure 24**). The MRGB suffered significant damage and broke away from the main fuselage. Both engines were intact and remained connected to the MRGB. Upon recovery, the yellow and red main rotor blades were cut at the root under supervision of the ASIT to allow transportation to HMAS *Harman.*

Figure 24: MRGB and Main Rotor Head (MRH)

36. All four main rotor blades exhibited significant damage, with the outer sections of the blue and black blades experiencing substantial delamination and structural disruption. All blade attachment points, with their attachment pins, remained intact and connected to the Main Rotor Head (MRH). The blue blade had damage from its root throughout the blade structure (**Figure 25**). The yellow blade (**Figure 26**) was broken at approximately 0.6 m outboard of the attaching pins. Through significant force, the yellow blade broke at the top surface and folded downward. The outer section of the black blade separated at the approximate location of the taper of the aerofoil section to the blade root. The trailing edge side of the red blade (**Figure 27**) was significantly damaged. All four Main Rotor Blade De-Icing Looms remained connected to the head, except the blue loom, which was completely detached from the blade socket assembly.

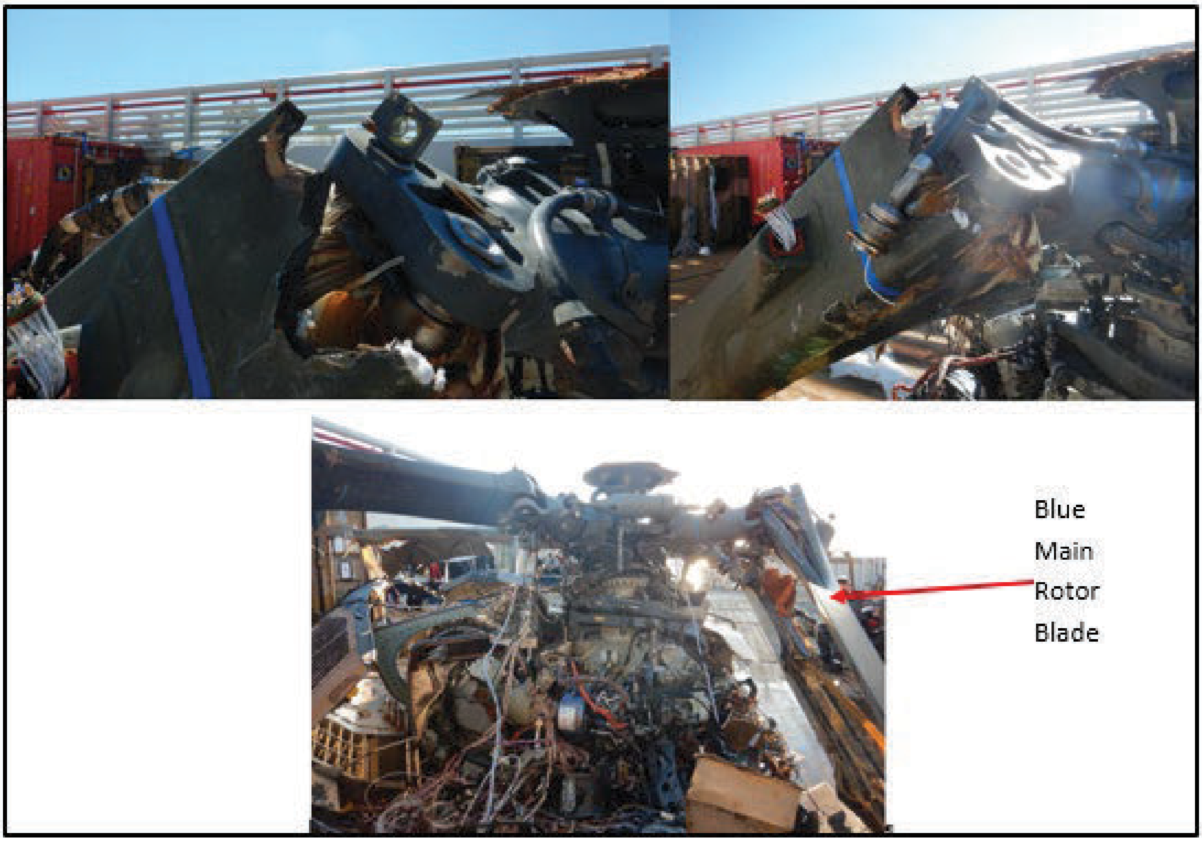

Figure 25: Blue Main Rotor Blade

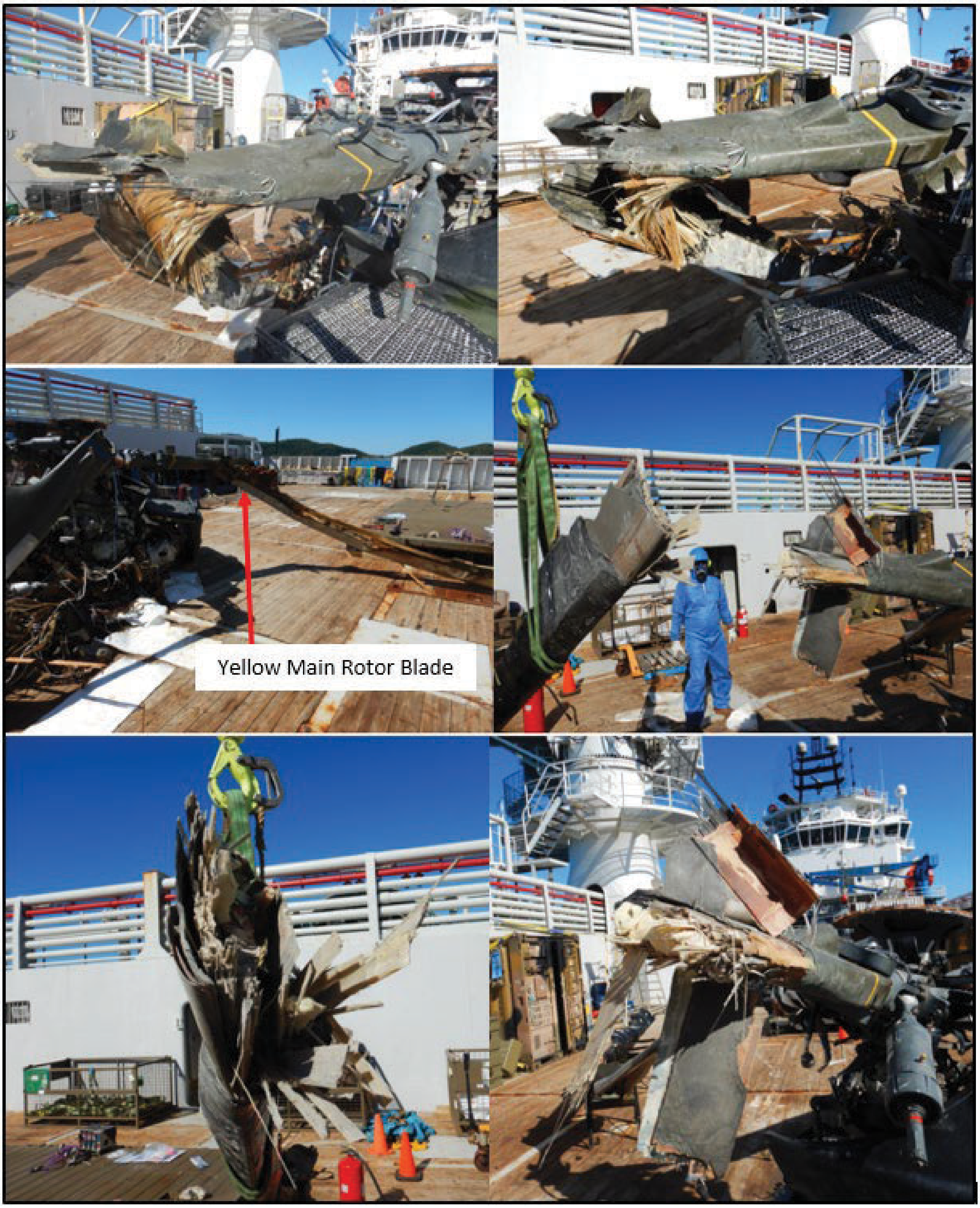

Figure 26: Yellow Main Rotor Blade

Figure 27: Red Main Rotor Blade

37. All four main rotor PCRs and four main rotor dampers were attached to the recovered MRH. The Black and Blue PCRs exhibited significant damage with bent and fractured rods. The Red PCR exhibited no visible deformation and only minor paint damage to the top end. The Yellow PCR was significantly bent but still attached. **Figure 28** and **Figure 29** exhibits the recovered PCRs.

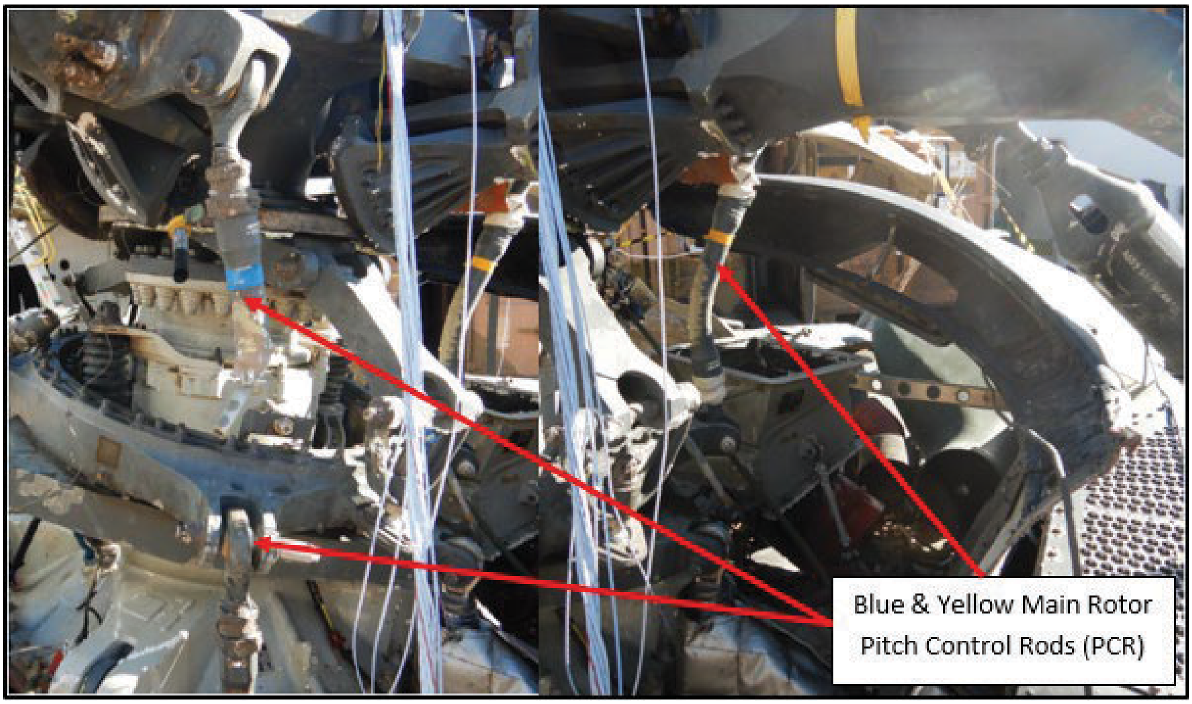

Figure 28: Main Rotor PCR

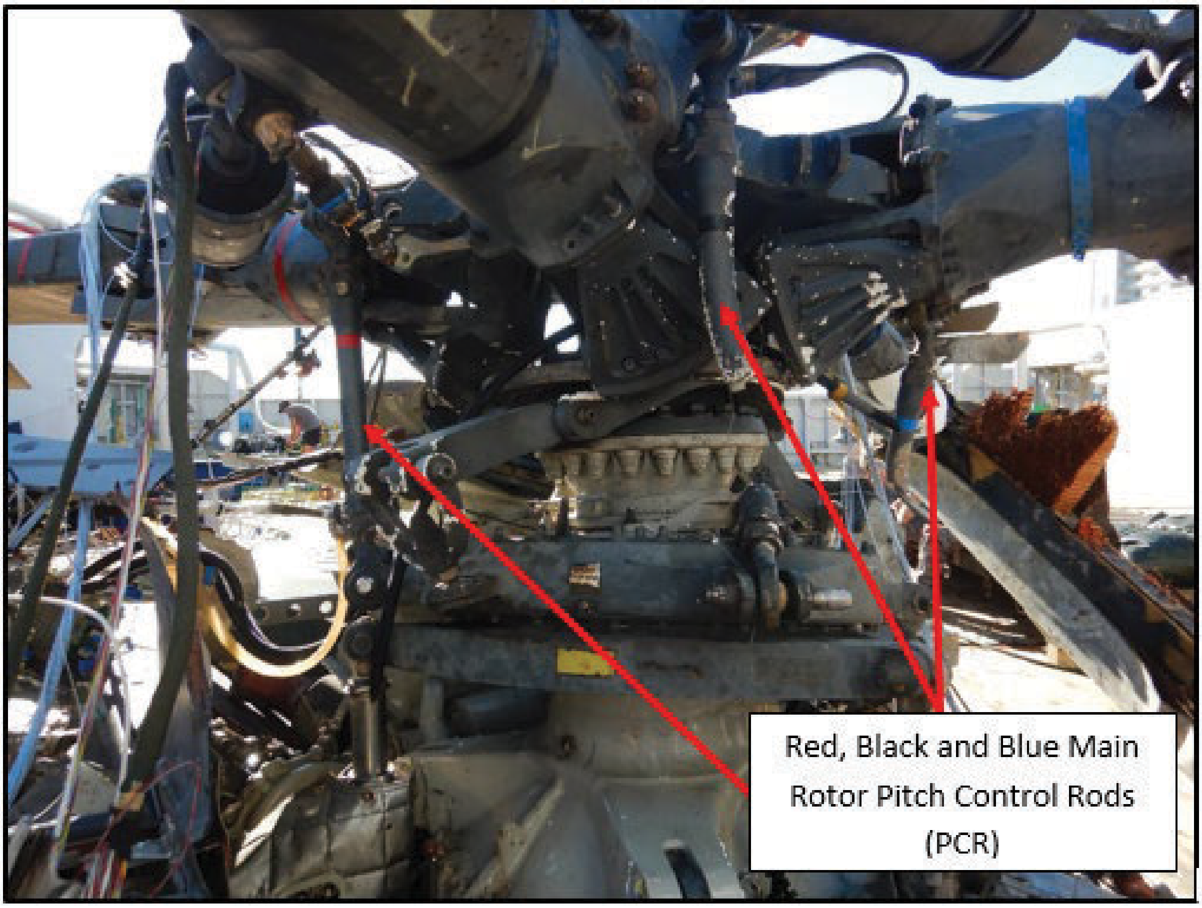

Figure 29: Blue, Black and Red main rotor PCR

38. The Four main rotor dampers were attached to the MRH structure. The Black and Blue Dampers remained intact and had minimal damage. The Red Damper fractured at the threaded section near the Red Blade Damper attachment point. There was no other damage visible on the Red Damper. The Yellow Damper, detached at the trailing elastomer housing which exhibited significant damage and was fractured in two pieces. **Figure 30** to **32** show the condition of the recovered main rotor dampers.

Figure 30: Yellow Main Rotor Damper assembly

Figure 31: Red Main Rotor Damper assembly

Figure 32: Black and Blue Main Rotor Damper assembly

39. Examination of the SARIB arms (**Figure 33** and **Figure 34**) identified significant damage to all four, with the RH-side aft SARIB arm exhibiting the least damage with only minor bending and twisting. The RH FWD SARIB arm exhibited significant bending and twisting. The LH FWD SARIB arm exhibited significant bending and tearing of the rod section of its arm. The LH aft SARIB arm exhibited an axial tensile overload fractured rod section.

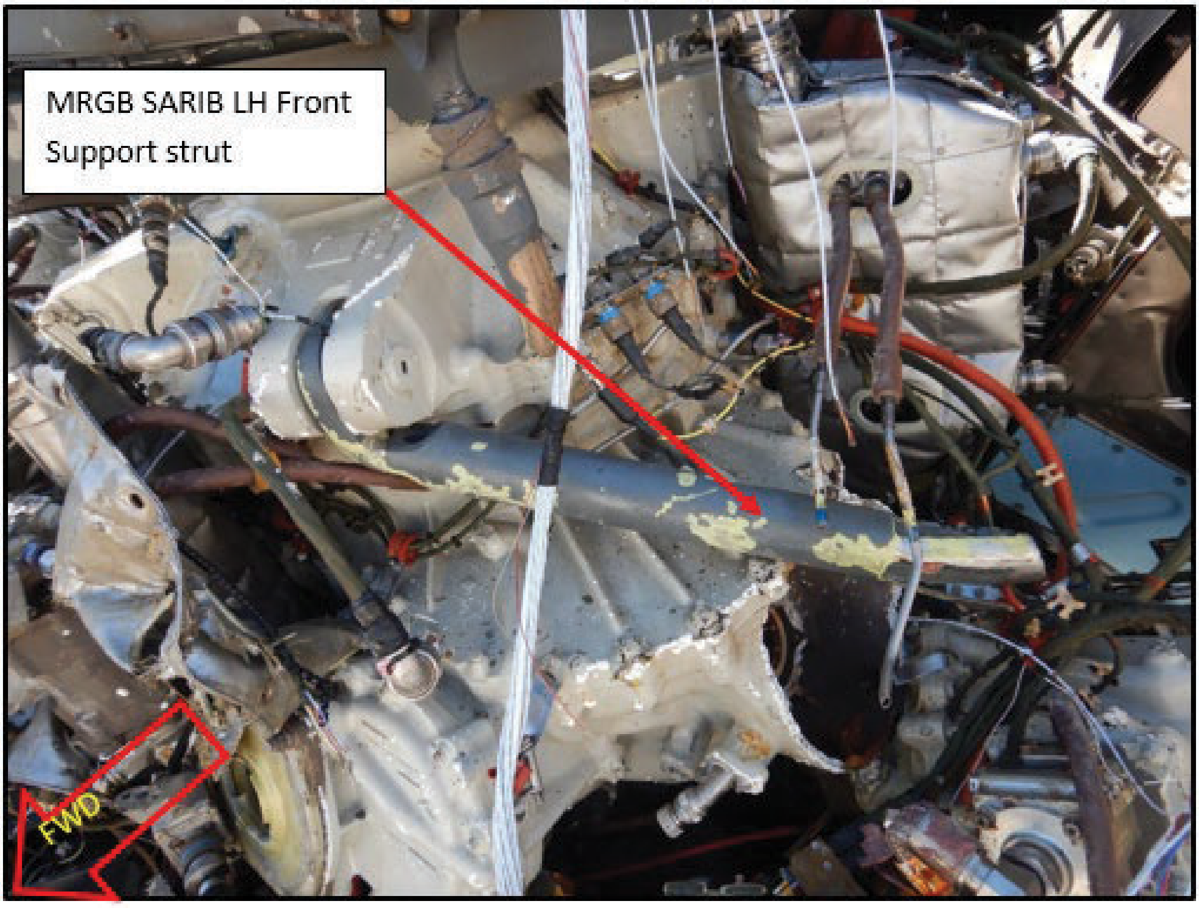

Figure 33: Left-hand Front MRGB SARIB Support Strut

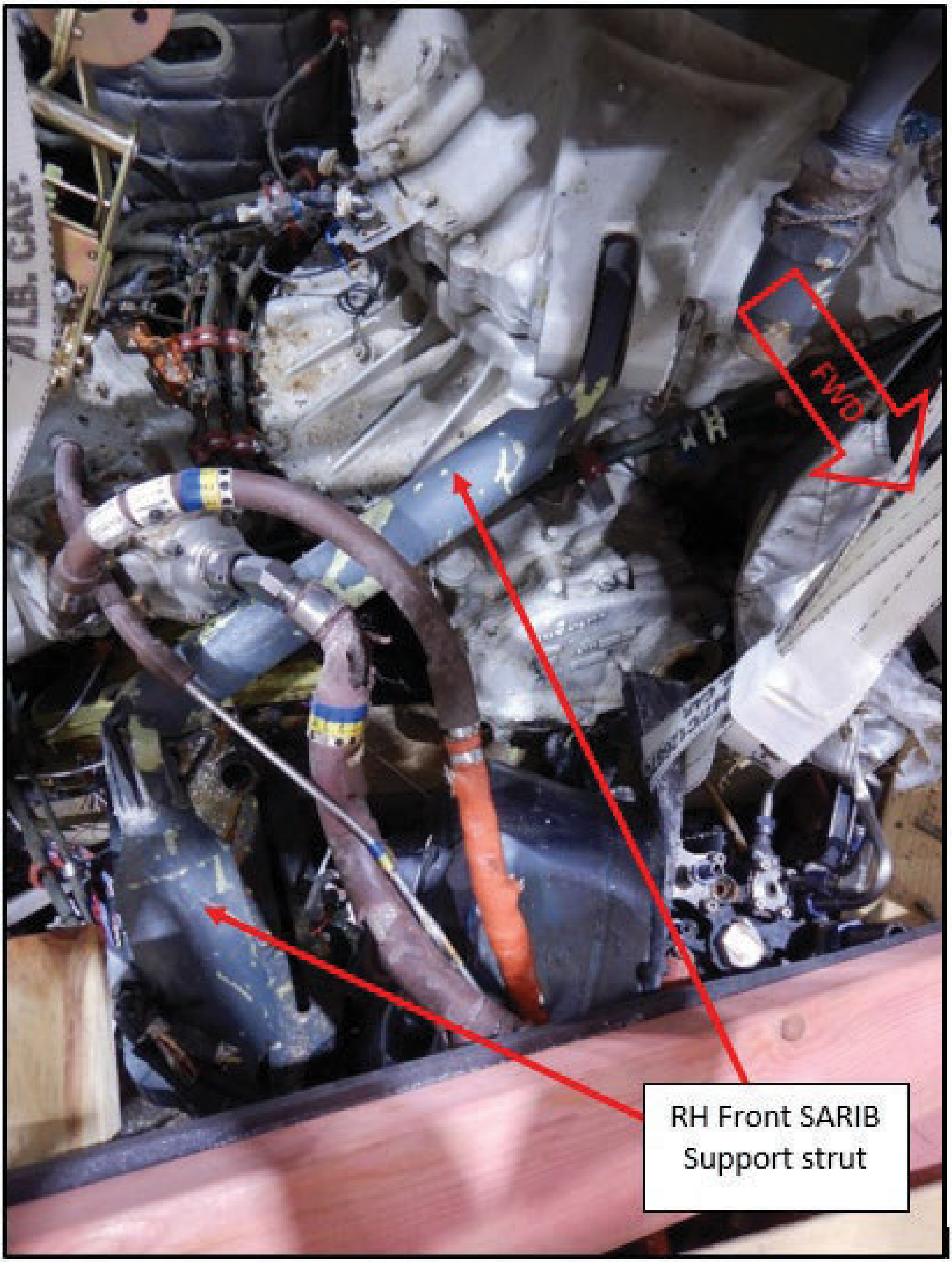

Figure 34: Right-hand Front SARIB Support Strut

40. The LH-side Input Module Gearbox was separated after recovery from the MRGB (**Figure 35**). Examination of the LH-side MRGB input module housing identified two areas of damage. Paint damage was present at a joint in the housing (yellow arrow), consistent with a torsion/twisting force. There is evidence of a hole on the FWD side of the housing where a section of the housing was forced inwards (red arrow).

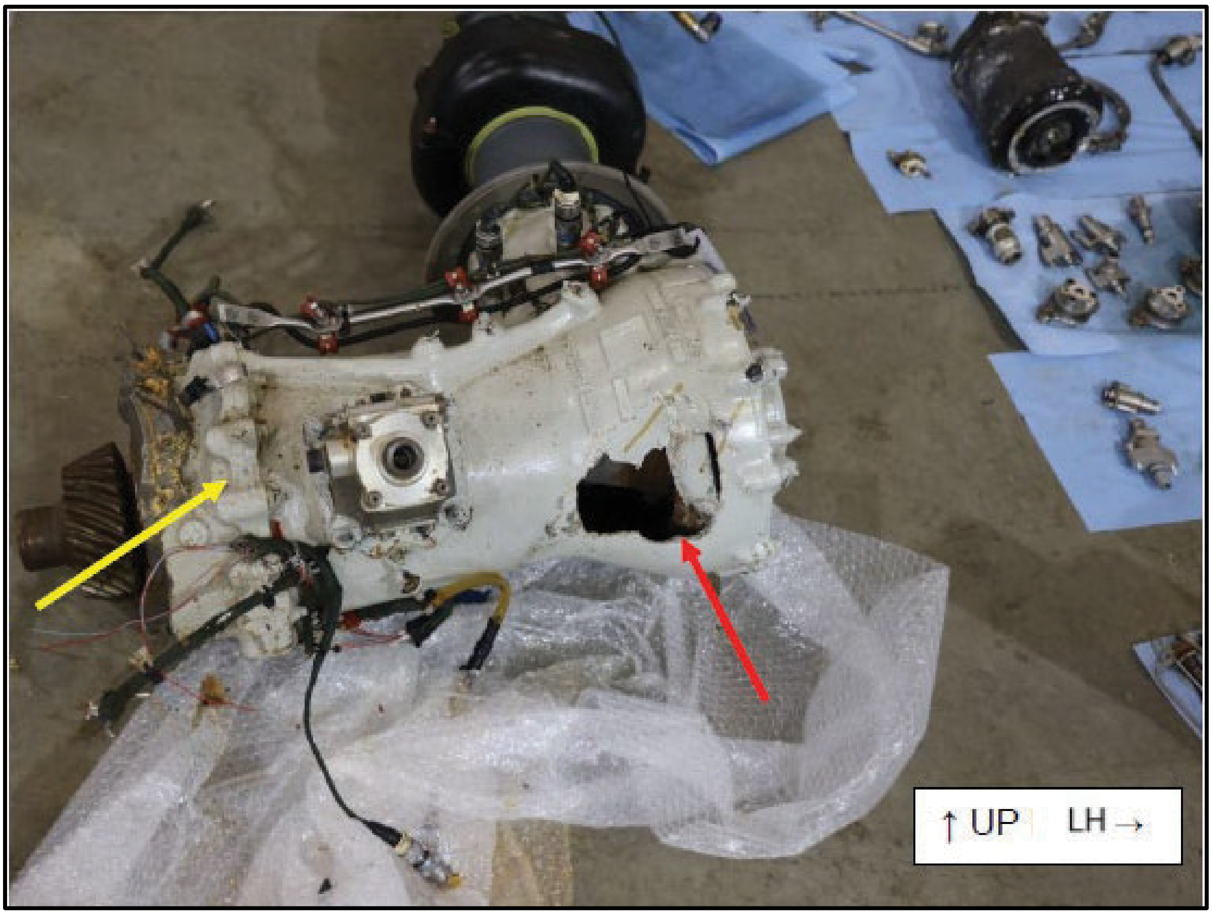

Figure 35: LH-side Main Gearbox Input Module housing

41. The RH-side Input Module Gearbox (**Figure 36**) was partially separated from the MRGB (red arrow), with cracking indicating the input module twisted forward and in a counter-clockwise direction relative to the MRGB. There was evidence of paint cracking at the same joint in the RH MRGB Input Module housing which was significantly less than the LH side. The RH engine to main gearbox shaft was found sheared in the outer housing **Figure 37.**

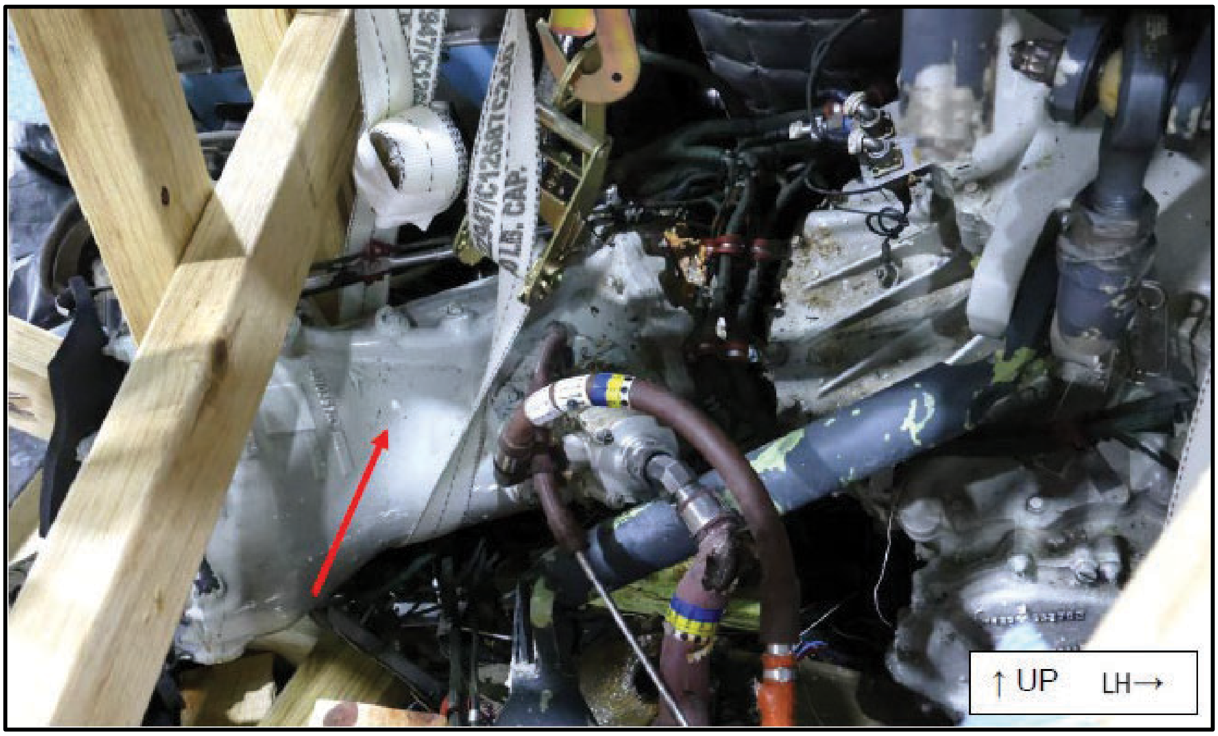

Figure 36: RH-side MRGB Input Module

Figure 37: Engine to Main Gearbox shaft

42. **Tail section.** The tail section was recovered from the seabed with TRGB and tail rotor blades attached. The tail section separated from the tail pylon and aft fuselage (**Figure 38**) at the weakest point of the structure, as stated in the AAP inspection report (Reference F). The damage on the tail rotor was consistent with impact damage. Upon detailed visual inspection, there was no indication of material fatigue or mechanical damage on the tail section.

Figure 38: Recovered tail section

43. The entire TRDS was recovered in three sections. The largest section was still attached and contained within the fuselage/tail pylon section, the FWD drive shaft section between the aft fuselage and MRGB (**Figure 39**), and the IGB input spline (**Figure 40**). The majority of the recovered tail rotor assembly was intact from the IGB to the tail rotor head.

Figure 39: FWD Tail Rotor Drive Shaft (TRDS) section

Figure 40: Intermediate Gearbox (IGB) Input Spline

44. The Tail Rotor Spline, which drives the tail rotor system from the MRGB was undamaged and intact. The attaching No. 1 TRDS Input Spline had spiralling damage around the circumference of the matching spline (**Figure 41**). The No. 1 TRDS sustained damage including a gouge mark aft of the O-ring recess at the FWD end (**Figure 42**). The O-ring was dislodged and partially sitting within the gouged area (red arrow). The shaft had circumferential scoring (black marks and paint scoring) to the FWD half of the shaft. The mid-alignment bracket was sitting loose on the shaft, having dislodged from the centre area (**Figure 43**).

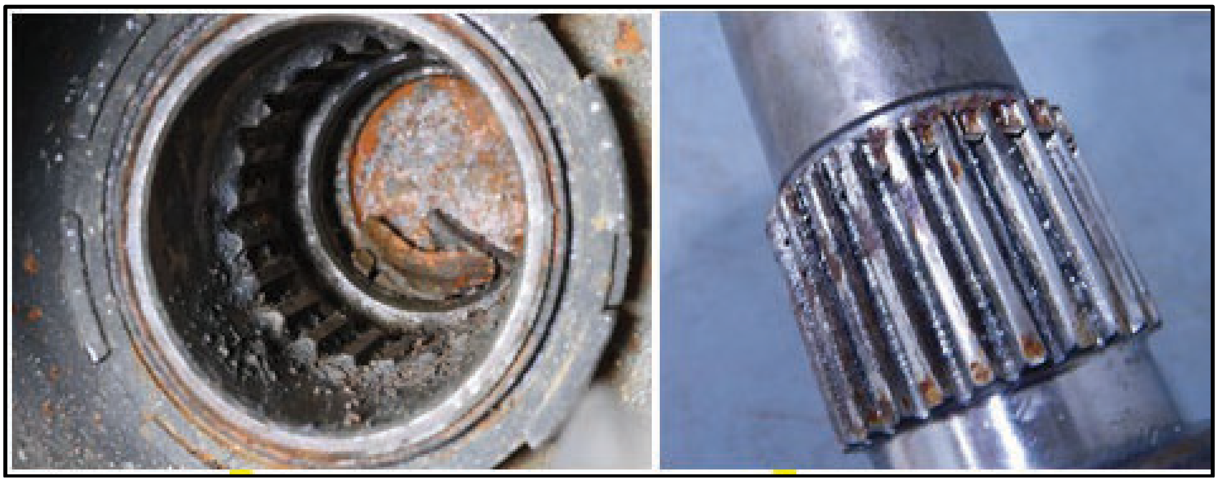

Figure 41: MRGB Tail Rotor Spline and No. 1 TRDS Input Spline

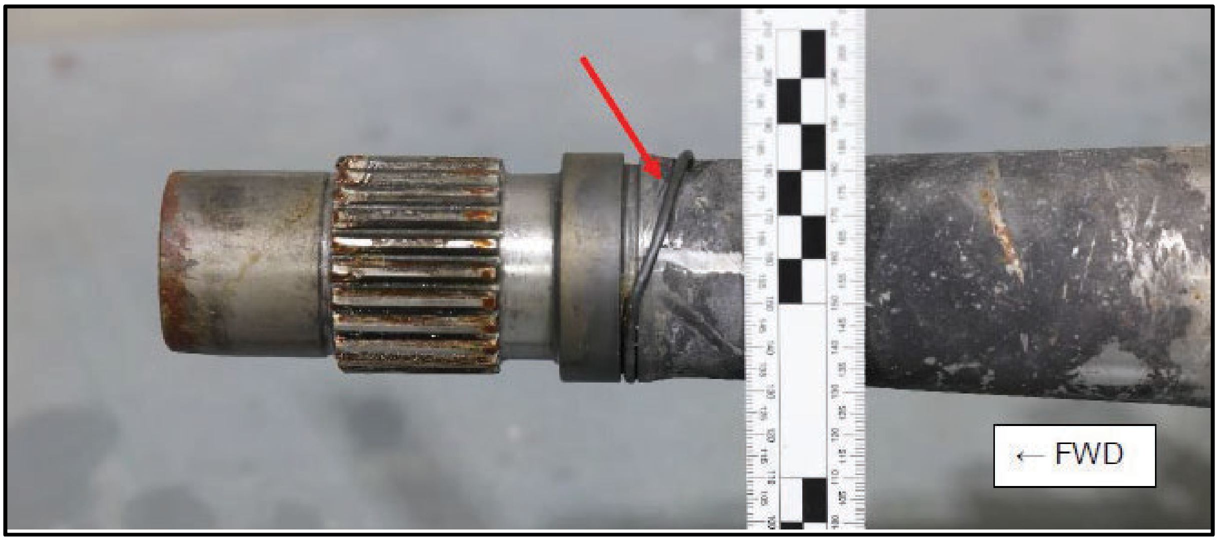

Figure 42: No. 1 TRDS FWD Spline end damage

Figure 43: No. 1 TRDS

45. The aft end connecting links of the No. 1 TRDS, fractured by overloading and bending at the midpoint, but remained attached to the drive shaft. The intermediate portion between the attachment bolts was missing, later found attached to the next connecting drive shaft in line, **Figure 44**. There were witness marks on all four quadrants of the shaft attachment points on both ends of the shaft, in addition to the attaching connecting links. The marks across the shafts indicate a significant compressive force on the tail rotor drive.

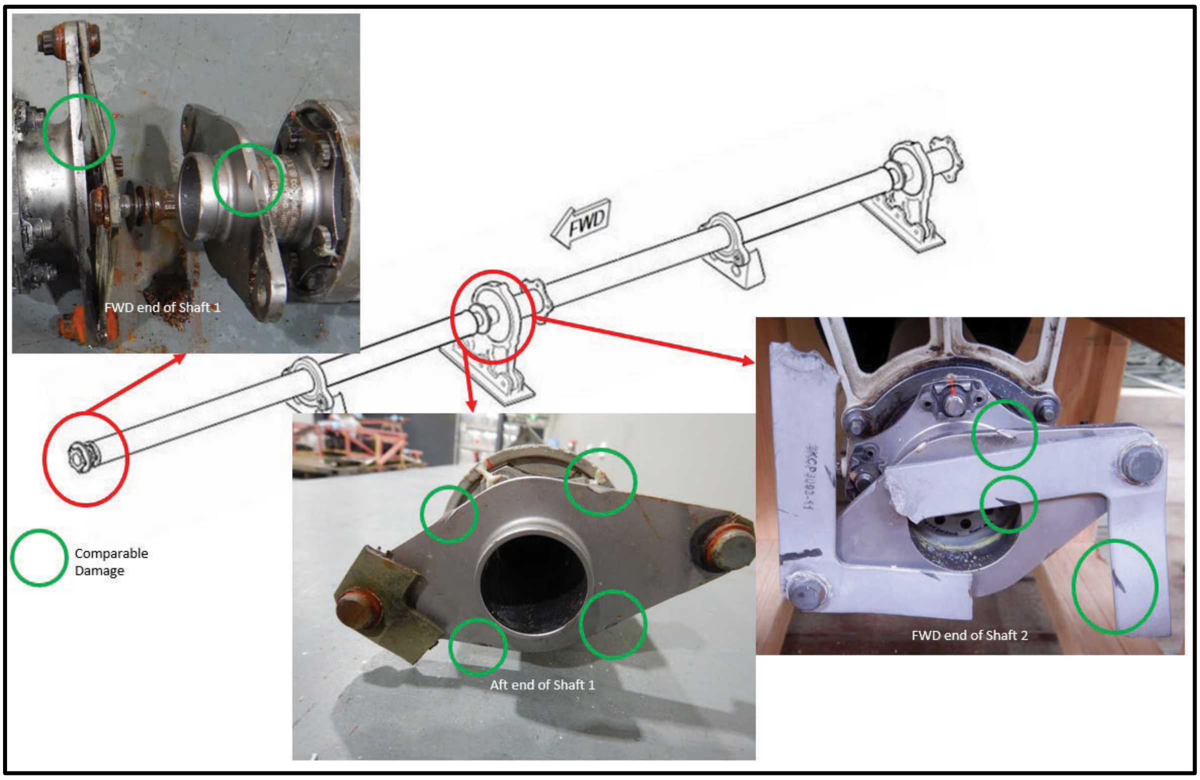

Figure 44: No. 1 TRDS attachment hardware damage

46. The TRDS section through the tail boom was intact and contained within the aft fuselage (**Figure 45**). The FWD end of No. 2 TRDS exhibited similar witness-mark damage as No. 1 TRDS at the aft end and connecting link as shown in **Figure 44**.

Figure 45: Internal of tail pylon drive shaft area

47. At approximately 0.6 m aft of the FWD end of the tail pylon section, there was a gouge/dent mark on the shaft around its circumference (**Figure 46** left). At 2 m aft of the FWD end of the tail boom, there was a penetration mark on the TRDS cowling (**Figure 46** right). Borescope inspection did not identify any damage on the TRDS assembly.

Figure 46: No. 2 TRDS damage and FWD drive shaft cowling penetration

48. The rear shaft into the IGB exhibited similar damage on the shaft ends to those found on all other shafts (**Figure 47**). The flexible coupling assemblies had fractured due to overloading, with matching fractures at both ends of the two shafts and spline portions. The IGB and shaft splines were undamaged, however, there was gouging on the upper FWD face near the spline area.

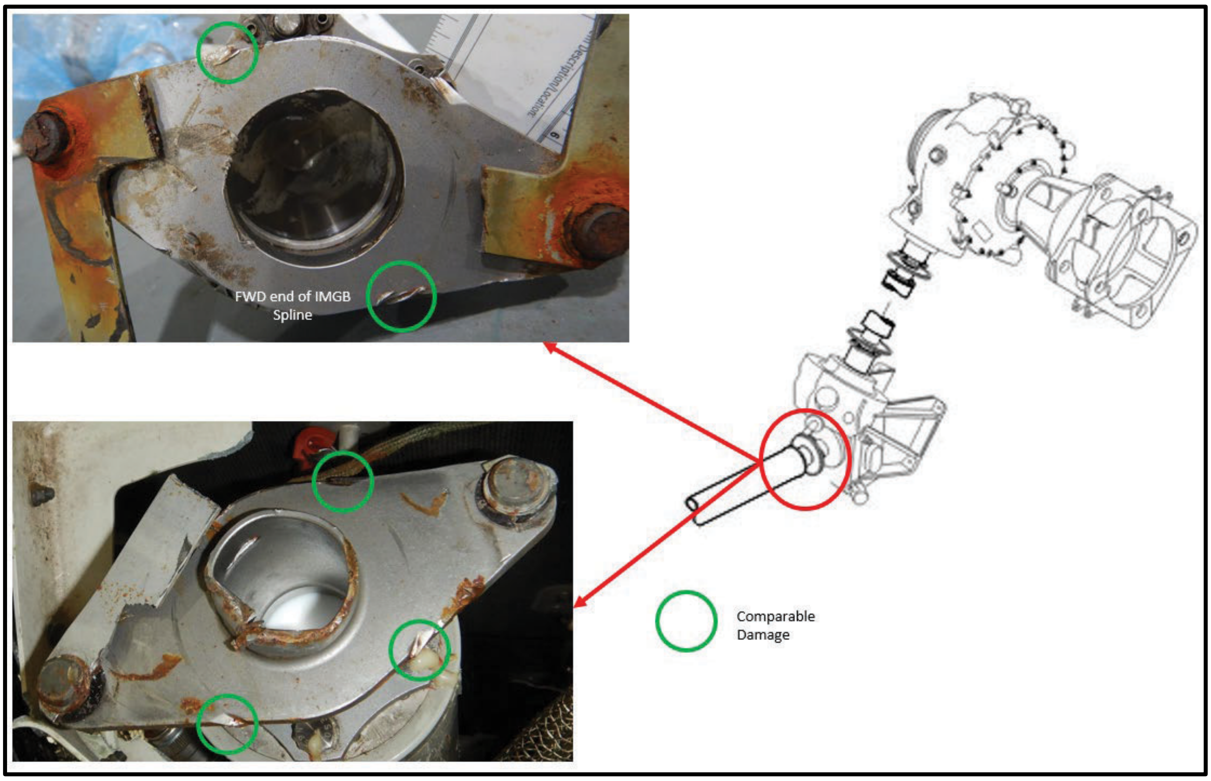

Figure 47: TRDS into IGB

49. Examination of the tail rotor assembly identified significant damage to the top and leading edge of the yellow blade (**Figure 48**) with delamination/cracking of the leading edge and the blade root. Blade root damage was caused by contact with the rotor blade bracket and fractured bracket bolts. Examination of the Blue Tail Rotor Blade identified minor indentations on the blade tip and a fracture of the blade near the blade root (without complete separation) (**Figure 49**) resulting in the blade folding over on itself.

50. The Black Tail Rotor Blade did not exhibit denting or other significant damage to the blade leading edge or tip, whereas the Red Tail Rotor Blade exhibited significant scraping, paint damage and chipping to the outer surface near the blade tip, **Figure 50**. There was minimal damage on the lead-lag dampers, brackets and bolts on the tail rotor assembly with the exception of the Yellow Blade Bracket bolts described above.

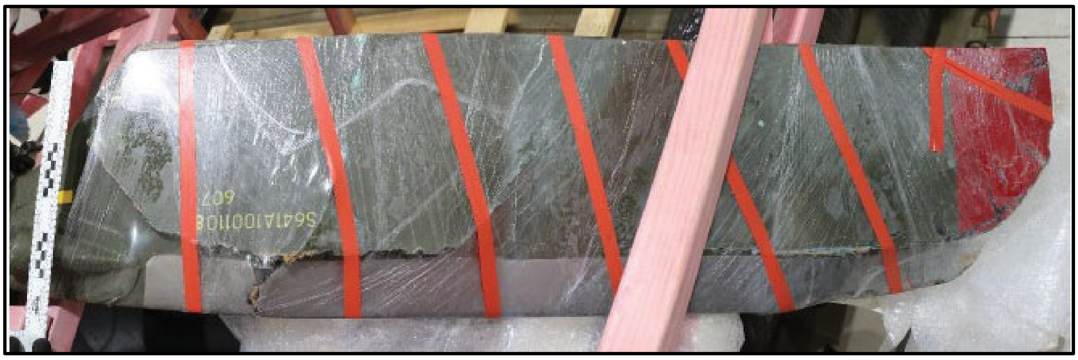

Figure 48: Yellow Tail Rotor Blade

Figure 49: Blue Tail Rotor Blade bent in half

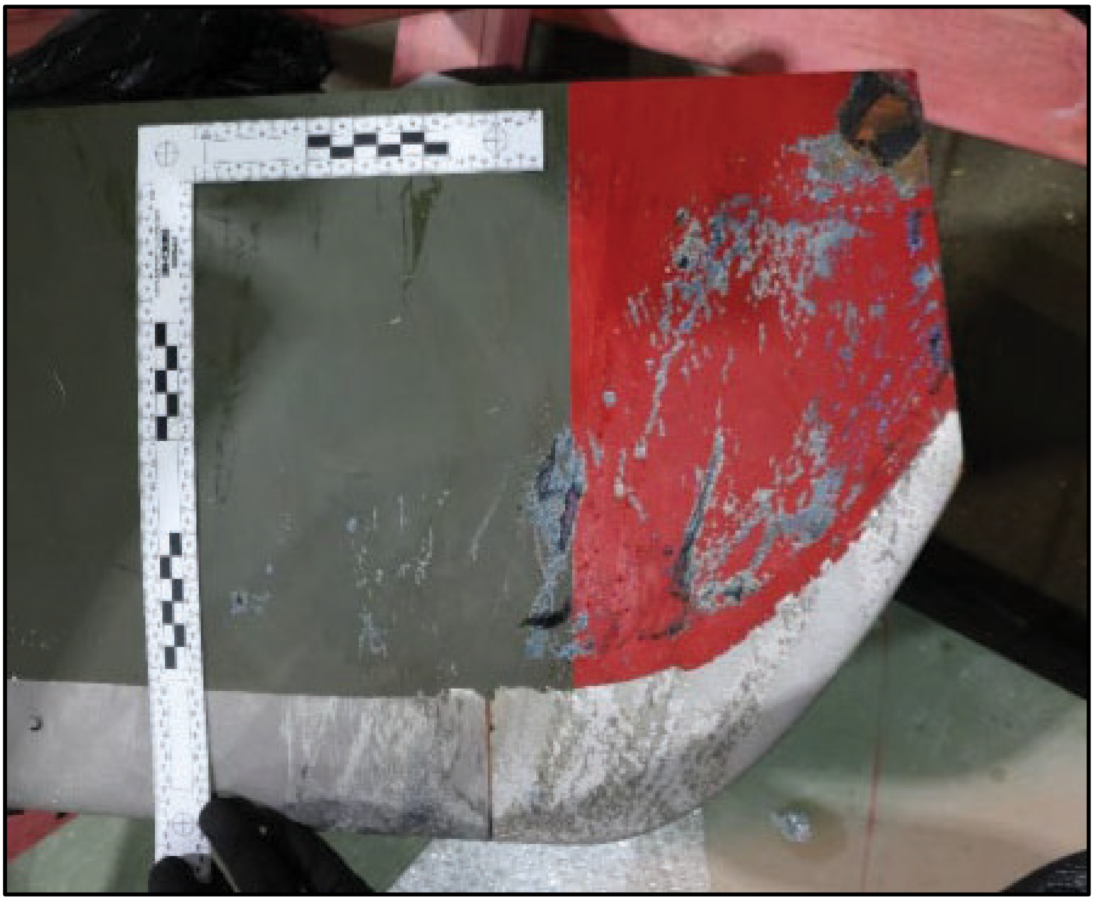

Figure 50: Red Tail Rotor Blade tip

51. **Engines.** The engine assembly was found attached to the main rotor assembly, and recovered on board the ship where the ASIT conducted initial inspections (**Figure 51**). The recovered engines showed no evidence of engine fire. The engine and main rotor assembly structure sustained impact damage and had broken away from the front and rear assembly structures. The engine cowlings remained latched to the structure and the cowling skin contained minor instantaneous damage (cracks and broken structure) from impact forces.

Figure 51: Recovered top structure containing engines

52. Once the engine cowlings were removed, both engines were found inside their compartments with minor damage to the engine accessories (**Figure 52**). Both engines were removed from the main structure and transported to HMAS *Harman* where ASIT and DSTG members conducted further detailed inspections and borescope examinations.

Figure 52: No1 Engine (left) and No. 2 Engine (right)

53. The engine accessories and fittings were removed to gain access to the borescope ports on the engine. The inspection of the engine fittings identified greater damage on the LH Engine accessories. On the LH Engine, fuel pipes and fittings exhibited deformation and damage from the combustion chamber section to the power turbine section. **Figure 53** shows the deformed fuel pipe at the top left position (approximately at 270-360 °) on the LH Engine. **Figure 54** shows the LH Engine accessory gearbox components have higher levels of corrosion than the RH Gearbox components.

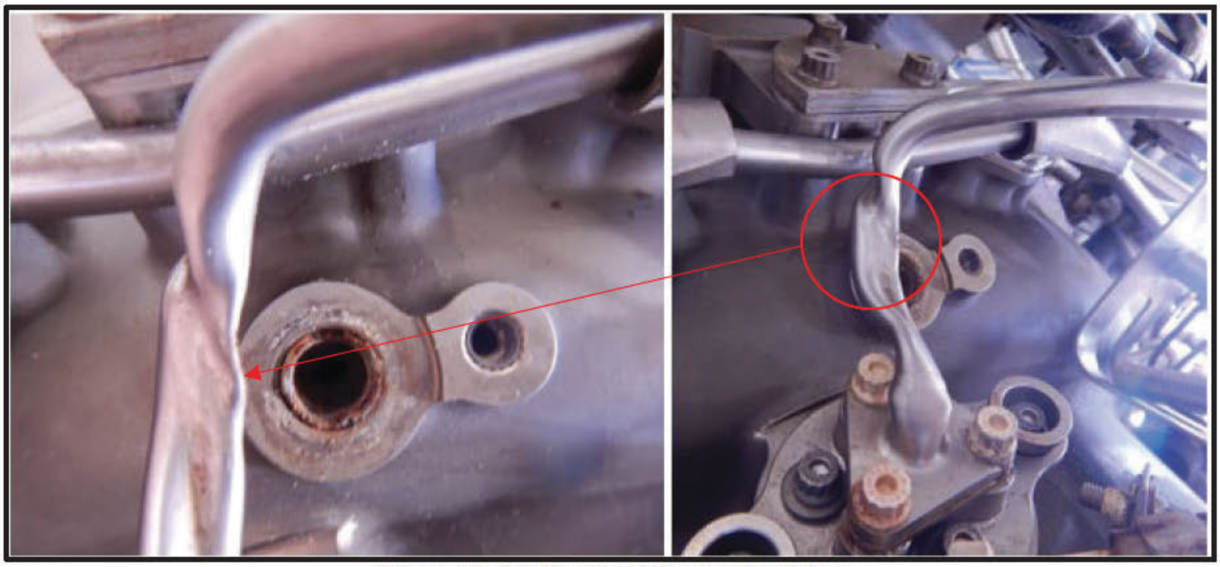

Figure 53: LH Engine deformed fuel pipe

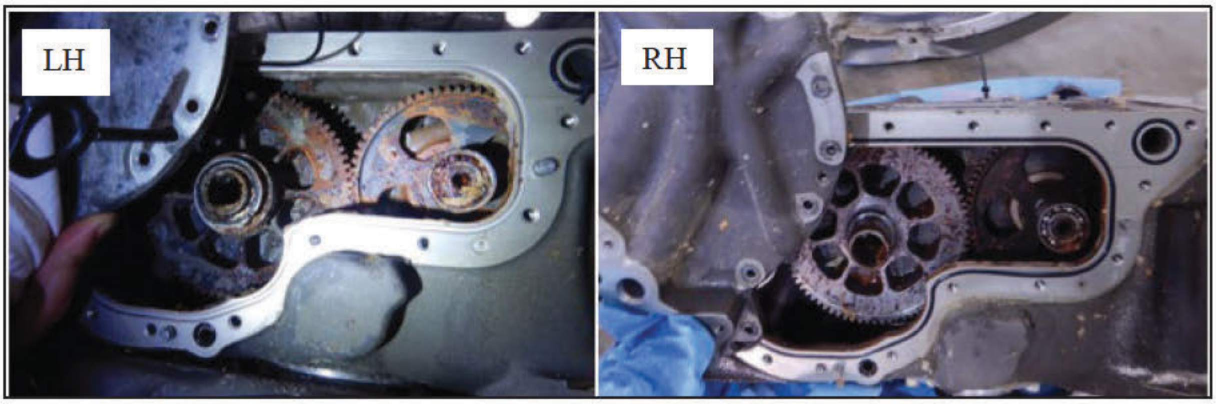

Figure 54: LH and RH Engine accessory gearboxes

54. Borescope examination was restricted to the first- and second-stage compressor blades through a portion of the combustion chamber, and to the downstream end of the second-stage High Pressure Turbine (HPT) blades. Only an external examination of the second stage Power Turbine (PT) blade was possible. The borescope could not reach other locations within the engine, nor could the engines be rotated to visually examine all blades.

55. **LH Engine.** The LH Engine exhibited debris and salt-like deposits on the first-stage compressor through to the second-stage compressor. There were minimal deposits on the combustion chamber and HPT stage. There were two chipped blades (**Figure 55**) and a bent blade (**Figure 56**) on the first-stage compressor. The combustion chamber contained minor carbon deposits (**Figure 57**). Borescope inspection found uniform coloration on internal components and found no evidence of metallisation inside both the engines. There was no evidence of damage on the second-stage PT.

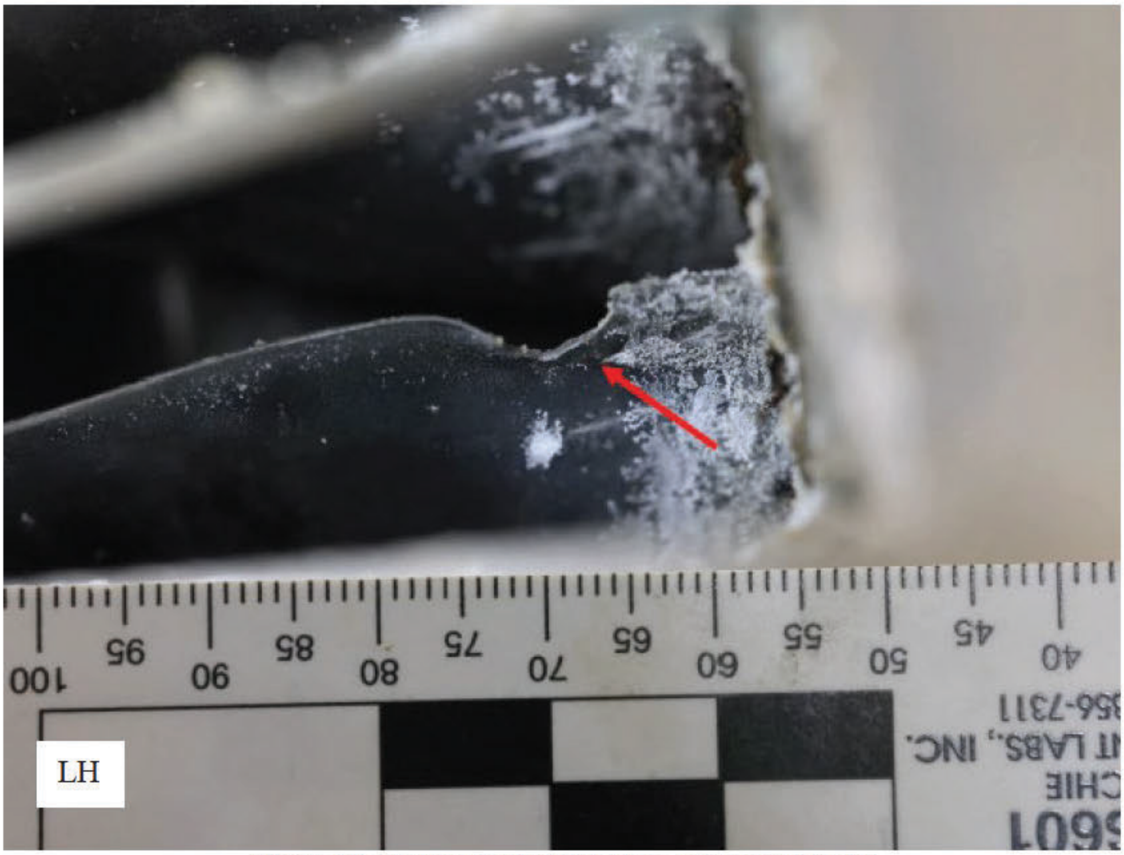

Figure 55: Damage on the first-stage compressor blade

Figure 56: A bent first-stage compressor blade

Figure 57: Minor carbon deposits on combustion chamber

56. **RH Engine.** The RH Engine exhibited an increased concentration (compared to the LH Engine) of debris and salt-like deposits at the first-stage compressor through to the second-stage compressor. Similar to the LH Engine, there were minimal salt-like deposits on the combustion chamber and HPT stage. There was damage on one first-stage compressor blade (**Figure 58**). There was no evidence of damage on other engine modules.

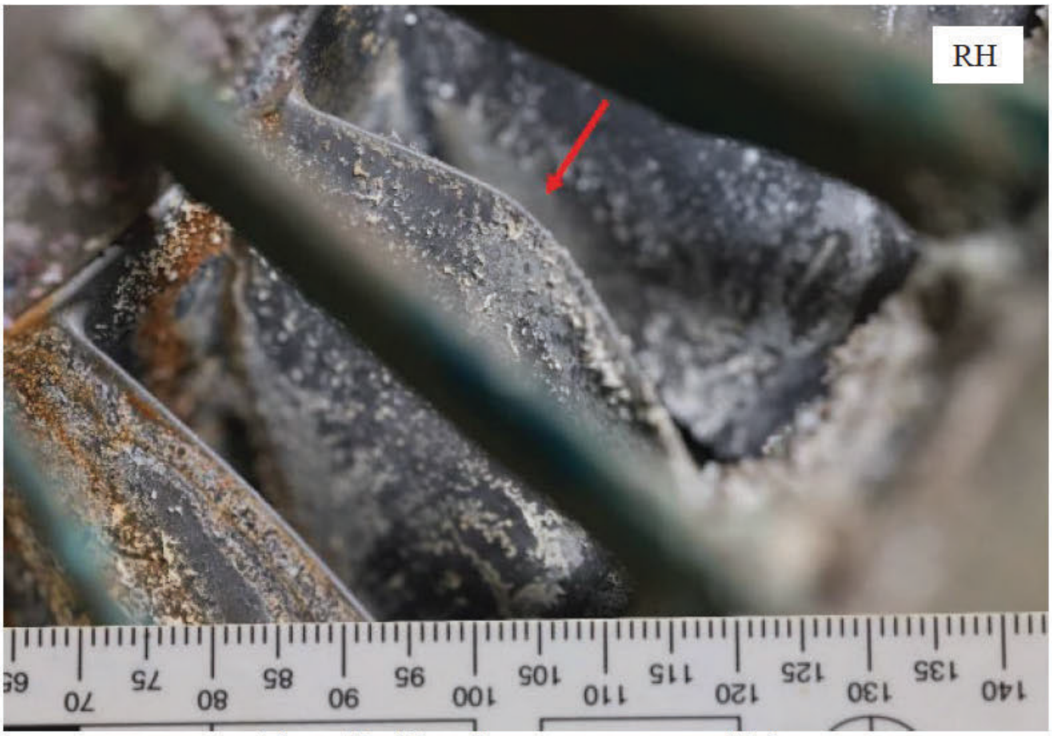

Figure 58: A bent first-stage compressor blade

57. **Air Speed Indicator (ASI).** The recovered ASI showed an airspeed of approximately 125 knots (kts) at impact (**Figure 59**). The information from the recovered ASI broadly aligned with airspeed data downloaded from the CSMU. The CSMU's last valid data point was taken 1 to 2 seconds prior to impact and indicated the speed as 135 Knots Indicated Air Speed (KIAS).

Figure 59: Recovered analogue ASI

58. **Artificial horizon.** The recovered Standby Artificial Horizon (**Figure 60)** indicated an apparent aircraft attitude of approximately 30° nose down and approximately 120° of angle of bank to the left. However, this did not match data from the CSMU. DSTG-CR-2024-0011 (Reference E) describes the tear down and examination of the artificial horizon. DSTG found the instrument was indicating a 20° nose down pitch attitude and that roll attitude was indeterminate at impact.

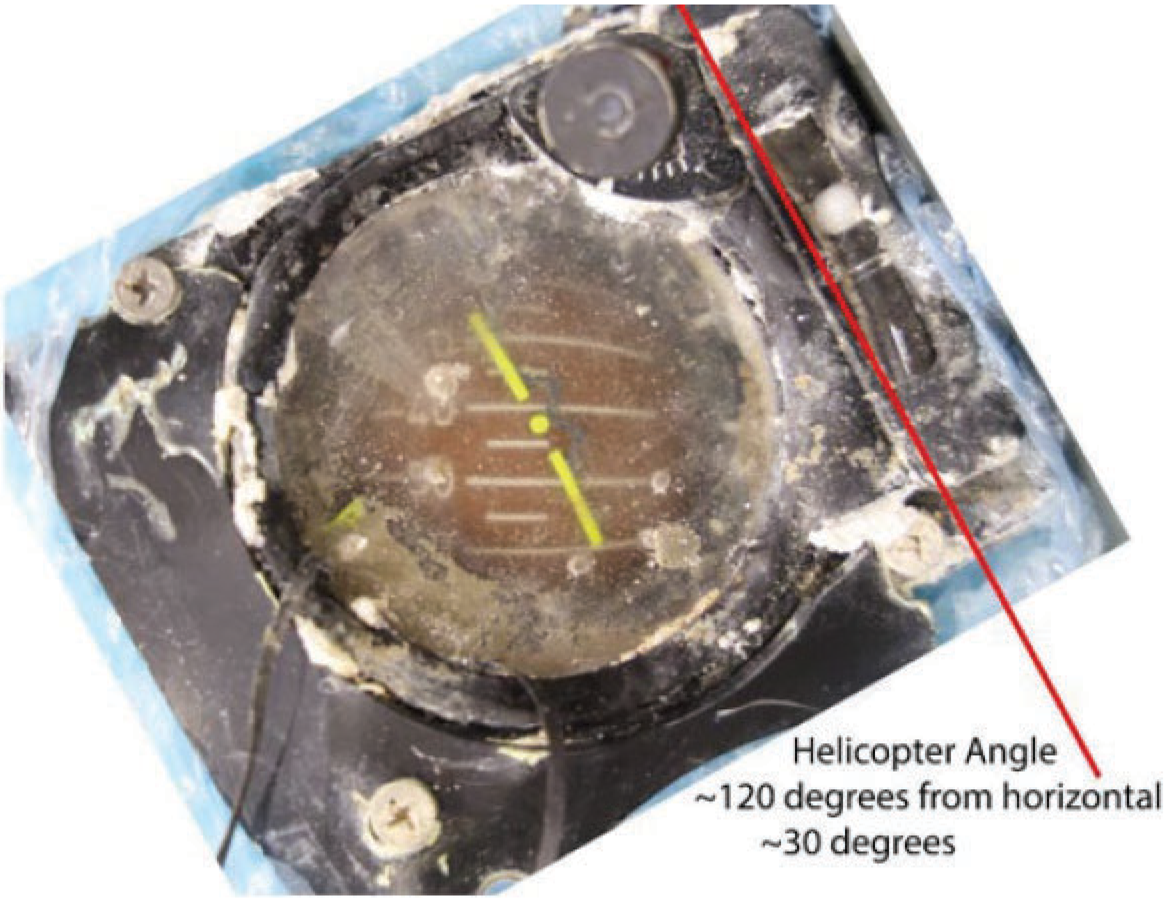

Figure 60: Recovered Standby Artificial Horizon

Flight data

59. The ASIT requested DSTG, AAP and NHI conduct independent reviews of aircraft flight data downloaded from the CSMU. Comparison of the ASIT's analysis of VFDR data with the independent reports provided by DSTG, AAP and NHI concluded that there was no evidence of abnormalities or failures of the airframe or aircraft major systems throughout the flight and the key sequence of events prior to impact with water. Pilot control inputs were correctly interpreted by the FCS and the aircraft responded accordingly.

60. Full details of the AAP, NHI, and DSTG reports, including analysis, are contained in References D, E, and F. Key data from those reports indicate the following aircraft performance and operation:

a. Control inputs show that the helicopter was flown manually.

b. The helicopter responded to control inputs throughout the entire flight.

c. An indicated airspeed of 135 KIAS during the last 1 to 2 seconds before impact.

d. In the last 6 seconds, the aircraft decreased its pitch attitude up to 28^{o} nose down.

e. The longitudinal and lateral accelerations remained within normal range during the entire flight before impact.

f. Oil temperature and pressure of the MRGB and the Remote Accessory Gearbox were within limits. There were no warnings associated with these systems during the entire flight.

g. Hydraulic pressures were within limits with no warnings activated during the entire flight.

h. Fuel quantity did not show any abnormal indication. The fuel flow provided to the engines was consistent with the engine data.

i. Engine parameters were within limits and both engines operated within the expected performance margins. The engines were both matched for Torque (TQ) and Power (Np) outputs and responded correctly to the pilot's control inputs. Each engine's free power turbine (NF) demonstrated expected synchronisation with the main rotor system.

j. At 12:36:22.5, the aircraft experienced a vertical acceleration of zero G and both engines recorded a brief low oil pressure warning due to the oil sensors detecting a low pressure due to the reduced G. The engines recovered to normal operating oil pressure immediately with the onset of positive G.

k. At the last data point 12:36:26.00, the collective was raised in one second from 17.8% to 56.1%. This led to a torque increase from 500 to 620 Nm (mean of LH and RH engines) and a rotor speed (Nr) decrease from 96.4% to 94.8%, triggering the low rotor RPM indication (Nr < 95%).

TECHNICAL ANALYSIS

Airframe attitude at impact

61. **Aircraft structure.** Examination of the wreckage did not indicate any pre-existing damage to the aircraft before the flight or damage that occurred before to its impact with the water. Data recovered from the VFDR supports evidence that the aircraft was serviceable prior to impact. The speed and attitude derived from flight data was similar to that shown on the analogue ASI and the standby artificial horizon pitch attitude at impact. The presence of cockpit instruments in the tail section, and the rearward movement of a main cabin crew seat to the crew escape hatch in the rear fuselage, supports assessments, that the aircraft impacted the water at high speed (125–135kts) with a nose down attitude (0–20° degree).

62. Due to the high-speed impact, it is very likely the forward part of the fuselage, including the cockpit, fragmented, as the aft fuselage continued on the flight path into the cockpit debris. The rear fuselage broke away from the main structure forward of Frame 11. The force of water impact from the nose-low impact attitude induced a compressive load to the tail section causing it to break away from the rear fuselage and tail pylon aft of Frame 14.

63. **Impact angle.** Based on VFDR data, the aircraft impacted the water on the left-hand side of the airframe in a nose-low attitude. DSTG (DSTG-CR-2024-0011) at Reference E concluded from damage to main rotor blades, PCRs, and the artificial horizon, the aircraft's attitude at impact was approximately 20° nose low rolling to the left. Other indications of a nose low with left roll impact are greater damage on the LH Engine accessories, including deformed components and corroded accessory gearbox. This analysis supports the FDR data that indicated a lateral cyclic displacement of -35% to the left in the last seconds before impact.

Main rotor assembly (head speed (Nr)) at impact

64. **Rotor head speed.** Analysis of rotor components indicate that the rotors were turning at high speed upon impact. The various degrees of damage on the main rotor blades and dampers indicate that there were significantly different speeds and loads on each blade at impact. Black rotational witness marks on the forward aft TRDS section also indicates that the rotors (and shaft) were turning at impact. The SARIB arms exhibited damage consistent with a tensile load on the LH-side forward gearbox mount, compressive loading on the RH-side forward mount and twisting on the RH-side aft mount. This suggests a significant clockwise movement (**Figure 61**) of the MRGB relative to the fuselage, which was very likely caused by the rotor blades being forcibly stopped while the engines were still providing power.

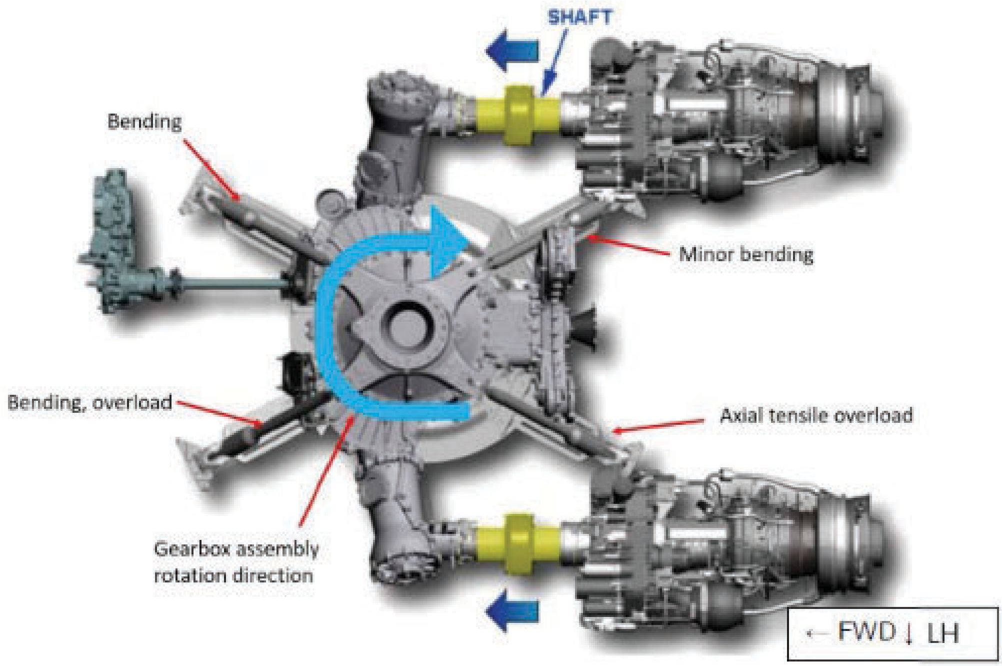

Figure 61: Damage to the SARIB with likely direction of movement

65. **Engine operating**. The evidence of the main rotor turning and rotational witness marks on the aft TRDS, (**Figure 41**), suggested the engines were operating and powering the rotors until impact. The shear damage on the engine to main gearbox shaft, (**Figure 37**) indicates a sudden stoppage during high-speed rotation.

66. Despite impacting the water at high speed, the damage to the engines is localised to the first-stage compressor blades due to the position of the engines and the protection provided by the engine cowling. The salt deposited in the first- and second-stage compressors indicates the engines were rotating and ingested water, which resulted in the engines flaming out. This also confirms the engines were operating at impact. The flight data confirmed the engine parameters were within the normal range of operation until the last data point, when a low rotor RPM indication was triggered just prior to impact.

Aircraft control input

67. **Flight Control System (FCS)**. Approximately 65% of the collective and cyclic systems were recovered; therefore, it was not possible to reconstruct the complete system. The yaw control system sustained significant damage to all components. The shearing or deformation damage was consistent with the characteristics of a high-energy impact. Analysis of VFDR flight data confirmed there were no abnormalities associated with the operation of the FCS.

68. **Control input versus output**. The DSTG report states that the final position of the swashplate actuators indicate the pilot control inputs of pulling up and rolling to the left. However, it is not possible to confirm accurately whether these particular inputs had an effect on the position of the actuators. The flight data indicated the aircraft responded appropriately to pilot control inputs during the entire flight.

69. **Attitude (ATT) versus Tactical Mode (TAC).** Apart from the differences in trimming function between ATT and TAC Mode, there is no difference in mechanical controllability of the aircraft in either mode. As a fly-by-wire aircraft, AAP states in their report (Reference I) that the time lag from Intermediate Transmission Unit to actuators is less than 45 milliseconds. From a piloting point of view, this time lag has no effect on the intended trajectory of the aircraft; therefore, the aircraft's response was timely and correct to all pilot control inputs.

CONCLUSION

70. This technical report details the analysis of A40-040's wreckage and VFDR data to determine the status of the aircraft's major systems including engines, gearboxes, main and tail rotor transmissions, and flight control systems throughout the flight and at impact. The technical investigation also analysed the aircraft's attitude at impact as a means of comparison with VFDR data and input into the Operational LOE. DFSB sought independent analysis and reports from DSTG, AAP and NHI as a means to validate and verify the conclusions and findings of the Technical LOE.

71. Examination of the wreckage did not indicate any pre-existing airframe or major system damage or malfunction throughout the flight or prior to impact. Analysis of VFDR data and damage to main rotor blades, gearboxes, transmissions and engines indicates that all major aircraft systems were operating and serviceable at impact. There was no evidence to suggest any anomalies of the FCS between pilot control input and aircraft flight control output during the flight.

72. Analysis of the wreckage and VFDR data indicates the aircraft impacted the water at approximately 130 KIAS and 20° nose down in a left-hand angle of bank, with pilot cyclic control inputs commanding a pull up and roll to the left. Of note, the Preliminary Report indicated that the aircraft may have impacted the water in a right-hand angle of bank. However, the ASIT has since determined the last record of aircraft attitude sampled by the CSMU was more than likely just prior to impact while the aircraft was rolling to the left, which explains the discrepancy.

73. Through thorough analysis within the scope of the investigation, the ASIT could not find evidence that the aircraft was unserviceable prior to impact.

Released by:

David SMITH 12 Digitally signed by David SMITH 12 Date: 2025.03.28 07:19:55 +11'00'

D Smith
GPCAPT
Officer-in-Charge

Aviation Safety
Investigation Team

References:

A. ASR DEFEV2371190 – *BSMN83 Collision with Terrain*

B. ARMY MAO-AM DIRECTIVE 04/2023 – *Appointment of an Aviation Safety Investigation Team for the Ditching of an MRH-90 Taipan on 28 July 2023*

C. DFSB Aviation Safety Investigation Team Preliminary Report – *MRH-90 (A40-040) Collision with Terrain – Whitsunday Islands, QLD 28 July 2023*, of 29 Aug 23

D. Defence Science and Technology Group – *DSTG-CR-2024-0011 – MRH-90 A40-040 Accident – DSTG Assessment of Recovered Wreckage at HMAS Harman,* of May 24

E. NHIndustries – *EQAI-017-2023-v1.1 TAU040 FDR Factual Report Final*, of Sep 23

F. AAP – *A40-ER-004376 Rev A A40-040 Aircraft Data Analysis*, of Sep 23

G. Defence Science and Technology Group – *MRH90 A40-040 Collision with Terrain 28 July 2023- DSTG Preliminary Review of Flight Data*, of Sep 23

H. Aeronautical Life Support Logistics Management Unit – ALSLMU Investigation into Recovered Aeronautical Life Support Equipment MRH-90 Taipan (A40-040) Accident, of 28 July 2023

I. Defence Science and Technology Group – *DSTG-CR-2024-0020 – MRH-90 A40-040 Survivability Report*, *of Oct 24*

ENCLOSURE 3

DSTG MRH90 A40-040 Collision With Terrain 28 July 2023 - DSTG Preliminary Review of Flight Data dated 06 Sep 23

Australian Government
Department of Defence
Defence Science and Technology Group

ENCLOSURE 3 TO BP44206784

Minute

DPN Objective Reference: [redacted]

[redacted] Deputy Director – Investigation-In-Charge, DFSB

For information:
Dr Greg Bain, Acting Chief Platforms Division, DSTG
Dr Ninh Duong, Chief Maritime Division, DSTG
Mr Nicolas Athiniotis, Forensics Team Principal, DSTG

MRH90 A40-040 COLLISION WITH TERRAIN 28 JULY 2023 - DSTG PRELIMINARY REVIEW OF FLIGHT DATA

References:

A. [redacted] DFSB Minute: Request for DSTG assistance in support of DFSB Aviation Safety Investigation into MRH-90 A40-040 Collision With Terrain 28 July 2023.
B. A40-029 Parameter Listing.csv
C. A40-006 Parameter Listing.csv
D. A40-040 Parameter Listing.csv
E. A40-008 Parameter Listing#1.csv

1. DSTG was requested by DFSB to carry out a forensic examination of the data downloaded from MRH90 A40-040's Voice and Flight Data Recorder (VFDR) to enable a comparison with DFSB's initial data analysis and provide the forensic level detail required to complete the investigation [A].

2. DSTG has created a preliminary replay of the four MRH90 helicopters involved in the accident flight, utilising the CSV datasets provided by DFSB (B, C. D and E). Note that the CSV file format is a reduced set of data channels that exists on the binary flight data recording format available on the MRH90 aircraft. Numerous fault codes, flight control system parameters and engine and drive train monitoring parameters have not been provided in the CSV file and therefore have not been analysed by DSTG at this stage.

3. DSTG has analysed, in particular, the flight of the accident aircraft up to the time it impacts the water near Hamilton Island. A timeline is provided in the Enclosure. Key points of the timeline are:

a. Aircraft A40-040 was Aircraft 3 of the four aircraft formation, and appears to fly and respond normally to pilot inputs up to approximately 55 seconds before impacting the water.

b. From approximately 55 seconds before impact with the water, the flight data indicates the aircraft has a lateral acceleration and begins to drift to the right during a turn to the left. There is pilot input of pedal that is noticeably different to the other aircraft in the formation which continues almost until the end of the flight. The flight path of A40-040 shows that it began to deviate from its lateral position in the formation and may indicate a difficulty in maintaining lateral station/location in the formation. After the turn is complete, A40-040 performs a moderate climb above the formation, with a corresponding increasing airspeed before significant banking and pitching motions occur. From there, the aircraft then rapidly descends and impacts the water. The flight data suggests the pilot(s) had control of the aircraft with it responding to inputs to throttle, collective and cyclic pitch and roll until impact. The pilot's ability to fully control motion of the yaw axis with the pedals, and the aircraft's ability to respond exactly or appropriately in yaw is yet to be determined.

c. At approximately 17 seconds before impact with the water, when the aircraft climbs out of formation, it climbs approximately 150 ft. above Aircraft 1 and 2. There follows the cyclic lateral inputs resulting in the aircraft rolling left and right, followed by increasing airspeed with increasing collective and forward cyclic (pitch down) inputs. These manoeuvres may possibility relate to the pilot attempting to determine relative proximity to Aircraft 1 and Aircraft 2 in front, but could be explained by other reasons. Importantly during this time, A40-040 is gradually closing the separating distance with Aircraft 1 and Aircraft 2 at the front of the formation.

d. At Universal Time Coordinated (UTC) 12:36:25, A40-040 impacts the water with considerable airspeed, likely to be greater than 130 knots indicated airspeed, and with an increasing and very high descent rate, greater than 5000 ft/minute just prior to impact. The aircraft impacts the water with greater than 20 degrees pitch down, a bank angle of 30 degrees (right) and considerable lateral acceleration indicating the presence of sideslip. The last data recording shows a significant forward input on the cyclic despite there being significant forward speed and a very high vertical speed downwards. The engines are operating under high torque and collective at the time of impact. Just prior to impact with the water and during the descent, Aircraft 3 is momentarily abeam Aircraft 2, and passes at a distance estimated by DSTG as 90 ft. laterally.

4. Although the aircraft appears to be responding appropriately to pilot inputs at least on the collective, throttle, cyclic forward, back, left and right, the increasing speed well above that of the rest of the formation, as well as the considerable control inputs in roll and pitch prior to the impact with the water suggest several potential lines of enquiry which include but are not limited to:

a. Significant loss of situational awareness, i.e. impairment of the pilots' ability to comprehend the position of other aircraft in the formation, the aircraft's speed and vertical descent rate, as well as its longitudinal and lateral attitude prior to impact with the water.

b. Significant pilot distraction due perceived or real events in the cockpit or occurring to the aircraft, such as warnings and cautions or due to mechanical or other system failures

c. An inability of the pilot or the aircraft to respond to the changing flight conditions appropriately or as intended.

Please feel free to make contact to discuss any aspects detailed herein,

Regards,

Mr Michael Grant Grant, Michael Digitally signed by Grant, Michael Date: 2023.09.06 18:44:11 +10'00'

Senior Researcher Platform Systems, DSTG
506 Lorimer Street Port Melbourne, Victoria 3207
[redacted]

06/09/2023

3

Enclosure:
Timeline of flight of MRH90 A40-040 aircraft on 28/07/2023

Enclosure

Timeline of flight of MRH90 A40-040 on 28/07/2023

Note all times are in Universal Time Coordinated (UTC), which is +10 hours Australian Eastern Standard Time (AEST).

First Valid Time Step on the CSV file is 9:54:22 UTC.

Aircraft 3 is operating on the ground with engine running, however no noticeable change of position, i.e., latitude, longitude, or altitude recorded.

At 11.45:40 weight on-wheels indication turns false; Aircraft 3 begins to hover at 30-35 ft.

At 11:47:37 weight on-wheels indication turns true, Aircraft 3 still in same latitude and longitude location, but is now back on the ground.

Between 11:47:37 and 11:52:25 Aircraft 3 remains on the ground and is at one point refueled on the ground while the engine remains running.

At 11:52:25 weight on-wheels indication turns false; Aircraft 3 begins a hover again at an altitude of 30-50 ft.

At 11:54:07 weight on-wheels indication turns true, Aircraft 3 still in same latitude and longitude location and on the ground with engines running.

At 12:14:12 weight on-wheels indication turns false; Aircraft 3 takes off and begins the accident flight.

Aircraft 3 climbs and then cruises in formation with another three MRH90 aircraft at low altitude (<500ft) to an area near Hamilton Island and Lindeman Island and begins to perform a racetrack pattern.

Indications of Aircraft 3 appear normal for most of the flight. It may or may not be noteworthy, but some indications appear true continuously throughout all of the accident flight and have been observed on other aircraft in the flight. The indications are

Hydraulic Pump 2 Pressure Low (A)

Hydraulic Pump 1 Pressure Low (A)

Hydraulic Elec Pump Temp high (A)

Landing Gear Pressure low 1

The significance of these warnings has not been assessed at this point.

First noteworthy occurrence is at 12:35:30, or about 55 seconds before the last quality data point captured on the CSV file which is assumed to be the approximate time of accident. There is an abrupt change in the pedal input. It occurs at or just prior to the beginning of the second turn of the racetrack pattern. It is significant because of the noticeable difference to the amount of pedal input when compared to the other aircraft at this time and is also a noticeably different pedal input to the accident aircraft’s first turn of the racetrack. It is also significant as the pedal input is not transient and is present and distinctly different to the other three aircraft for nearly the entire period until Aircraft 3 impacts the water. Only three seconds prior to impact with the water does the rudder pedal input for Aircraft 3 return to similarity with the other aircraft in the formation, however by then Aircraft 3 has considerable pitch and is descending towards the water at 2000-3000 ft/min.

5

Figure 1 shows the pedal input as recorded for all four aircraft for the entire flight up to the time Aircraft 3 is assumed to impact the water.

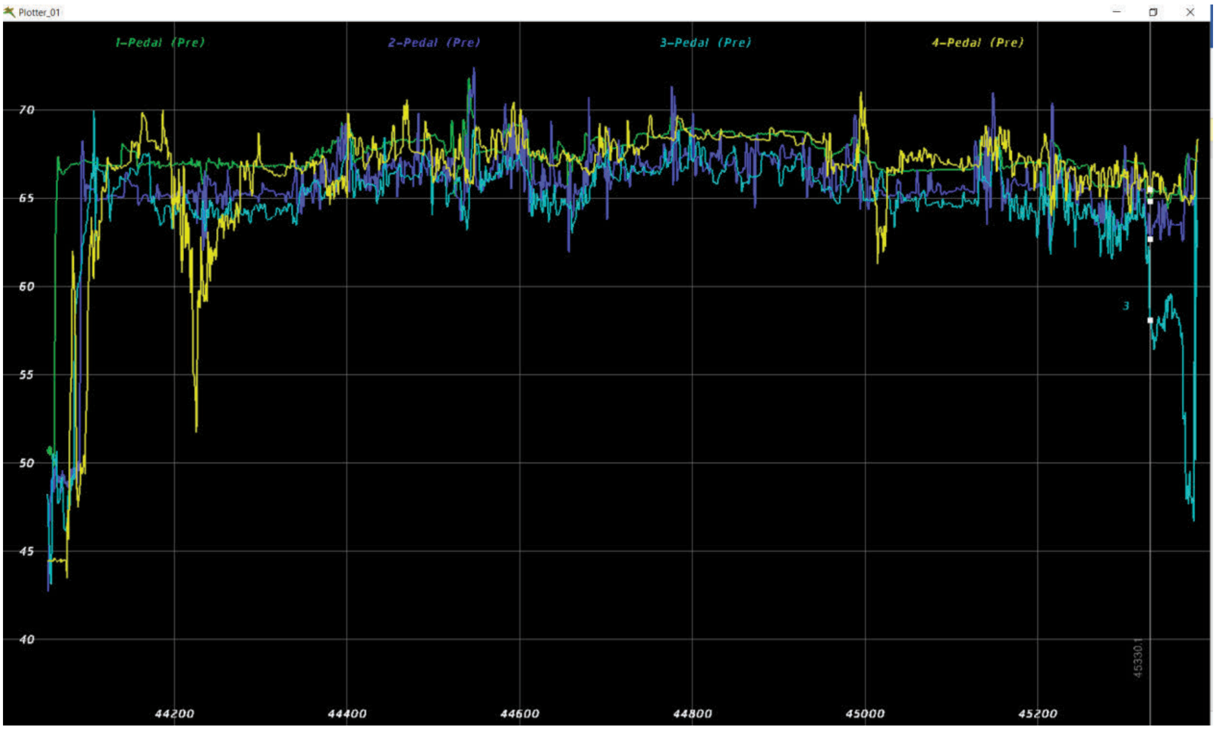

Figure 1 - Pedal Inputs of all MRH90 aircraft in the Formation on 28/07/2023. Aircraft 3 is in cyan and the white vertical trace marks the beginning of abrupt pedal input.

There is a need to define the pedal input as recorded as either being pilot only input or pilot input plus some contribution from the trim or other augmentation by systems associated with the aircraft's flight control system. However different pedal input is used and becomes more significantly different relative to the other aircraft in the formation, up until just prior to impact when the pedal becomes more in line with that of the other aircraft.

At this time of 12:35:30 there is a peak response of yaw rate and the pedal input to the actuation control channel [redacted], in response to the increased pedal. This means that the aircraft is responding to the pedal input and which may result in the aircraft taking up a sideslip and having a lateral acceleration (This require further analysis). The lateral acceleration is present and increasing up to the time of the accident and is different to that of the other aircraft in the formation. This indicates sideslip was present up to the time Aircraft 3 impacts the water.

At 12:35:36 the aircraft are continuing their second turn of the racetrack and Aircraft 3 appears to either be no longer able to maintain the same position it has held for nearly all the flight or alternatively this may possibly be a commanded or intentional change by the pilot(s) of Aircraft 3. The position of Aircraft 3 in the formation hitherto, was relatively in longitudinal alignment with the lead aircraft (Aircraft 1), albeit slightly left of the lead aircraft's flight path. Aircraft 3's position relative to the rest of the formation is best shown in the image below, Figure 2, which is a ground map view of the formation's flight path. Aircraft 3 (in cyan) has for nearly all the flight has been behind and to the left of Aircraft 1 (Green) and considerably more left of Aircraft 2 (Blue). Aircraft 4 (Yellow) is on the far left side of the entire formation.

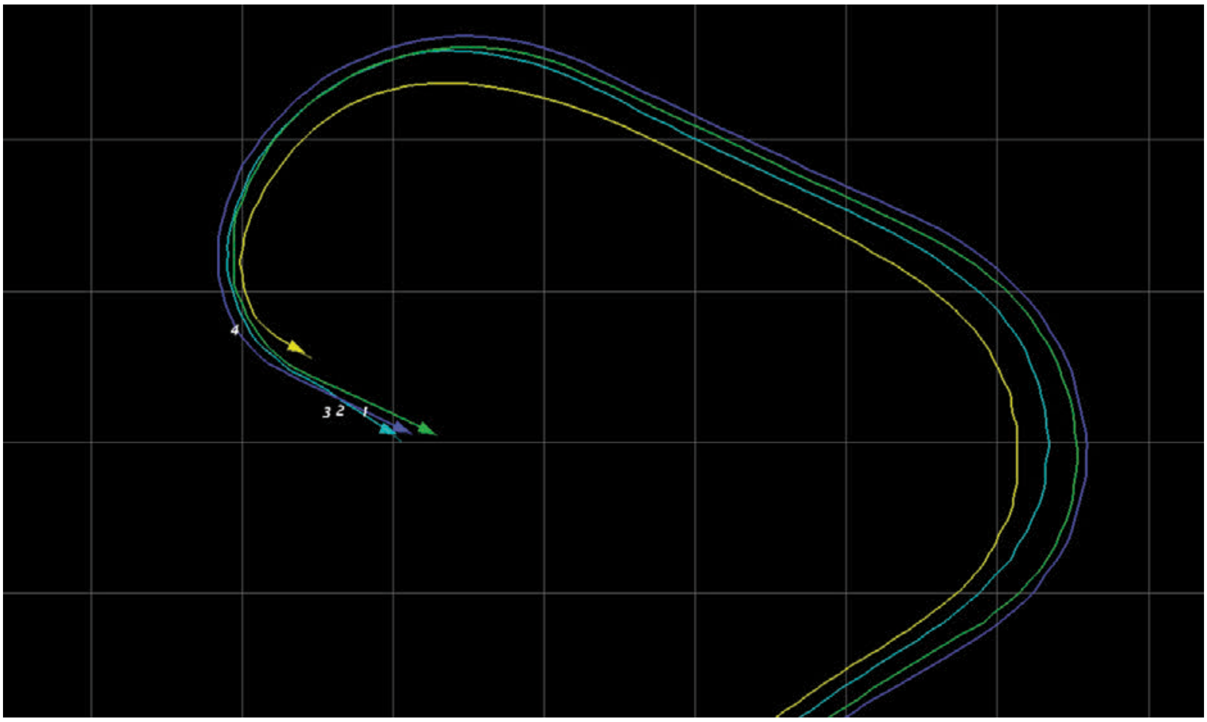

Figure 2 - Flight path over the ground plane of all aircraft in the formation on 28/07/2023.

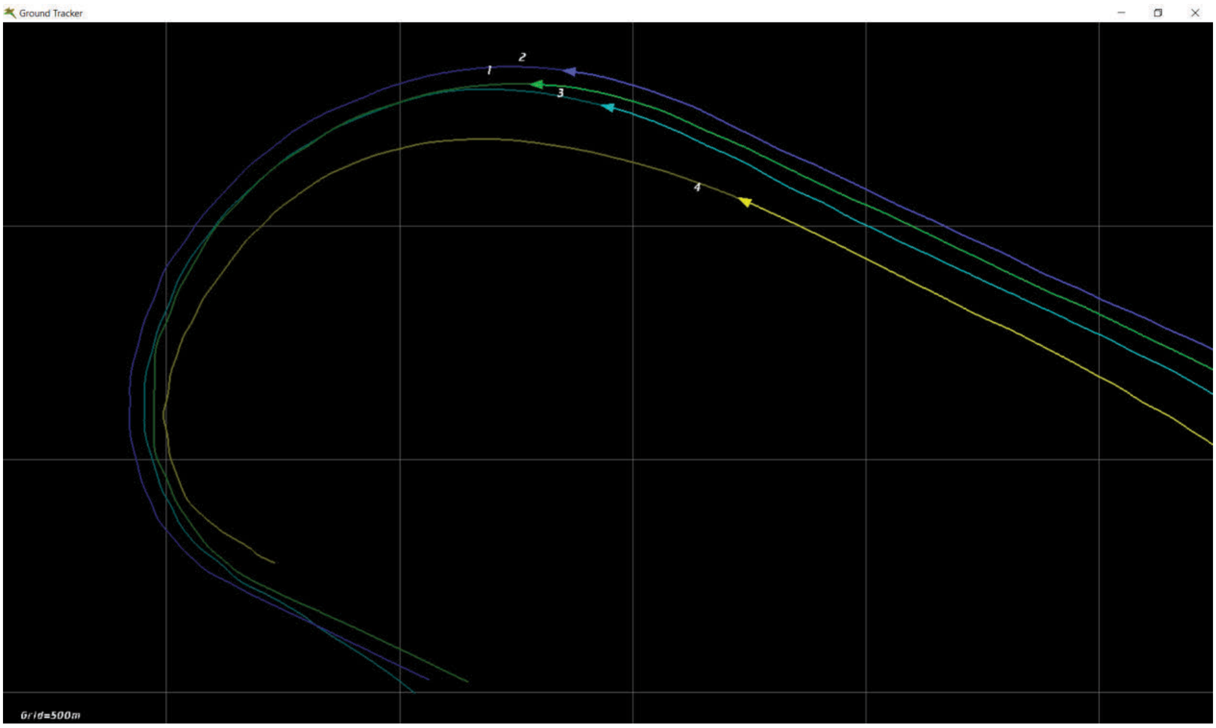

Figure 3 - Close up of flight path over ground plane of all aircraft in the formation on 28/07/2023. Note Aircraft 3's flight path (in Cyan) begins to drift right in the second turn of the racetrack. The drift continues throughout the turn such that both Aircraft 3's flightpath, which for most of the flight has remained to the left of both Aircraft 1 and 2's flight path, will eventually be off to the right of Aircraft 1 and Aircraft 2's flight path. Aircraft 3 is the only aircraft to break with the formation for the entire flight up until the time it impacts the water.

In Figure 3, it can be seen that during the second turn Aircraft 3 crosses Aircraft 1's flight path from behind and from left to right, such that it is now following Aircraft 1's flight path during the turn. Aircraft 3 is using less bank angle than the Aircraft 1 and Aircraft 2 in the turn. Aircraft 3 maintains the noticeable difference in pedal and lateral acceleration previously mentioned indicating the presence of sideslip in the turn.

7

At 12:36:08, Aircraft 1 and Aircraft 2 have completed turn 2 of the racetrack and Aircraft 3 is also just completing the turn. With a change in collective, Aircraft 3 begins to climb out of the formation. This may have been a commanded climb by the pilot(s) of Aircraft 3 in order to maintain safe separation from Aircraft 2 or for some other reason. One possible scenario here is that due to the sideslip of Aircraft 3 and its effect of a reduced bank angle in the turn, Aircraft 2 with more bank angle and tightening its turn due to a momentary speed increase, is perceived as being on a convergent course by the pilot(s) of Aircraft 3. Aircraft 2 has momentarily increased speed at this time, relative to the rest of the formation, and its flight path is seen crossing in front of Aircraft 3 just prior to the initiation of the climb, see Figure 4. Note Aircraft 3's slight drift or change of position in the formation towards the outside of the second turn in the racetrack may have all contributed to a perception of the pilot(s) of Aircraft 3 that Aircraft 2 was sufficiently close as to warrant some evasive action. However there are also many alternate possibilities to explain the climb at this time which could include the pilot responding to some other event or issue in or outside the cockpit. Note that the separation distance between Aircraft 2 and Aircraft 3 has typically been 300-400 ft. during the racetrack. At the time of Aircraft 3 initiating the climb, separation is 350 ft. between the two aircraft, suggesting a possible perception by the pilot(s) of Aircraft 3 rather than an actual reduction in safe separation between the aircraft, may have been the reason for Aircraft 3's climb.

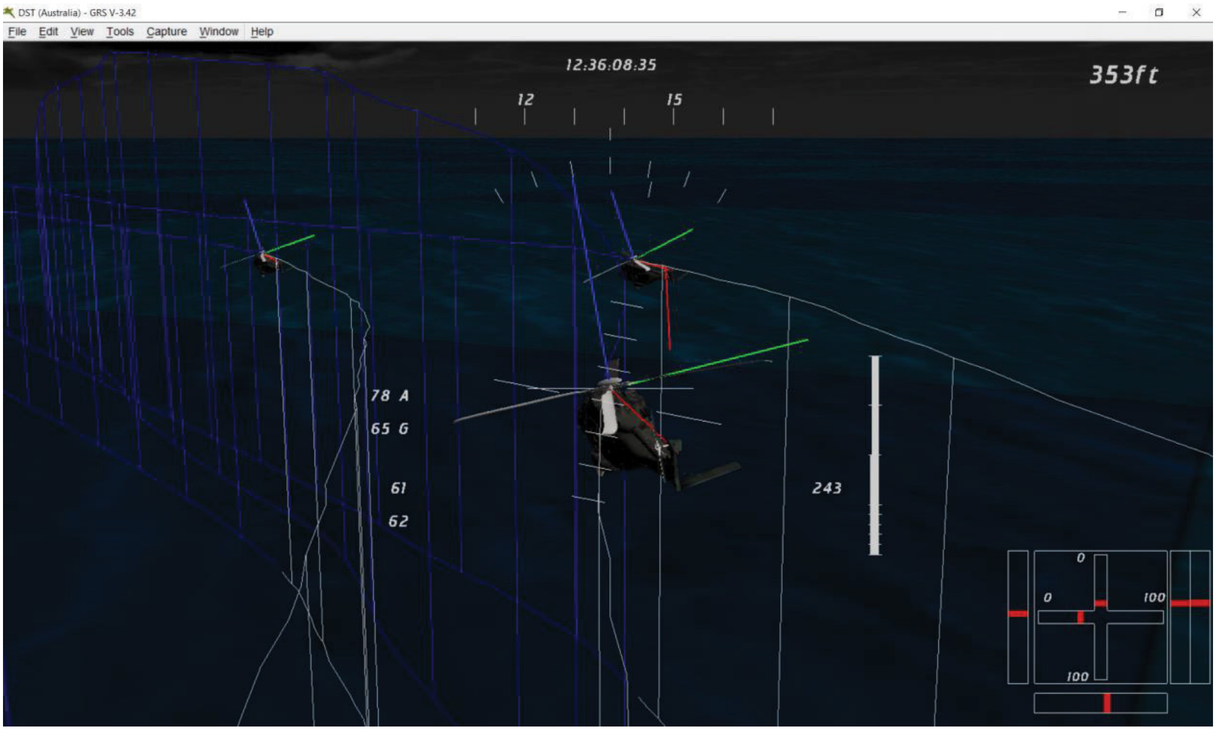

Figure 4 - Time 12:36:08 just prior to when Aircraft begins a climb out of formation

At 12:36:13, Aircraft 1, 2 and 3 have now completed turn 2 of the racetrack. Aircraft 3 is now above the formation at a radar altitude of 306 ft., about 100 ft. above the rest of the formation. Separation between Aircraft 2 and Aircraft 3 is 350 ft. Figure 5 shows image of the first three aircraft at this time. Note between 12:36:13 and 12:36:19, the pilot(s) roll first left 30 degrees and then right 45 degrees, a possible scenario is that this is an attempt to identify the locations of the first two aircraft in the formation again to ensure safe separation, prior to an attempt to descend and re-enter the formation. However, there are also many alternate possibilities to explain the behavior, e.g. a check of controls or control responsiveness.

8

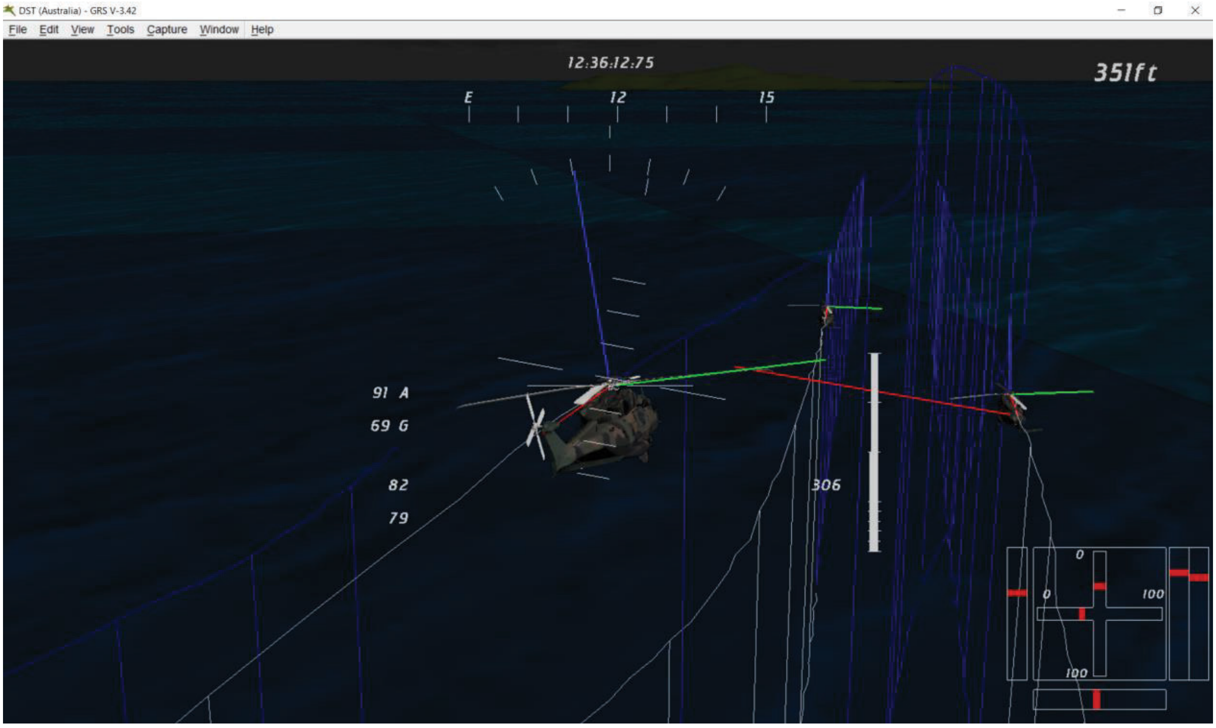

Figure 5 - Formation at time 12:36:13

At 12:36:15, Aircraft 3 is at a radar altitude of 332 ft., while all other aircraft in the formation remain at approximately 200 ft. altitude. Aircraft 3 begins to level out of the climb but is also considerably higher in airspeed with 92 knots indicated. This is in comparison to Aircraft 1 and Aircraft 2 which are cruising in straight line at approximately 80 knots. The increase in the airspeed of Aircraft 3 is likely the result of the collective and torque remaining high despite Aircraft 3 levelling out. Separation between Aircraft 2 and Aircraft 3 is 360 ft. Figure 6 shows image of the first three aircraft of the formation at this time.

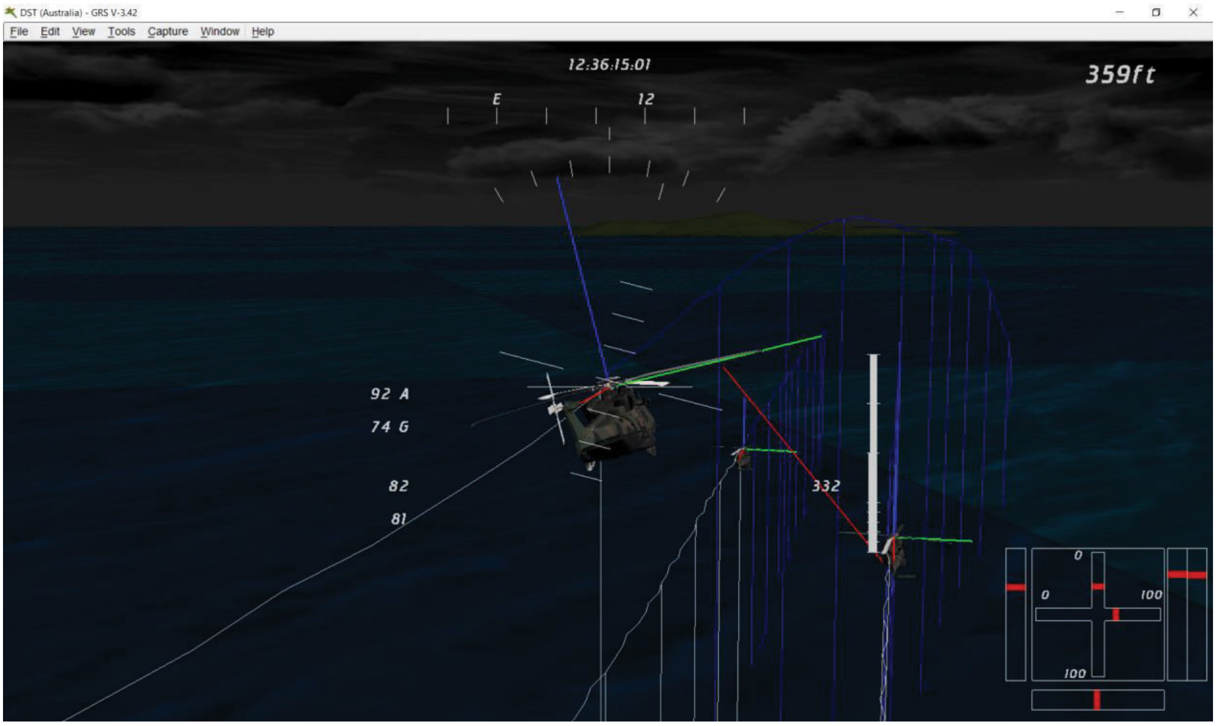

Figure 6 - Formation at time 12:36:15

At 12:36:16, Aircraft 3 rolls back and is momentarily straight and level at 94 knots indicated and 342 radar altitude. The aircraft then rolls to 20 degrees right, airspeed is increasing, sideslip is still to the left. Cyclic is forward and collective and torque are high which explains why airspeed is still increasing. Separation between Aircraft 2 and Aircraft 3 is 330 ft. and reducing.

At 12:36:17, Aircraft 3 is almost 30 degrees right roll, speed is now above 100 knots indicated and altitude is approximately 350 ft. Separation between Aircraft 2 and Aircraft 3 is 317 ft. See Figure 7.

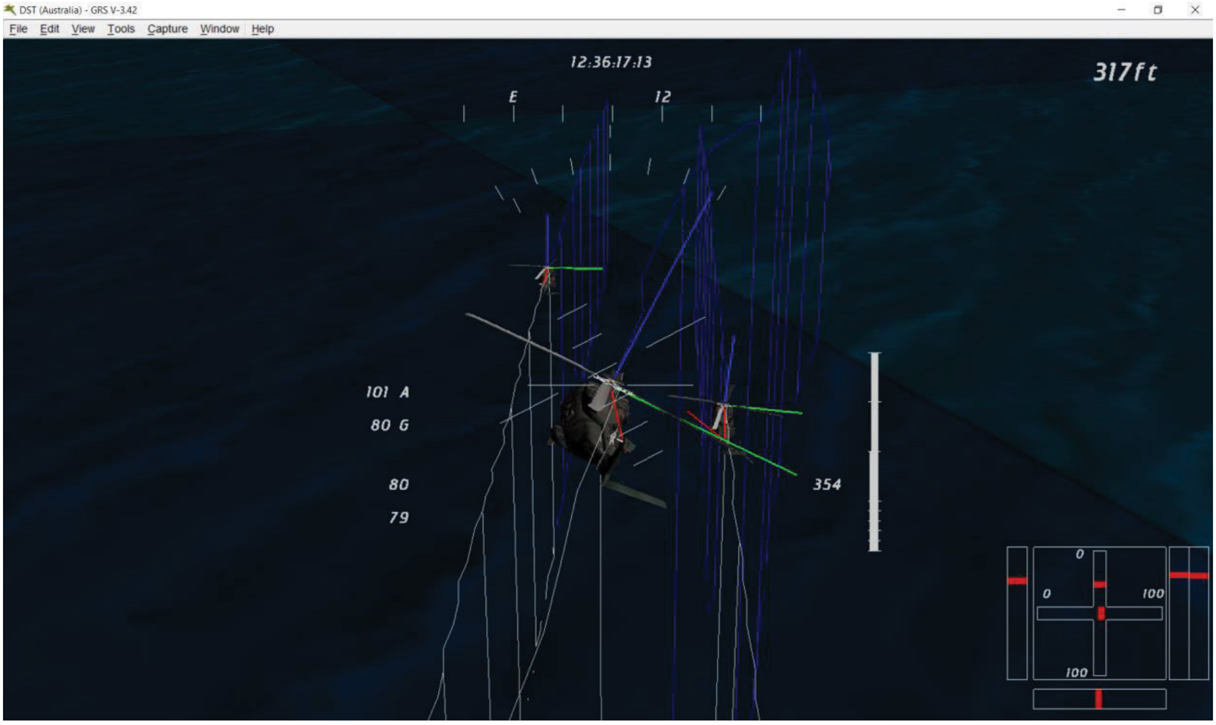

Figure 7 - Formation at time 12:36:17

At 12:36:19, Aircraft 3's flight path has crossed over Aircraft 2. Separation between Aircraft 2 and Aircraft 3 is now 272 ft. Aircraft 2's radar altitude is 218 ft. while Aircraft 3 is at 356 ft. radar altitude. Relative to Aircraft 2, Aircraft 3 has considerably more collective and torque, resulting in Aircraft 2 now having an airspeed of 111 knots indicated, while Aircraft 2 is still at typical formation speed of 74 knots indicated. Aircraft 3 although 150 ft. above Aircraft 2 is approaching from the rear. See Figure 8.

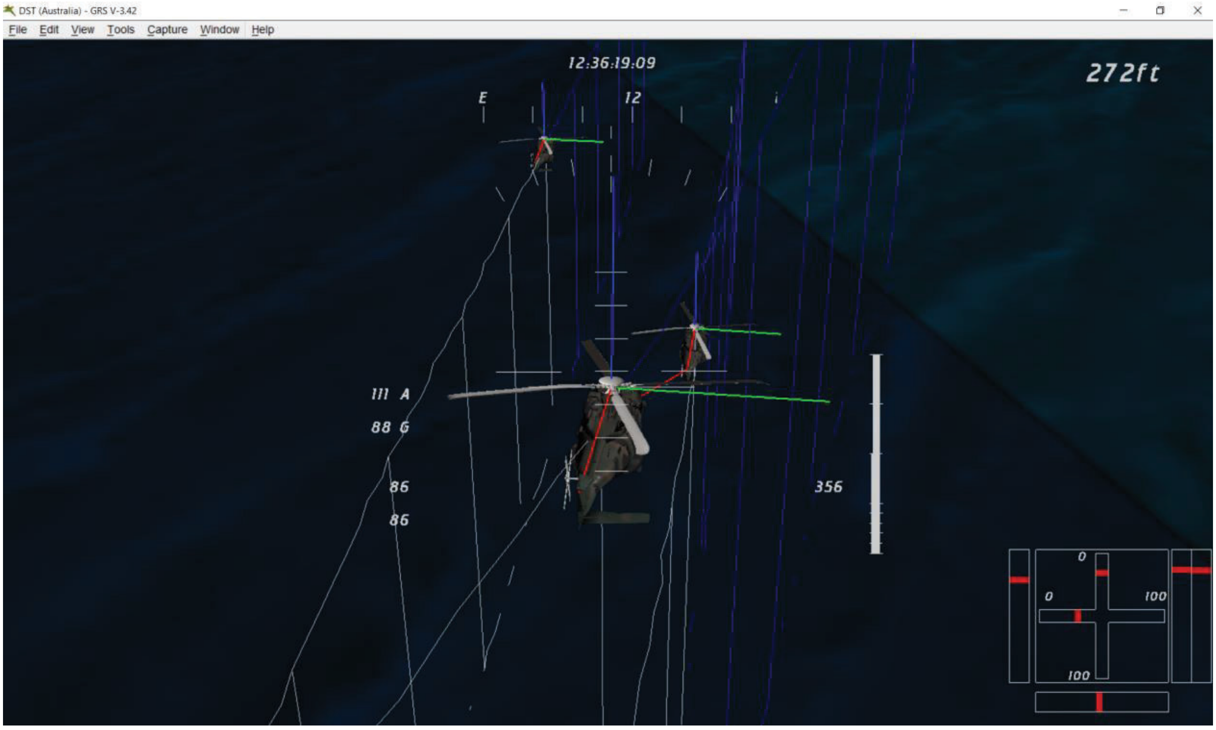

Figure 8 - Formation at time 12:36:19

At 12:36:20 the Aircraft is straight and level momentarily at 350 ft. radar altitude and at 107 knots indicated airspeed. Aircraft 3 is drifting to right of formation and Aircraft 3’s flight path is now right of Aircraft 2’s flight path. Aircraft 3’s collective and torque remains high but pedal is more centered. Pitch which has been somewhat constant between 4-6 degrees down is now 10 degrees down due to maximum forward cyclic input from the pilot. Aircraft 3 begins to descend at rate of 500 ft/minute. Separation between Aircraft 2 and Aircraft 3 is now 234 ft. See Figure 9.

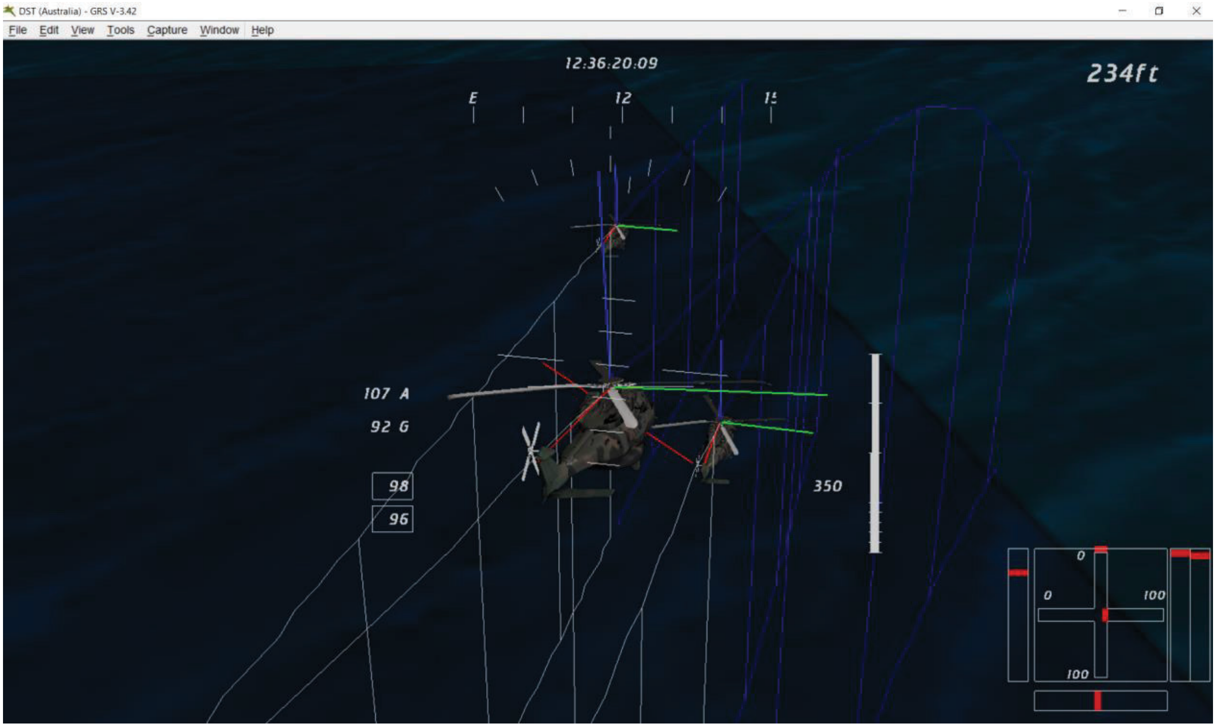

Figure 9 - Formation at time 12:36:20

11

At 12:36:21 the nose of Aircraft 3 pitches down 17 degrees, cyclic is near fully forward suggesting pitch down is responding to pilot input to pitch down. The angle of bank is 10 degrees right, speed is increasing to 115 knots indicated. Note collective is high. Aircraft is at 344 feet radar altitude but vertical speed down is now increasing from 780-1700 ft/minute. Cyclic is almost fully forward. Separation between Aircraft 2 and Aircraft 3 is now 195 ft.   See Figure 10.

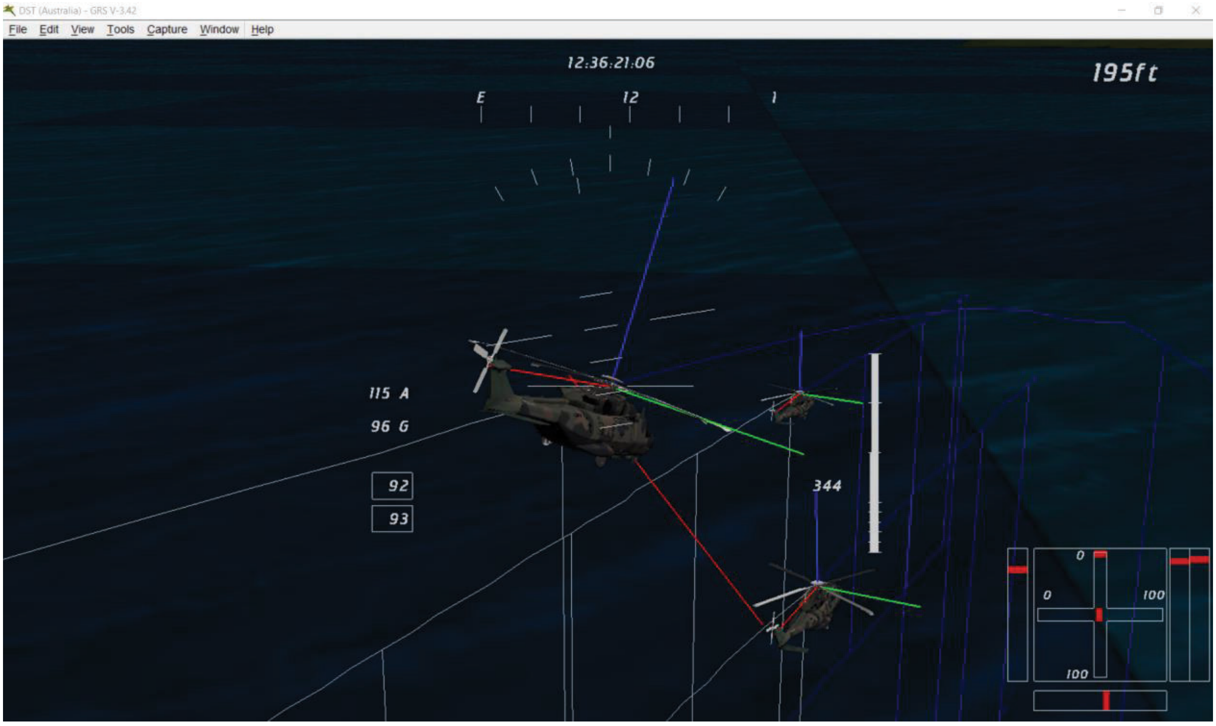

Figure 10 - Formation at time 12:36:21

At 12:36:22 the angle of bank is temporarily greater than 45 degrees right, Aircraft 3 is pitching down at over 25 degrees, the collective is high, and airspeed is 129 knots indicated, radar altitude is 331 ft. Separation between Aircraft 2 and Aircraft 3 is now 158 ft.   See Figure 11.

12

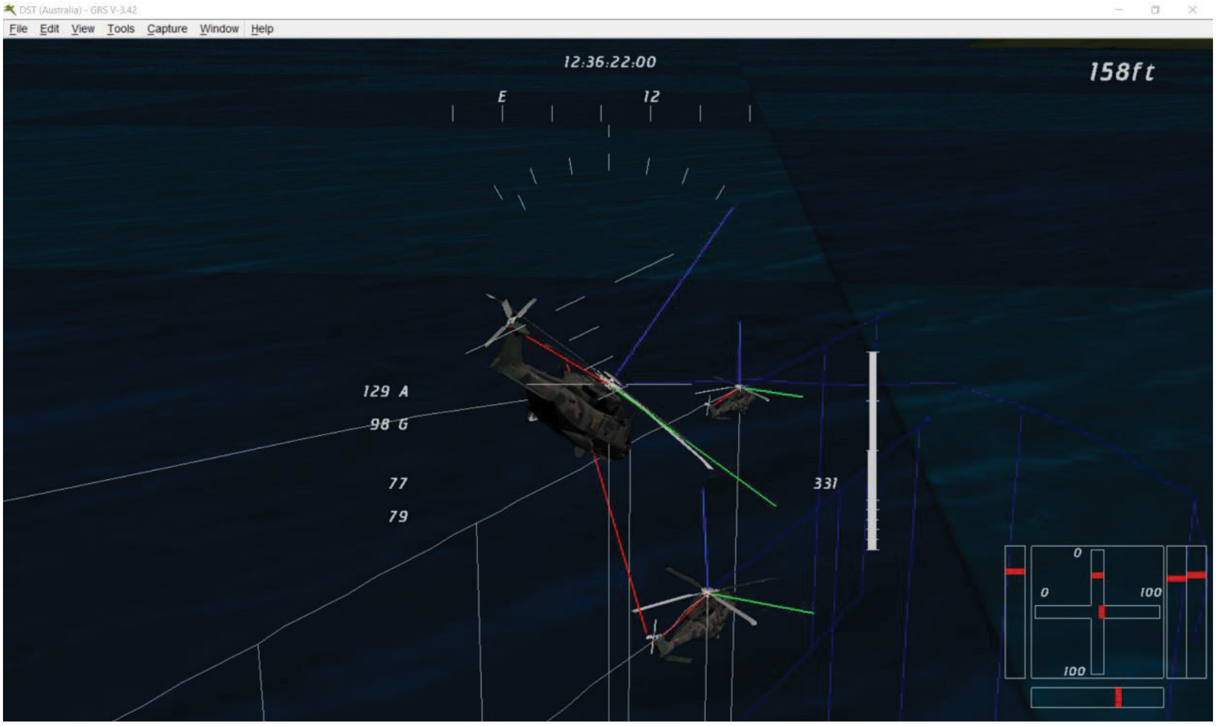

Figure 11 - Formation at time 12:36:22

At 12:36:23 the angle of bank is 41-43 degrees right, pitch is still 25 degrees down, the collective is high, airspeed is 126 knots indicated, radar altitude is 290 ft. Just prior to this time, the cyclic is only momentarily moved back almost to the centre, however it is then moved full forward again. Master Red Control Light activated at 12:36:23 and remains on till end of recording. Separation between Aircraft 2 and Aircraft 3 is now 115 ft. See Figure 12.

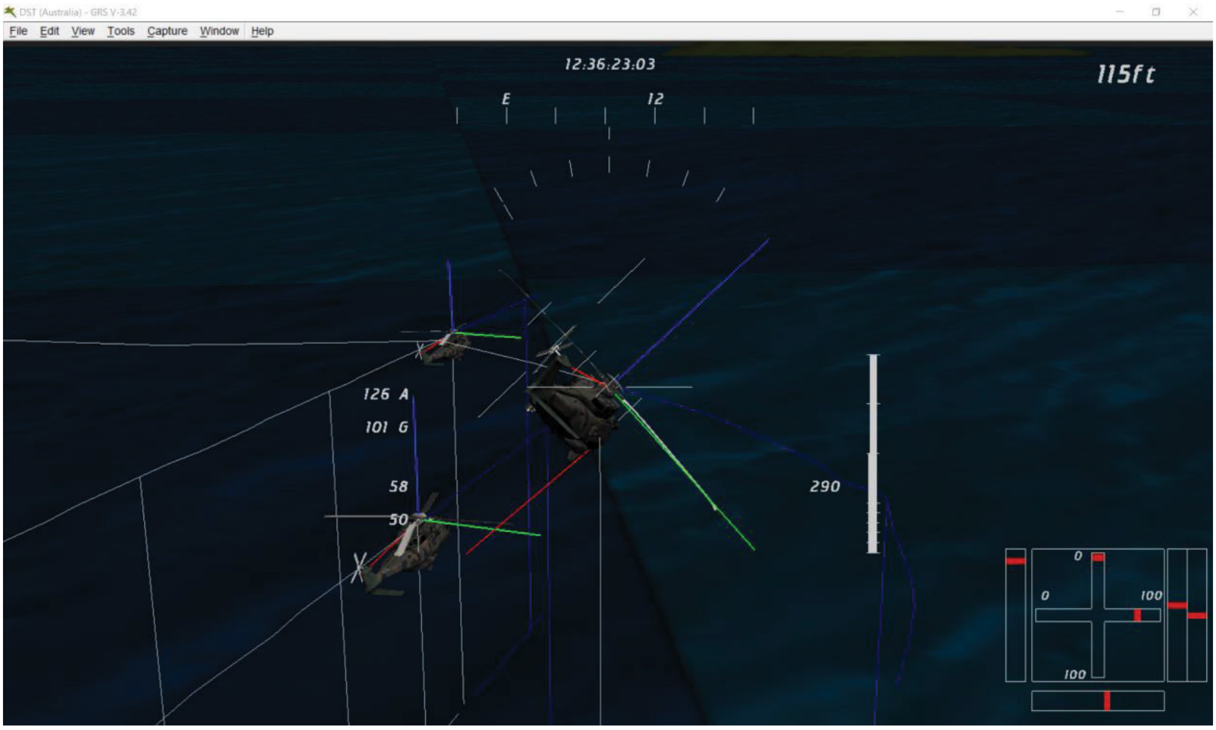

Figure 12 - Formation at time 12:36:23

At 12:36:24 Aircraft 3 is in descent passing through the altitude at which the rest of the formation is or approximately 200 ft. radar altitude. Aircraft 3 due to its significantly higher speed over the past

10 seconds is now almost abeam Aircraft 2. The miss distance between Aircraft 2 and Aircraft 3 is estimated by DSTG at this time to be approximately 90 ft. Aircraft 3 is at 137 knots indicated airspeed, has vertical speed of approximately 4,500 ft/min. Aircraft 3 is pitching 20 degrees down and bank angle is 45 degrees to the right. See Figure 13.

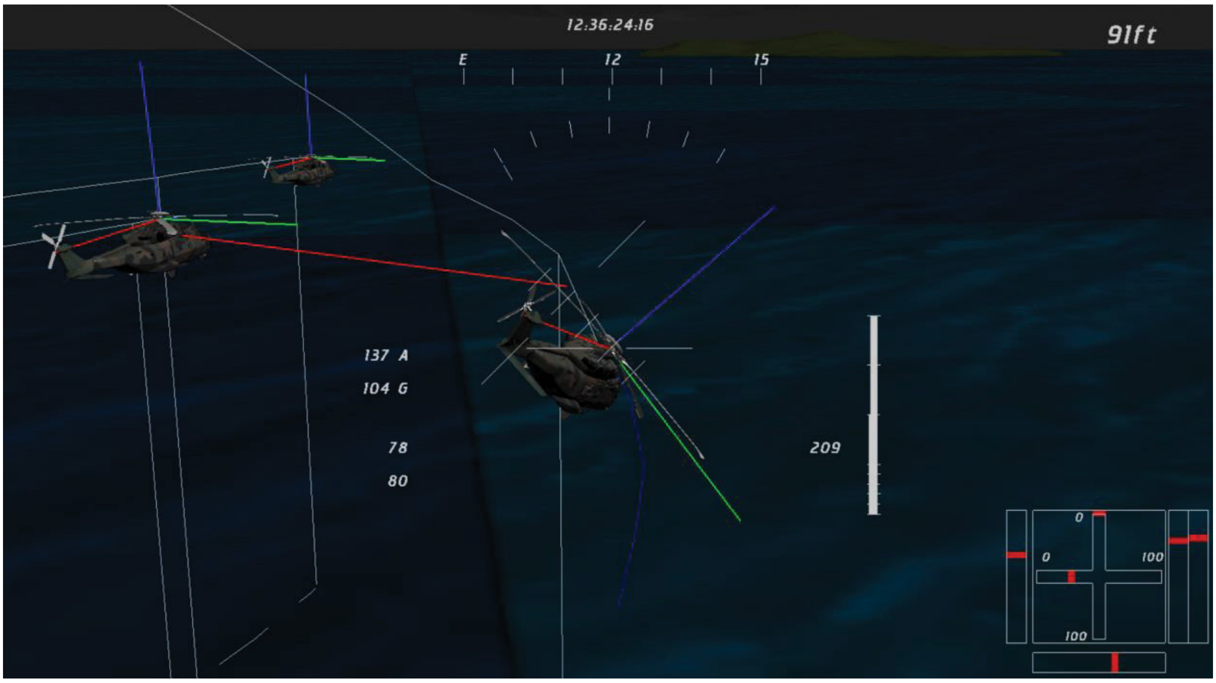

Figure 13 - Formation at time 12:36:24

Last quality data point of the CSV data is 12:36:25, 134 KIAS, vertical Speed 5,197 ft/min (down) Radar Altitude 157 ft. Pitch 23 degrees down, roll 31 degrees right. Within the next one second, Aircraft 3 impacts the water and flight data begins to corrupt, making any further analysis difficult. Figure 14 below is the last frame from DSTG's replay of the accident flight.

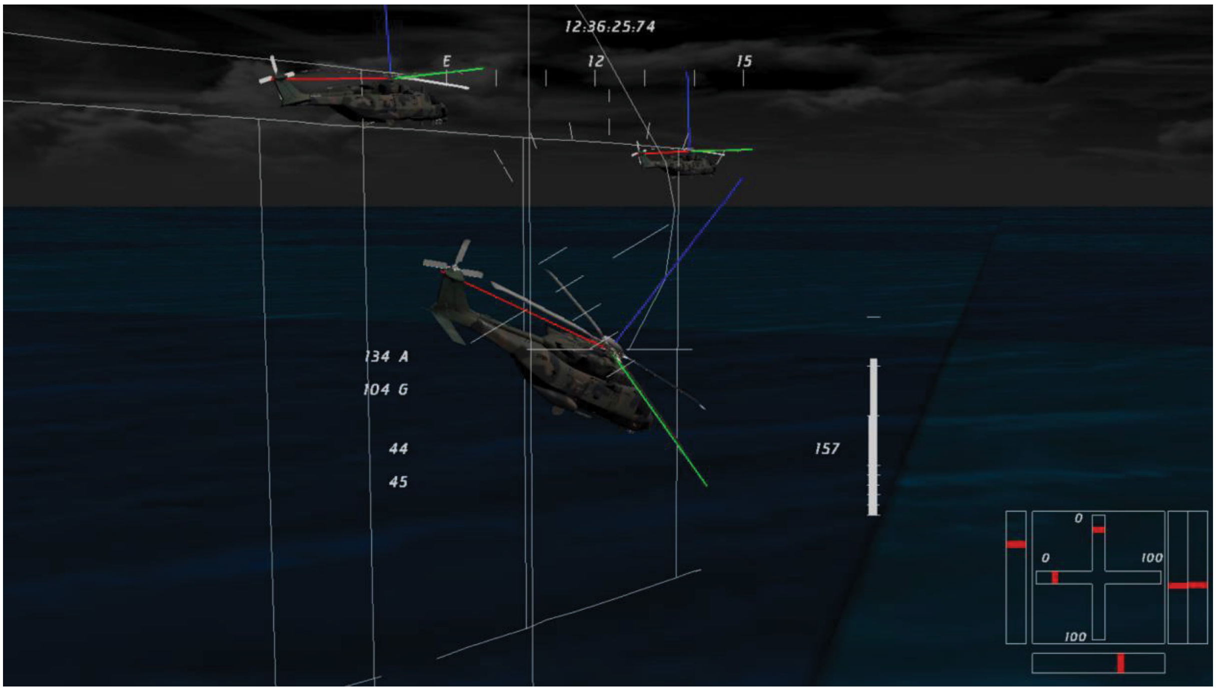

Figure 14 –Last quality data point from Aircraft CSV data. Time is almost 12:36:25.

ENCLOSURE 7

DSTG MRH-90 A40-040 Collision With Terrain 28 July 2023 – Miss Distance Calculation from DSTG Preliminary Review of Flight Data

Australian Government
Department of Defence
Defence Science and Technology Group

ENCLOSURE 7 TO BP44206784

Minute

DPN Objective Reference: [redacted]

[redacted] Deputy Director – Investigation, DFSB

For information:
Dr Greg Bain, Acting Chief Platforms Division, DSTG
Dr Ninh Duong, Chief Maritime Division, DSTG
Mr Nicholas Athiniotis, Forensics Team Principal, DSTG

MRH90 A40-040 COLLISION WITH TERRAIN 28 JULY 2023 – MISS DISTANCE CALCULATION FROM DSTG PRELIMINARY REVIEW OF FLIGHT DATA

References:

A. [redacted] DSTG Minute – MRH A40-040 COLLISION WITH TERRAIN 28 JULY 2023 – DSTG PRELIMINARY REVIEW OF FLIGHT DATA

B. [redacted] Email: A40-ER-004376 rev A –MRH040 data analysis, dated 7 September 2023

1. In [A], DSTG provided an analysis of the flight data of four MRH90 aircraft involved in the accident flight on 28th July 2023, near Hamilton Island and Lindeman Island in the Whitsundays. In order to support the analysis, DSTG utilised its graphical replay software to animate the flight of the formation using aircraft digital flight data recorder (DFDR) information. In addition, the replay software was used to estimate the separation or miss distance between all aircraft in the formation. Just prior to its impact with the water, Aircraft 3 of the formation passed Aircraft 2 in a rapid descent, passing abeam on a near-parallel course. DSTG estimated that the separation distance between Aircraft 2 and Aircraft 3 at this time was approximately 90 feet [A] which was an estimate of the closest part, or component, of each aircraft to the other. Subsequently, DFSB, in [B] requested DSTG to provide the tolerance of the estimated separation distance quoted in [A].

2. DSTG analysis in [A] was based on a CSV data file which is a subset of the data recorded by the MRH90 DFDR. Given that there is only one source of time provided in the CSV format, and the synchronisation of this time or otherwise between Aircraft 2 and Aircraft 3 is an unknown, the estimate and associated tolerance of the separation distance has been revised to a range of between 82 feet and 147 feet. Importantly, the revised separation distance estimate(s) is now the difference between the GPS locations of Aircraft 2 and Aircraft 3 and does not include any elements of the aircraft geometry which would reduce the separation distance further. This has been done due to the complexities of integrating separately sourced geometric 3D models with DFDR data, in DSTG's graphical replay software.

3. Further analysis in the enclosure provides indicative separation distances between another aircraft pair in the formation. The purpose for inclusion is to provide a qualitative baseline for minimum separation distances observed during the flight. It suggests that the lower bound separation distance of 82 feet between Aircraft 3 and Aircraft 2 just prior to the accident was not significantly less than the lowest recorded separation distance of 101 feet recorded during the same period between Aircraft 1 and Aircraft 2. Further explanatory details are provided in the attached Enclosure.

Please feel free to make contact to discuss any aspects detailed herein,

Regards,

Grant, Michael
Digitally signed by Grant, Michael
Date: 2023.09.14 17:16:01 +10'00'

Mr Michael Grant

Senior Researcher Platform Systems, DSTG
506 Lorimer Street Port Melbourne, Victoria 3207
[redacted]

13/09/2023

Enclosure: Explanatory Details – Miss Distance Estimation

3

Enclosure: Explanatory Details – Miss Distance Estimation

There are three primary sources of error (or tolerances) with regards to the miss distance or separation distance calculation between the MRH90 aircraft within the formation.

1. Individual aircraft GPS position estimation
2. Aircraft Geometry
3. Aircraft Time Estimation.

Each source of error will be detailed separately.

1. Individual aircraft GPS position estimation.

There are numerous potential sources of error relating to the GPS data recorded on the DFDR. Assuming, GPS integrity of at least three satellites and good GPS performance at the time, the accuracy of GPS position is quoted in the MRH90 flight manual as seen in table below:

[redacted]

The CSV dataset provided to DSTG does not provide any indications of the state of GPS performance or satellite coverage shortcomings that would indicate performance degradation greater than that provided in the table above. [redacted] The manufacturers of the GPS equipment on the MRH90 aircraft may provide more informative data than that in the table above. It is anticipated that the combined or relative error between two GPS systems would be considerably lower than the absolute error of a single system as stated above, however that would also be information best provided by the manufacturer of the GPS equipment.

2. Aircraft Geometry

The MRH90 GPS antenna is located on the tail boom as designated by the number 12 in Figure 1 below. Note that the antenna is located at some distance from the centre-of-gravity and is unlikely to be near the inertial navigation reference point of the helicopter. When calculating miss distance the various rotations of the aircraft about the inertial reference point and the difference in location between GPS antenna and the inertial reference point would need to be considered.

4

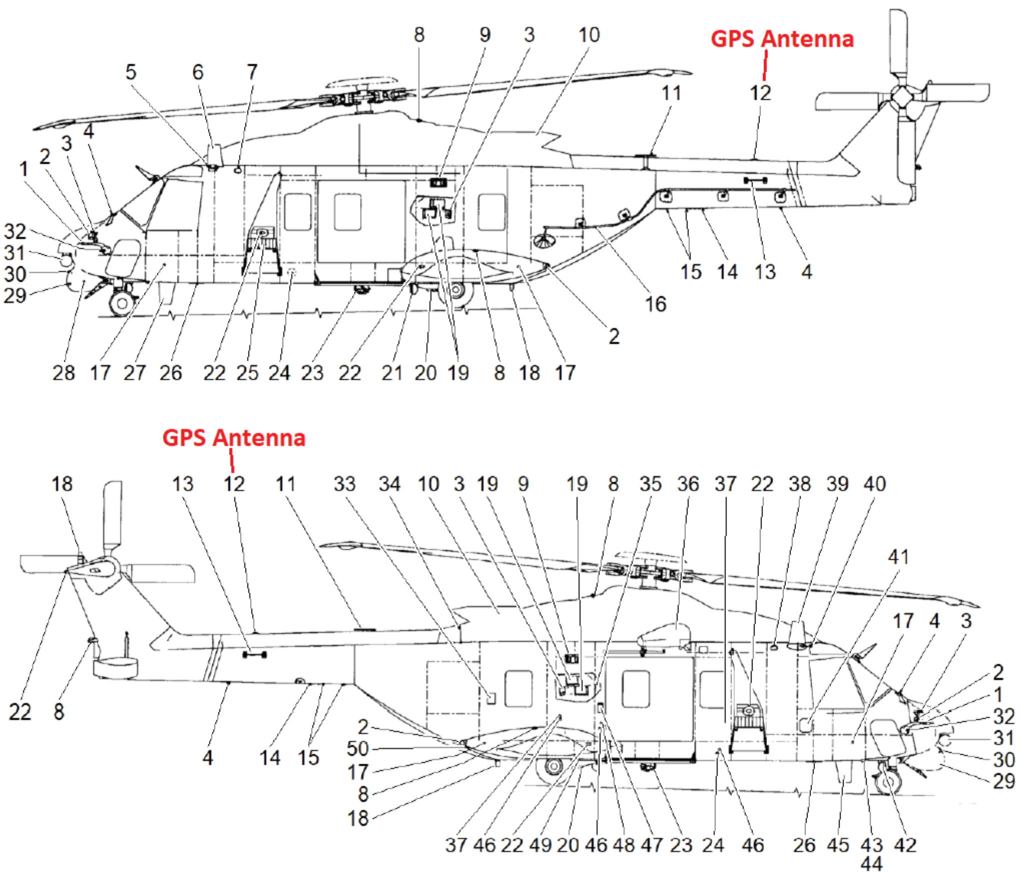

Figure 1 – Position of external equipment on the MRH90 aircraft, the GPS antenna is located at number 12 and marked by the red text.

In Reference A, DSTG used a bounding box method for each MRH90 aircraft, which described the volume the MRH90 geometry occupies as it translates and rotates in all six axes during flight. This volume also includes the components of the main and tail rotors. This was done to continually assess which component of Aircraft 2 was closest to Aircraft 3 at any given time. The method utilised an open source MRH90 3D geometry, which although visually acceptable in appearance has not been rigorously validated. Most importantly, the inertial reference location about which all aircraft rotations and positions are referenced about, by the DFDR data, had to be assumed. Actual location of the inertial reference point remains an unknown for DSTG. Knowledge of the reference location and use of a more accurate 3D geometry would result in only a minor increase in miss distance accuracy. Given that the most significant sources of uncertainty are in the time synchronization between the two aircraft and relative GPS accuracy, DSTG has decided to remove the effect of aircraft geometry and utilize GPS locations only to estimate miss distance.

3. Aircraft Time Estimation

Previous DSTG assessments of miss distance calculated for MRH90 aircraft have highlighted sources of error due to a range of time sources available on the DFDR binary data. In the current example DSTG only has access to CSV format DFDR data and therefore cannot assess if similar reductions or differences in synchronisation between Aircraft 2 and Aircraft 3 are present. [redacted]

[redacted] Given that DSTG does not know if there is a lack of synchronisation between the time on Aircraft 2 and Aircraft 3, DSTG has decided to estimate a range of potential separation distances given the following three scenarios:

1) Aircraft 3 [redacted] time is ahead of Aircraft 2 [redacted] time by 1 second
2) Aircraft 3 and Aircraft 2 [redacted] times are in fact synchronised
3) Aircraft 3 [redacted] time is behind Aircraft 2 [redacted] time by 1 second

The closest separation distances recorded between GPS locations in the last ten minutes of the flight until Aircraft 3 impacted the water are 147 feet, 134 feet, and 82 feet, respectively for cases 1, 2 and 3. All three separation distances are recorded just prior to when Aircraft 3 impacted the water. Note that these distances do not include any element of helicopter geometry, such as rotating main blades, which would reduce the separation by as much as 53.5 feet, i.e. one rotor blade diameter. The following three images, Figure 2, Figure 3 and Figure 4, illustrate the three scenarios detailed above, with lateral difference in feet on the horizontal axis and longitudinal separation in feet on the vertical axis for the last ten minutes of the flight up until Aircraft 3 impacted the water. Each image also illustrates the closest separation distance recorded during the time period.

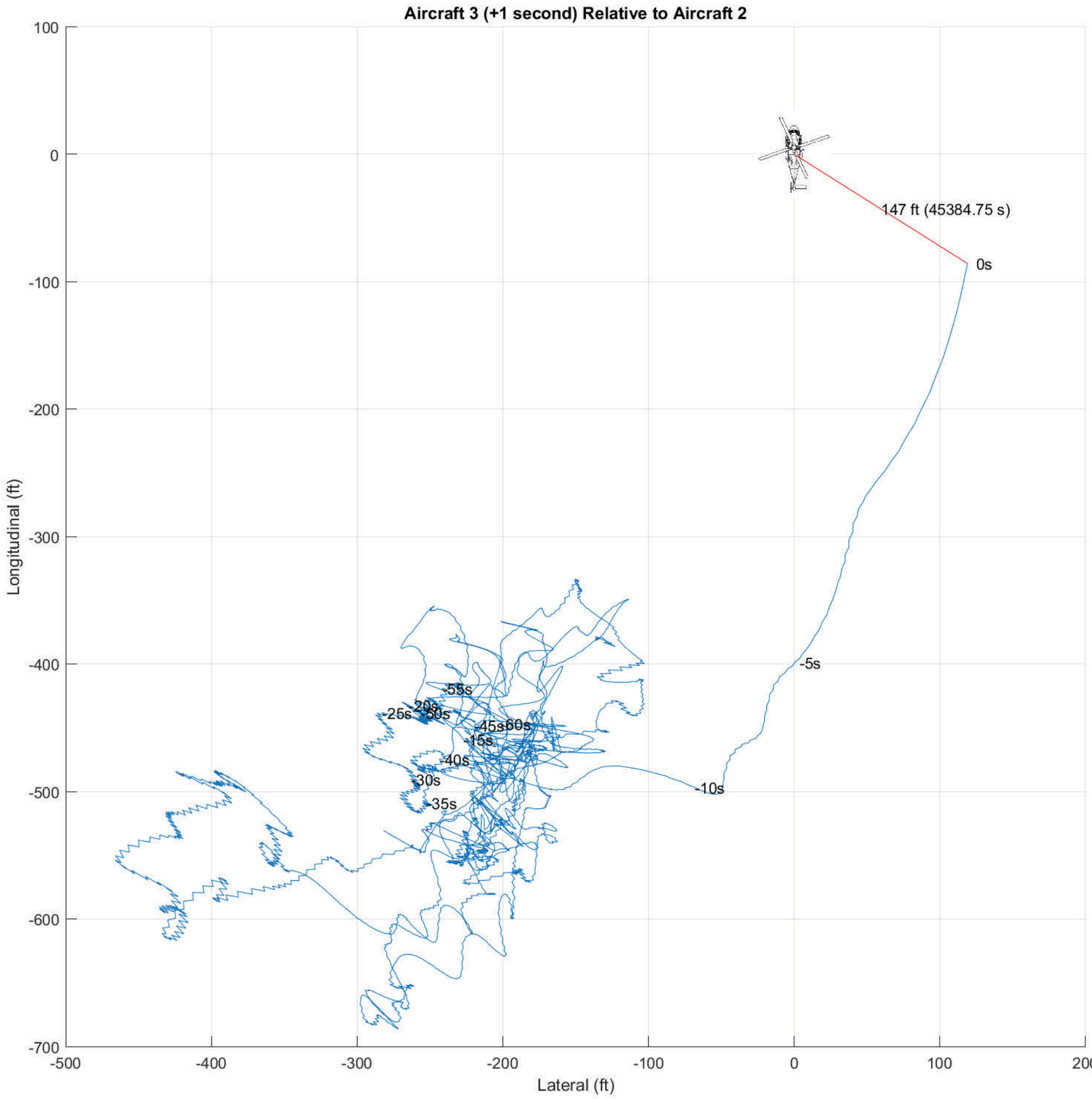

[redacted] 2 - Lateral and Longitudinal separation of Aircraft 3 relative to Aircraft 2 for last ten minutes of the flight, assuming [redacted] time of Aircraft 3 is one second ahead of the [redacted] time of Aircraft 2.

7

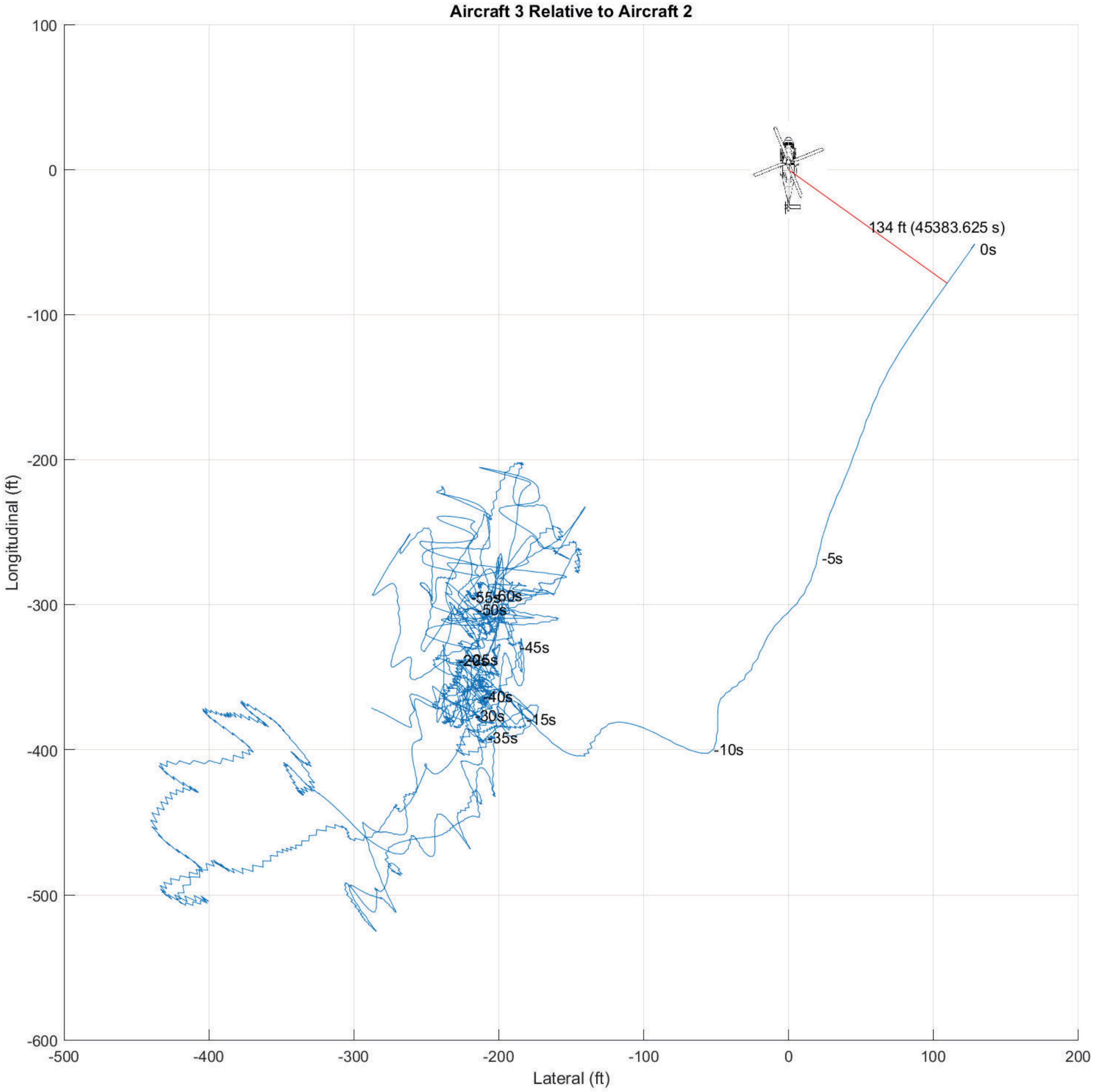

Figure 3 - Lateral and Longitudinal separation of Aircraft 3 relative to Aircraft 2 for last ten minutes of the flight, assuming Aircraft 3 and Aircraft 2 are synchronised in [redacted] time.

8

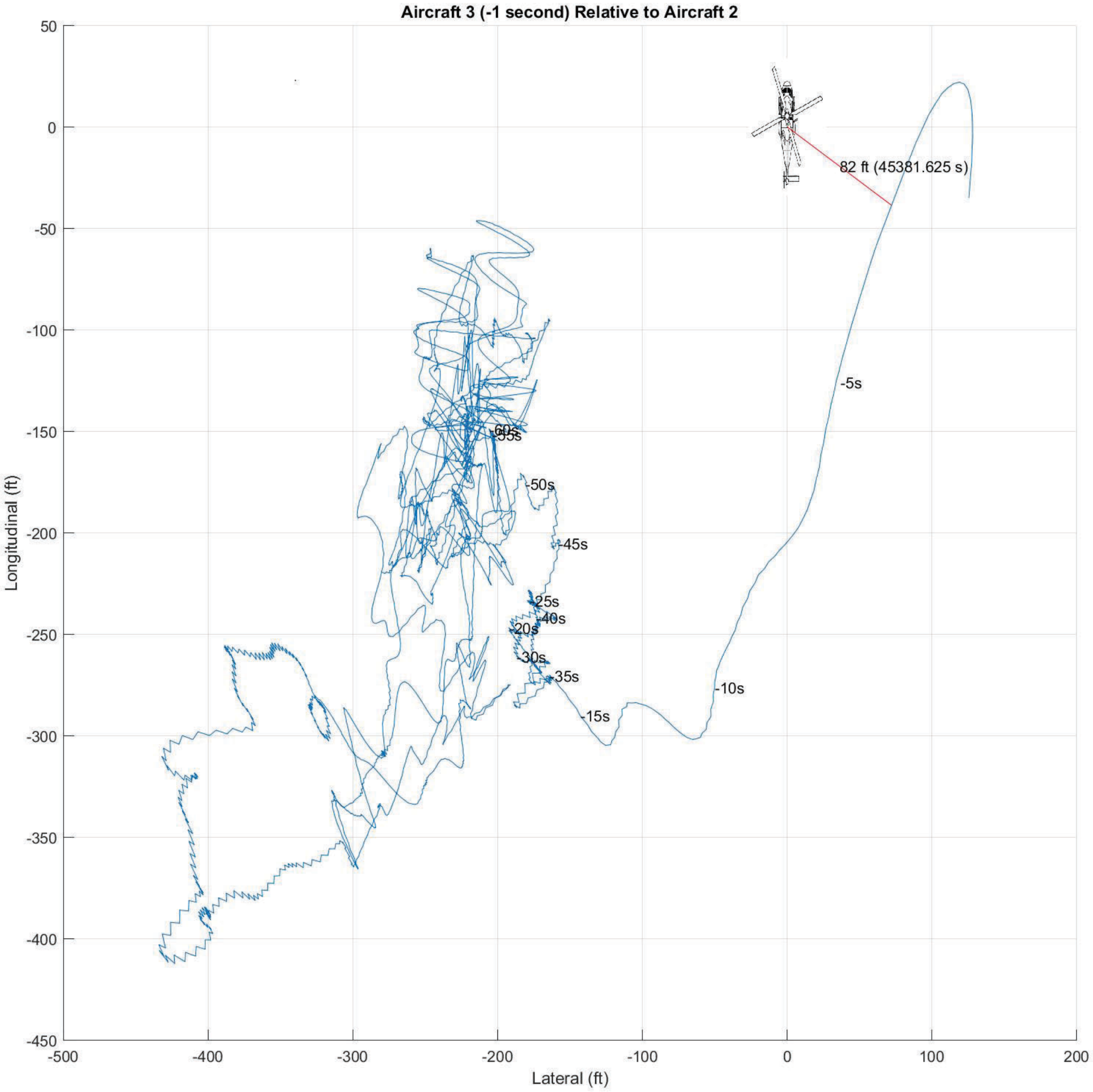

Figure 4 - Lateral and Longitudinal separation of Aircraft 3 relative to Aircraft 2 for last ten minutes of the flight, assuming [redacted] time of Aircraft 3 is one second behind the [redacted] time of Aircraft 2.

9

While the proximity of Aircraft 3 to Aircraft 2 at the time it passes abeam of Aircraft 2, just prior to impact with the water, may appear relatively close, the nature of helicopter formation flying should be considered. Formation flying involves aircraft being relatively close to each other and is best illustrated by the proximity that Aircraft 2 had with Aircraft 1 (Lead aircraft of the formation) during the same ten minute period of the flight. Figure 5 below shows again lateral difference in feet on the horizontal axis and longitudinal separation in feet on the vertical axis for the last ten minutes of the flight.

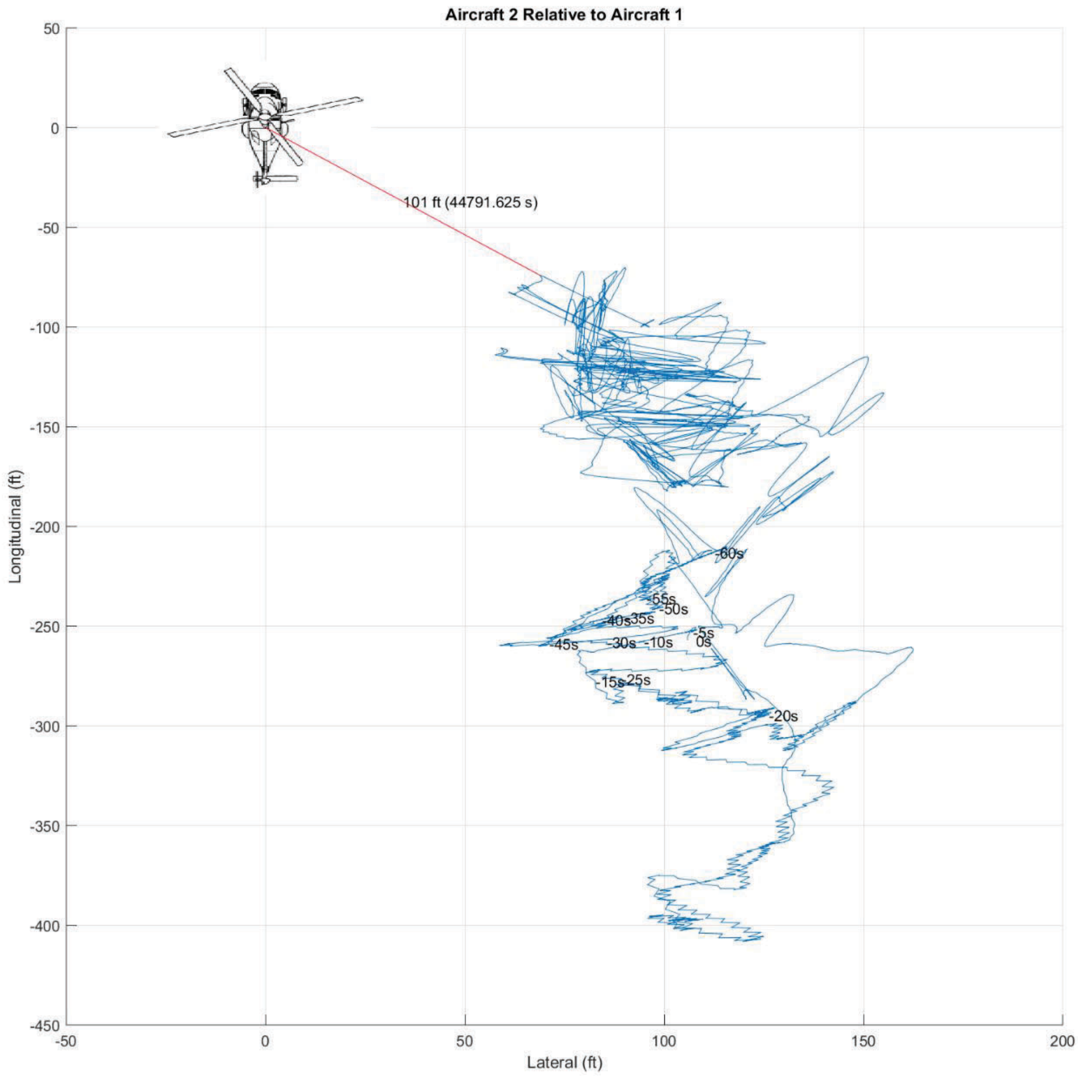

Figure 5- Latitude and Longitude separation of Aircraft 2 relative to Aircraft 1 assuming Aircraft 2 and Aircraft 1 are synchronised in [redacted] *time for last ten minutes of the flight.*

Figure 5 shows that Aircraft 2 spent a significant portion of the last ten minutes of the flight, approximately 120 feet behind in longitudinal separation and 80 feet in lateral separation (right). The closest separation distance between Aircraft 1 and Aircraft 2 during this time was estimated as 101 feet. Operational requirements aside, it appears to not be significantly more than the lower bound of the separation distance between Aircraft 3 and Aircraft 2 estimated just prior to impact with the water, i.e. 82 feet.

ENCLOSURE 8

Airbus (AAP) TAUA040 FDR Factual Report Issue V1 22 Sep 23

AIRBUS HELICOPTERS

ENCLOSURE 8 TO BP44206784

[Airbus Amber]

[redacted]
NHI
[redacted]

[redacted]
Issue V1
Donauwörth,22.09.2023

Copy: [redacted]

TAUA040 FDR Factual Report Issue V1

This report contains a summary of the FDR data received from Australian DFSB on August 31st 2023. The analysis of the data was performed between August 31st and September 18th 2023 and is limited to an overview of the most important parameters and time periods of the recorded data. The statements about consistency between control inputs and helicopter attitude are limited by the respective experience of the involved persons, who do not include a pilot or a flight mechanics specialist. Therefore, an involvement of this expertise would further enhance those statements.
Further insight into the probable causes of the accident would be possible by a synopsis together with voice data, recordings of the other helicopters of the formation, detailed weather information, mission and flight profile requirements and potentially a wreckage examination.

Table of Contents

Hausanschrift/Business address:
Airbus Helicopters Deutschland GmbH
Industriestraße 4, 86609 Donauwörth

Postanschrift/Postal address:
Airbus Helicopters Deutschland GmbH
86607 Donauwörth

Lieferanschrift/Delivery address:
Airbus Helicopters Deutschland GmbH
Dr. Ludwig-Bölkow-Straße 3, 86609 Donauwörth

Tel.: +49 906 71 – 0, Fax: +49 906 71 – 4011
www.airbushelicopters.com

Airbus Helicopters Deutschland GmbH
Vorsitzender des Aufsichtsrats/Chairman of the Supervisory Board: Bruno Even
Geschäftsführung/Managing Directors:
Stefan Thomé (Vorsitzender/Chairman), Dr. Hans Bartosch,
Grit de Vito, Helmut Färber, Frank Müller, Dr. Klaus Przemeck
Sitz der Gesellschaft/Registered Office: Donauwörth
Register: Amtsgericht Augsburg (District Court), HRB 16508
USt. Ident.Nr./VAT reg.no DE 129273267

Deutsche Bank AG, München/Munich
SWIFT: DEUT DE MM, IBAN: DE 67 70070010 0 190235200
UniCredit Bank AG, München/Munich
SWIFT: HYVE DE MM, IBAN: DE 31 70020270 000 2702100

[Airbus Amber]

1 Abbreviations

ACC	Actuator Control Computer	IAS	Indicated Airspeed
CSMU	Crash Survivable Memory Unit	IMC	Instrument Meteorological Conditions
DSFB	Defence Flight Safety Bureau	NR	Rotor speed
ED55	EUROCAE document 55 “MOPS for flight data recorder systems”	RT	Real Time
ET	Elapsed Time	UTC	Universal Time Coordinated
EUROCAE	European Organisation for Civil Aviation Equipment	MOPS	Minimum Operational Performance Specification
FDR	Flight Data recorder		

2 Data recording

There are two time scales in the FDR, elapsed time ET which starts at zero when the helicopter is powered up and real time RT which is the UTC. The time axis of the figures in this document are related to ET in terms of 10^3 seconds.
The valid data recording range of the FDR for values in percent is +/-101 %. However, the control input data for longitudinal, lateral, collective and pedal control are defined in a theoretical range of +/- 50 %. This represents the full control range of 100 % from one control stop to the other

- for longitudinal control from forward (-) to rear (+)
- for lateral control from left (-) to right (+)
- for collective down (-) to up (+)
- for pedal from left (-) to right (+)

Therefore, a data value of +/-50% in FDR file represents the maximum control input in the respective axis.
Due to control range adjustments in the mechanical part of the flight controls, the actual minimum and maximum control positions can be slightly above the theoretical 50% value by a few percent.

3 Data analysis

The following parameters are shown in the figures in this report:

ID	Name	Parameter
L167	ATTACT	ATT Mode active
L170	TACACT	TAC Mode active
L172	BPLYW	Feet-on Detection Yaw
L173	BPLRL	Hands-on Detection Roll
L174	BPLPT	Hands-on Detection Pitch
L175	BPLCL	Hands-on Detection Collective
L187	ICPP	Flight Controls Position Pitch
L189	ICPR	Flight Controls Position Roll
L191	ICPC	Flight Controls Position Collective
L193	ICPY	Flight Controls Position Yaw
L569	ENG1_NP	Engine 1 Power Turbine Speed
L598	ENG1_TQ	Engine 1 Torque
L642	ENG2_NP	Engine 2 Power Turbine Speed
L644	ENG2_TQ	Engine 2 Torque
L697	MGB	Main Rotor Speed
P291	IRSM_RA_HGT_COMP	Radar Altitude
P292	IRSM_GAMMA_X	Longitudinal (x) Acceleration
P293	IRSM_GAMMA_Y	Lateral (y) Acceleration
P294	IRSM_GAMMA_Z	Vertical (z) Acceleration
P348	IRSM_OPTIMAL_ROLL	Helicopter Roll Attitude
P349	IRSM_OPTIMAL_PITCH	Helicopter Pitch Attitude
P351	IRSM_Q	Helicopter Pitch Attitude
P352	IRSM_P	Helicopter Roll Attitude
P354	IRSM_OPT_V_V	Helicopter Vertical Velocity
P503	PMCM_MASTER_ALARM_RED	Master Warning Red
P609	IAS_ADC	Indicated Air Speed
P625	ENG1_MIN_OIL_PRESS	Minimum Oil Pressure Engine 1
P626	ENG2_MIN_OIL_PRESS	Minimum Oil Pressure Engine 2
P635	NR_MIN	Minimum Rotor Speed Exceedance
P653	MASTER_RED_CONTROL_LIGHTED	Master Warning Red illuminated

3.1 Whole Flight

Figure 1 shows the main parameters of the flight control inputs, the helicopter attitude and the accelerations during the whole flight (RT selected as 12:13:57 at first collective increase and 12:36:26 at last recorded value).

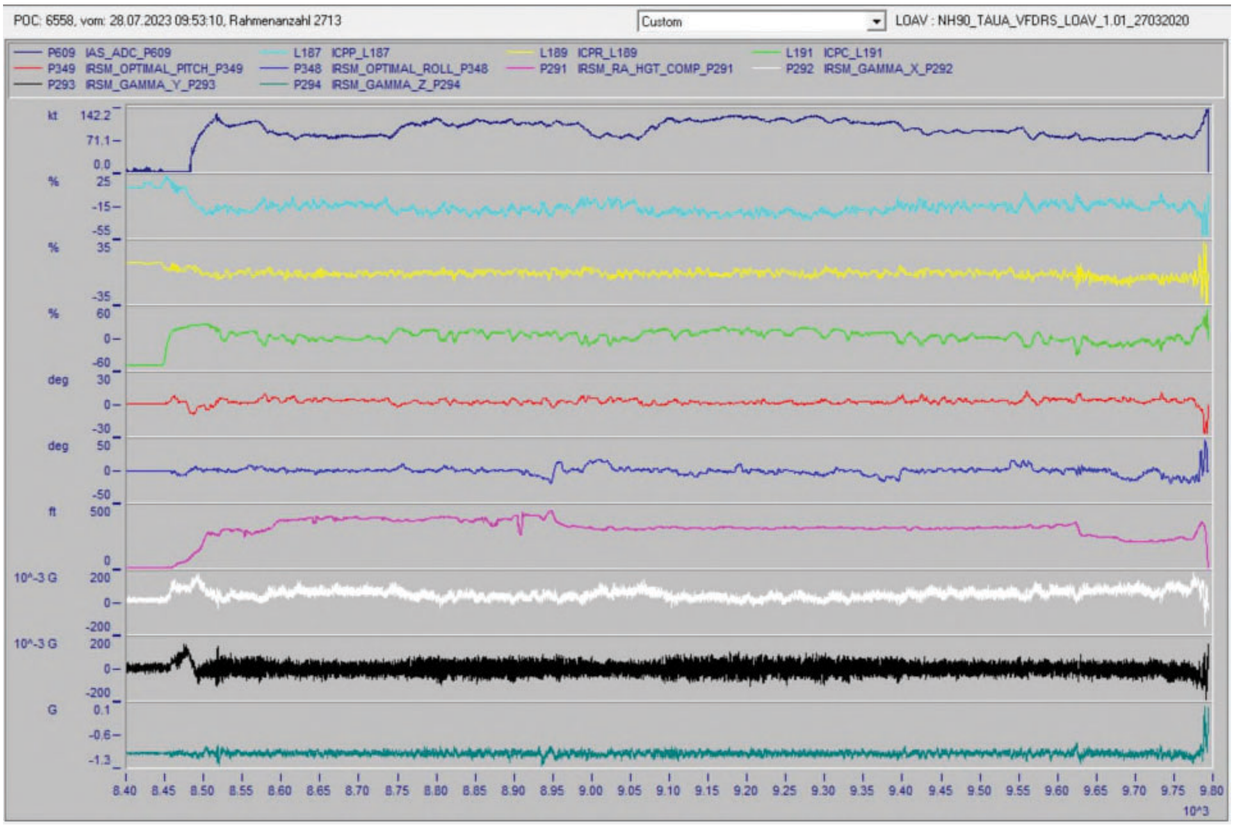

Figure 1: Full flight – Flight controls, attitude and accelerations

3.1.1 Control input

The value of the longitudinal control
- is between 0 and +23 % during the lift off
- is between -30 and 0 % for the remaining flight after gaining forward speed
- is between -52 and -30 % for the last three seconds of the flight

The absolute value of the lateral control
- is below 10 % during the whole flight until RT 12:36:10
- except of several excursions up to -16 %
- is between -20 and +20 % during the second to last 8 seconds (RT 12:36:10 - 18)
- is between -35 and +33 % during the last 8 seconds (RT 12:36:18 - 26)

The value of the collective control
- remains mostly below +20 % during the majority of the flight with a few excursions up to +30 %
- is between -32 and -10 % during RT 12:33:35-43
- remains mostly between -20 and +4 % with one excursion to -24 % (RT 12:33:43 - 12:36:06)

- increases to +42 % until RT 12:36:21
- oscillates for two down-up cycles between +18 % and +56 % for the last four recorded seconds (until RT 12:36:25)

All control inputs indicate that the helicopter was flown manually. The range of control inputs is moderate and calm except in the last phase of the flight (see Figure 6).

3.1.2 Helicopter speed and attitude

The indicated airspeed

- is between 80 and 120 kt for the majority of the flight after lift off
- is between 70 and 80 kt during the last approximately 20 % of the flight time (RT 12:32:38 - 12:36:10)
- Increases up to 142 kt during the last 16 seconds (RT 12:36:10 - 26)

The pitch attitude

- remains mostly well below +/-10° during the whole flight with a few nose up attitudes up to 13°
- shows an increased nose down attitude up to -28 ° in the last 6 seconds of flight (RT 12:36:20 - 25)

The roll attitude

- remains mostly below +10° during the whole flight with a few turns up to 21°
- shows two right roll peaks up to 31° and 48° in the last 10 seconds of flight (RT 12:36:16 - 25)

All helicopter motions and attitudes are moderate and calm except in the last phase of the flight (see Figure 6). The helicopter follows the control inputs throughout the complete flight.

3.1.3 Accelerations

- During start the highest x-acc is 0.17 g (RT 12:14:40)
- During start the highest y-acc is 0.13 g (RT 12:14:25)
- During final phase the highest x-acc is 0.19 g (RT 12:36:07)
- During final phase the highest y-acc is -0.28 g (RT 12:36:23)
- The z-acc remains at nominal 1 g condition +/- 0,3 g for the whole flight except in the final phase which is discussed in Chapter 3.2.3.

The longitudinal and lateral accelerations are apparently not out of the usual range during the whole flight. They will not be further considered for the following evaluation.

3.1.4 Engine Parameters

Figure 2 shows the rotor minimum RPM indication together with the rotor speed, the power turbine speed and torque of both engines over the full flight.

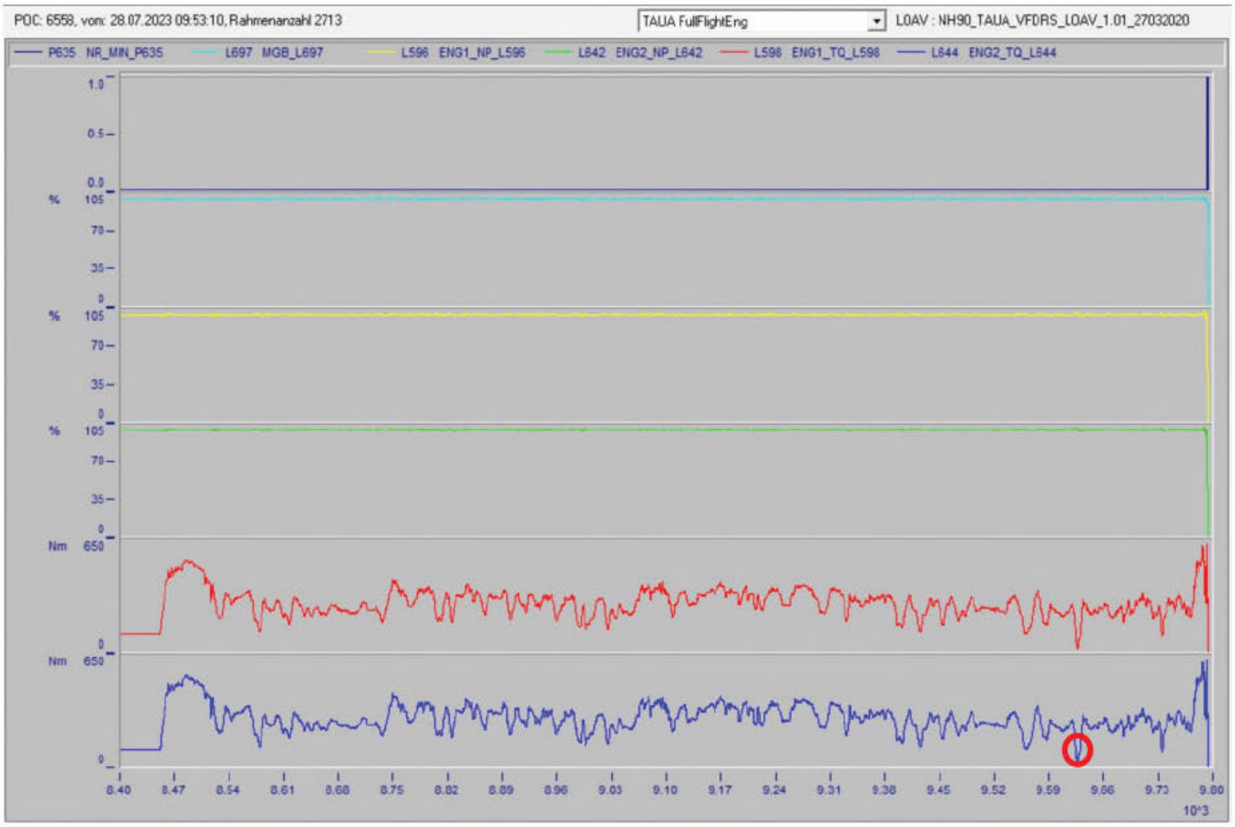

Figure 2: Full Flight - Engine Parameters

Except of small variations, the indicated speeds of main rotor and both engine power turbines are constant at nominal values and consistent with each other over the full duration of the flight. The last few seconds will be discussed in Chapter 3.2.2.

Both engines delivered torque over the full duration of the flight without any torque split (see Figure 3). During take-off and climb the values reach a maximum value of 530 Nm.
There is a significant drop (marked by a circle in Figure 2) down to 20 Nm at RT 12:33:39 which can be explained by the control input (RT 12:33:34.250 – 12:33:36.50 marked by vertical lines in Figure 4) in the pitch axis up from -12.1 to +1,6 % and in collective down from -4.8 to -32.4 % (see Figure 4).

[Airbus Amber]

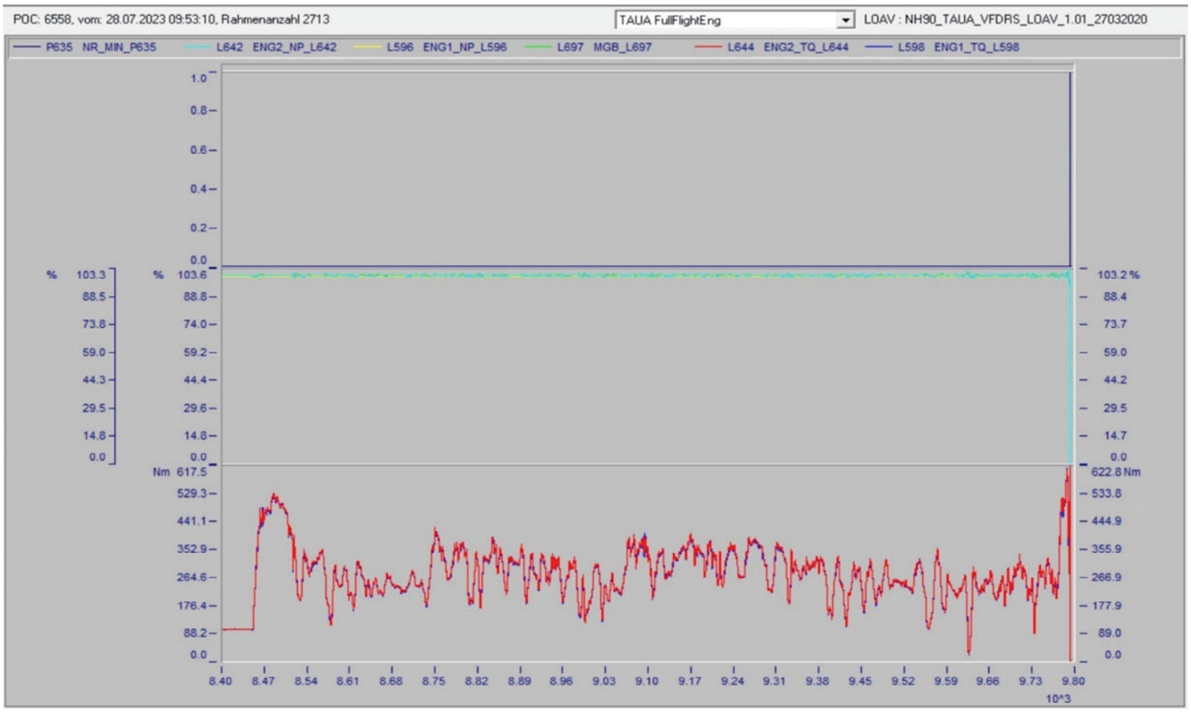

Figure 3: Full Flight - Engine Parameters Overlay

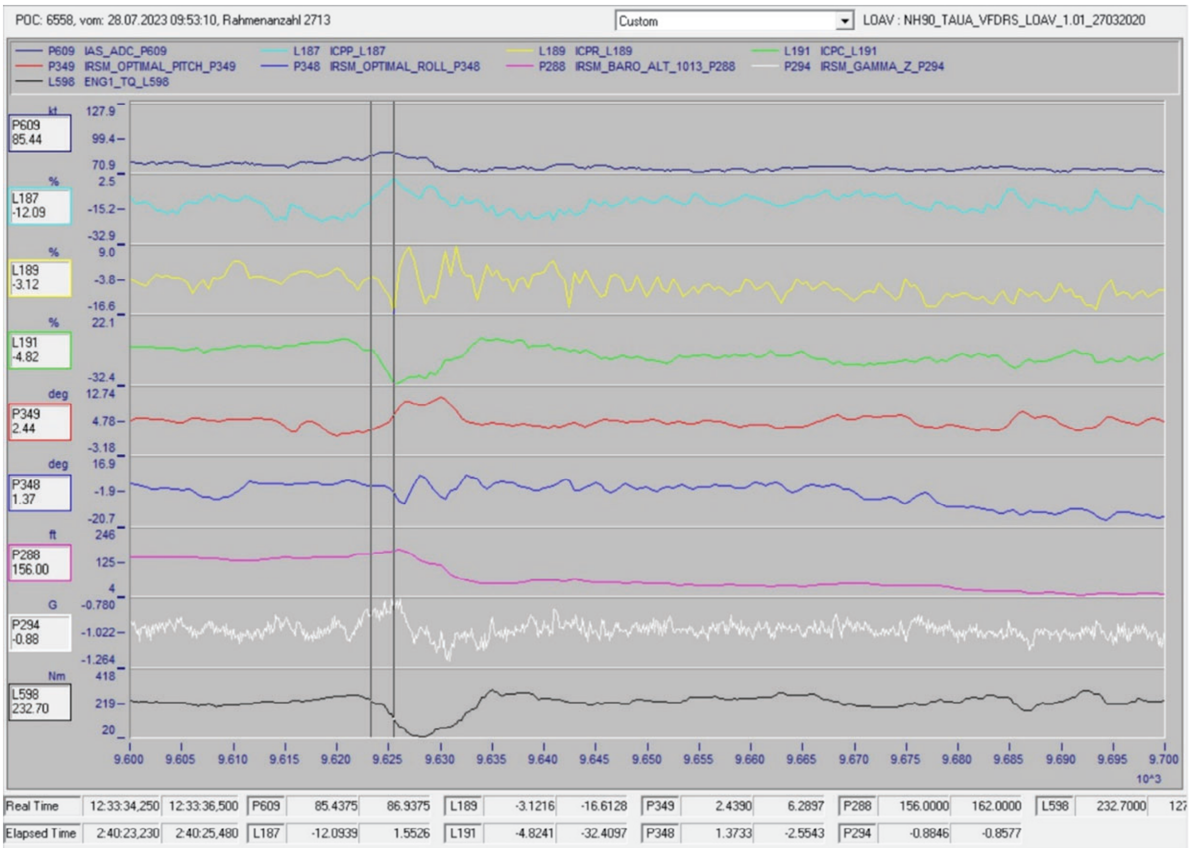

Figure 4: Engine Torque Drop

3.1.5 Flight Path

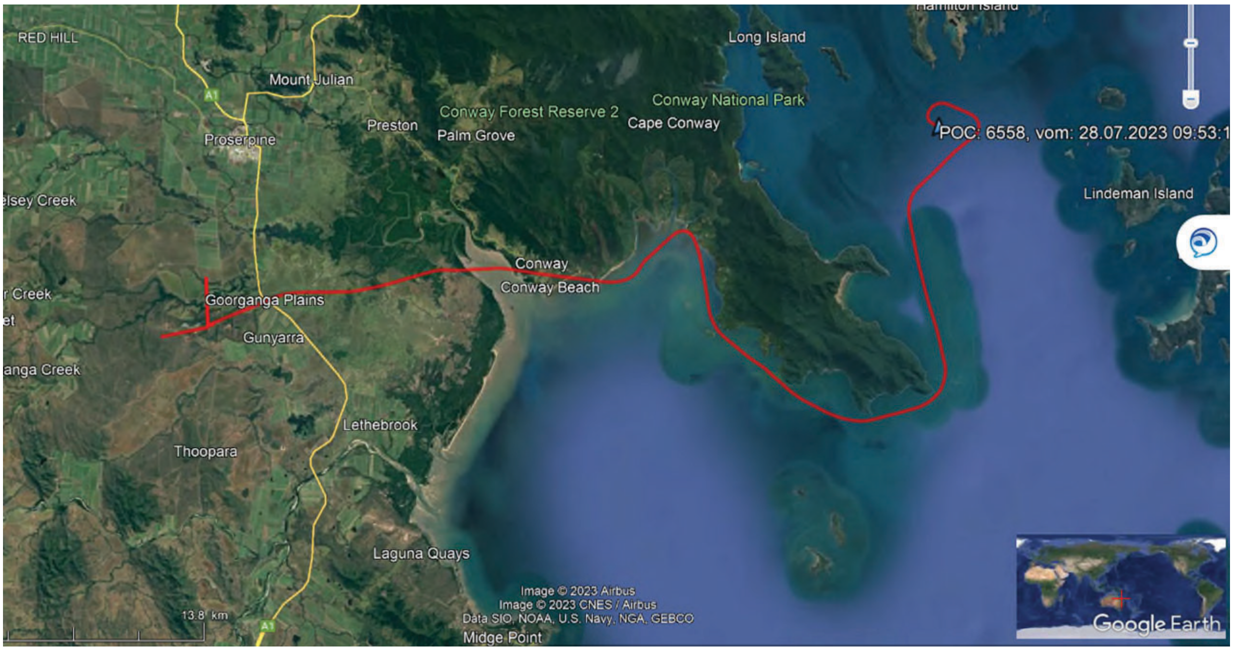

Figure 5: Flight path

3.2 End of Flight

Figure 6 shows the main parameters of the flight control inputs, the helicopter attitude and the z-acceleration during the last 45 seconds of the flight (RT 12:35:41 to 12:36:26). Two vertical lines indicate RT 12:36:08 and 12:36:20.

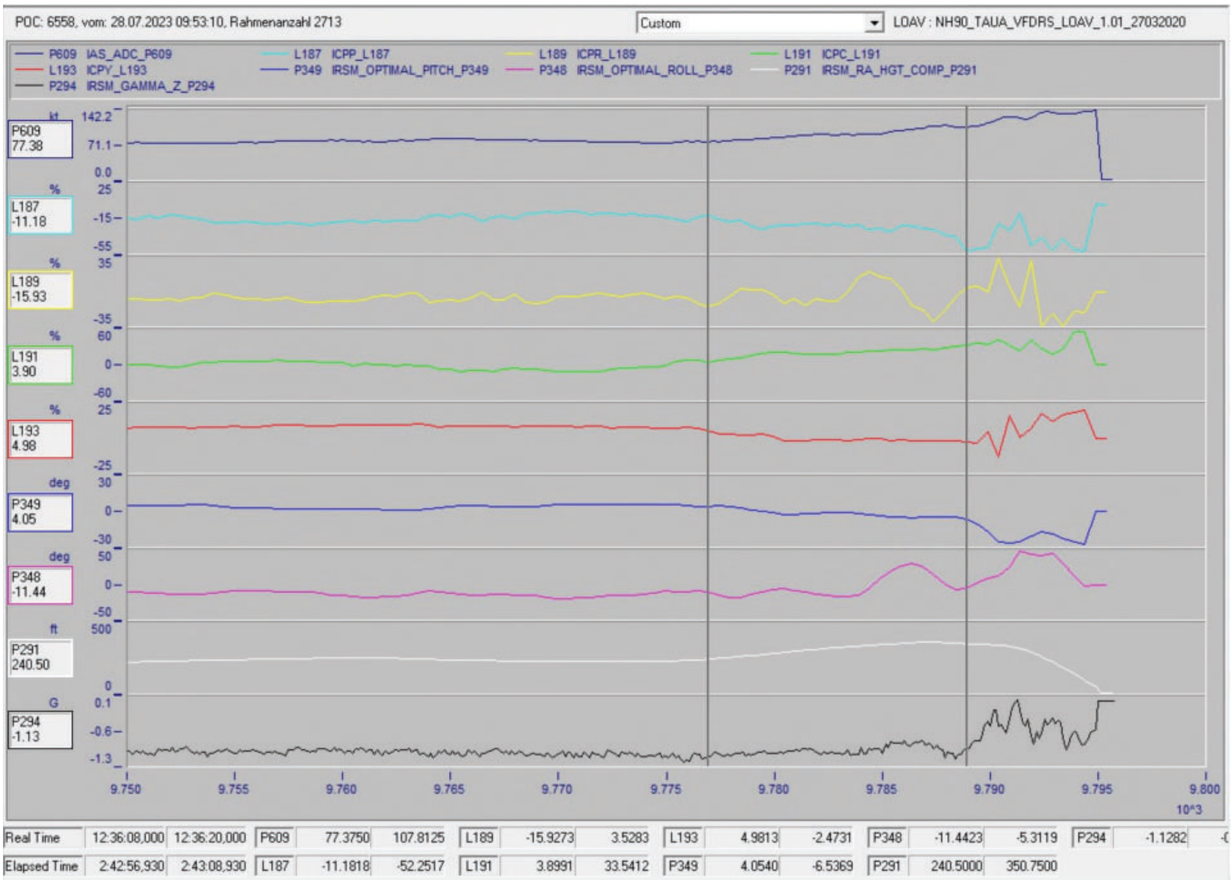

Figure 6: End of flight – Flight controls, attitude and z-acceleration

3.2.1 Control input

While the longitudinal control input value is more or less in the range of -10% for quite a time

- it decreases at RT 12:36:08 to approx. -20% in two seconds
- it further decreases at RT 12:36:17 to approx. -50% in three seconds
- it shows two oscillations up to -20% and -10% in three seconds at RT 12:36:20
- remains between -52 and -30 % for the last three seconds of the flight

In correlation with the negative pitch input and the collective rising in the same time an increase of the IAS from 78 to 142 kts and a nose down attitude from +4° to -28° can be observed. In addition, the final loss of altitude from 360 ft to 0 ft is attributed to the increasingly strong negative longitudinal input in the last eight seconds of flight

While the lateral control input value is more or less in the range of 0 to -10% for quite a time

- it starts to vary RT 12:36:08 - 20 with increasing amplitudes for approx. two and a half cycles
- it shows two oscillations between -35% and +33% in three seconds after RT 12:36:20 which are more or less in parallel to the longitudinal input oscillations
- remains between -35 and -21 % for the last three seconds of the flight

In correlation with the variable lateral input a respective roll attitude change between -18° and +42° can be observed.

The collective control is increased from 4 to 42% between RT 12:36:08 – 20. This leads in spite of the increasing nose down attitude initially to an altitude gain of 120 ft.

Also, collective and yaw control input show a similar oscillatory behavior in the last 6 seconds of the flight.

Figure 7 shows for pitch and roll axis the control input, the pitch and roll rate and the pitch and roll attitude. Two vertical lines indicate RT 12:36:08 and 12:36:20.

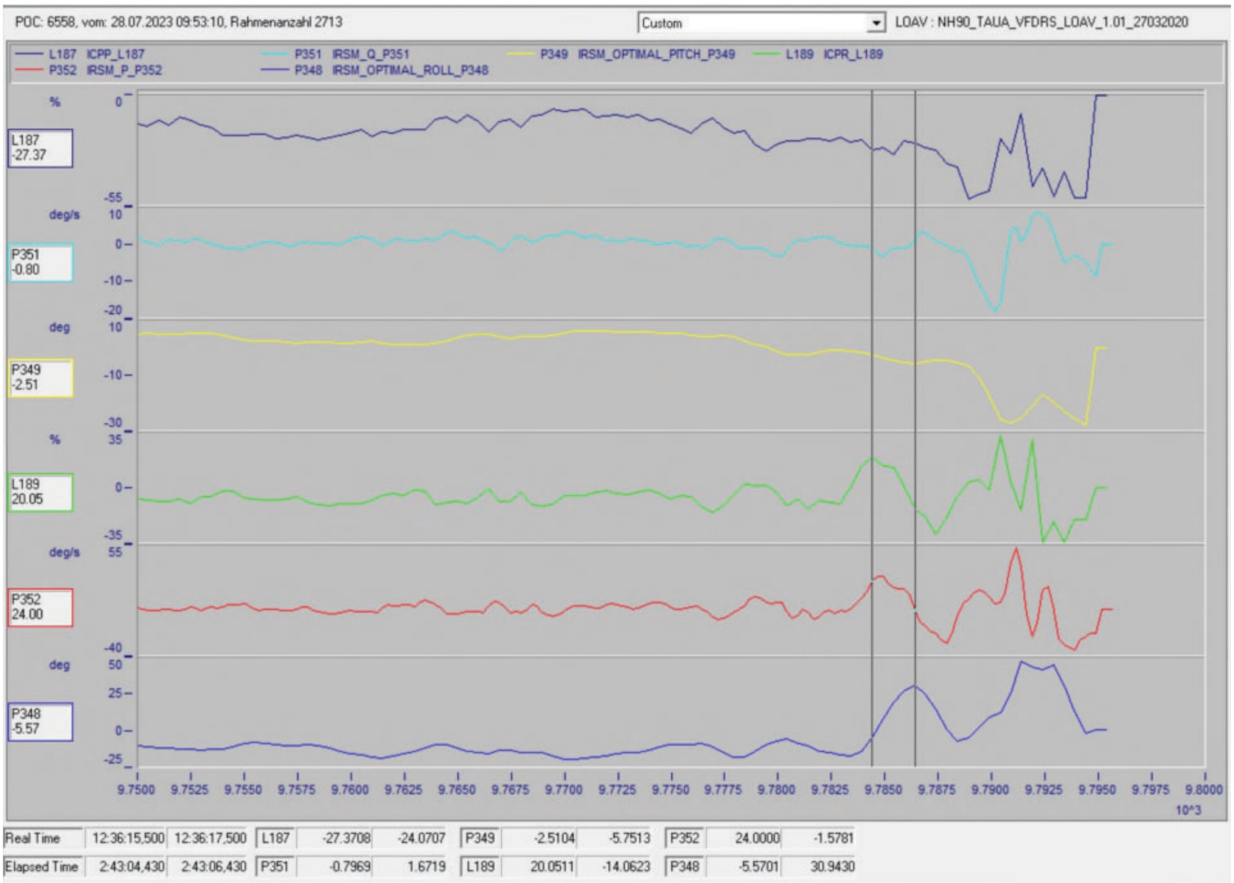

Figure 7: End of flight – Flight controls, pitch and roll rate and attitude

The control input in the pitch and roll axis results in a tilt of the main rotor plane which creates a pitch and roll moment acting on the helicopter. The pitch and roll accelerations (which are not recorded in the CSMU) are directly proportional to the pitch and roll moment and therefore respond to the control input. The pitch and roll rate are the integral of the respective acceleration under consideration of inertial and aerodynamic forces. Finally, the pitch and roll attitude are the integral of the respective rate.

The roll rate of the helicopter reacts immediately upon pilot roll inputs. Evolutions of bank angle is the direct result of pilot inputs and airframe inertia (see Figure 7).

Figure 8 shows the pitch attitude, collective control input, vertical speed, indicated airspeed and radar altitude. Two vertical lines indicate RT 12:36:04 and 12:36:16.

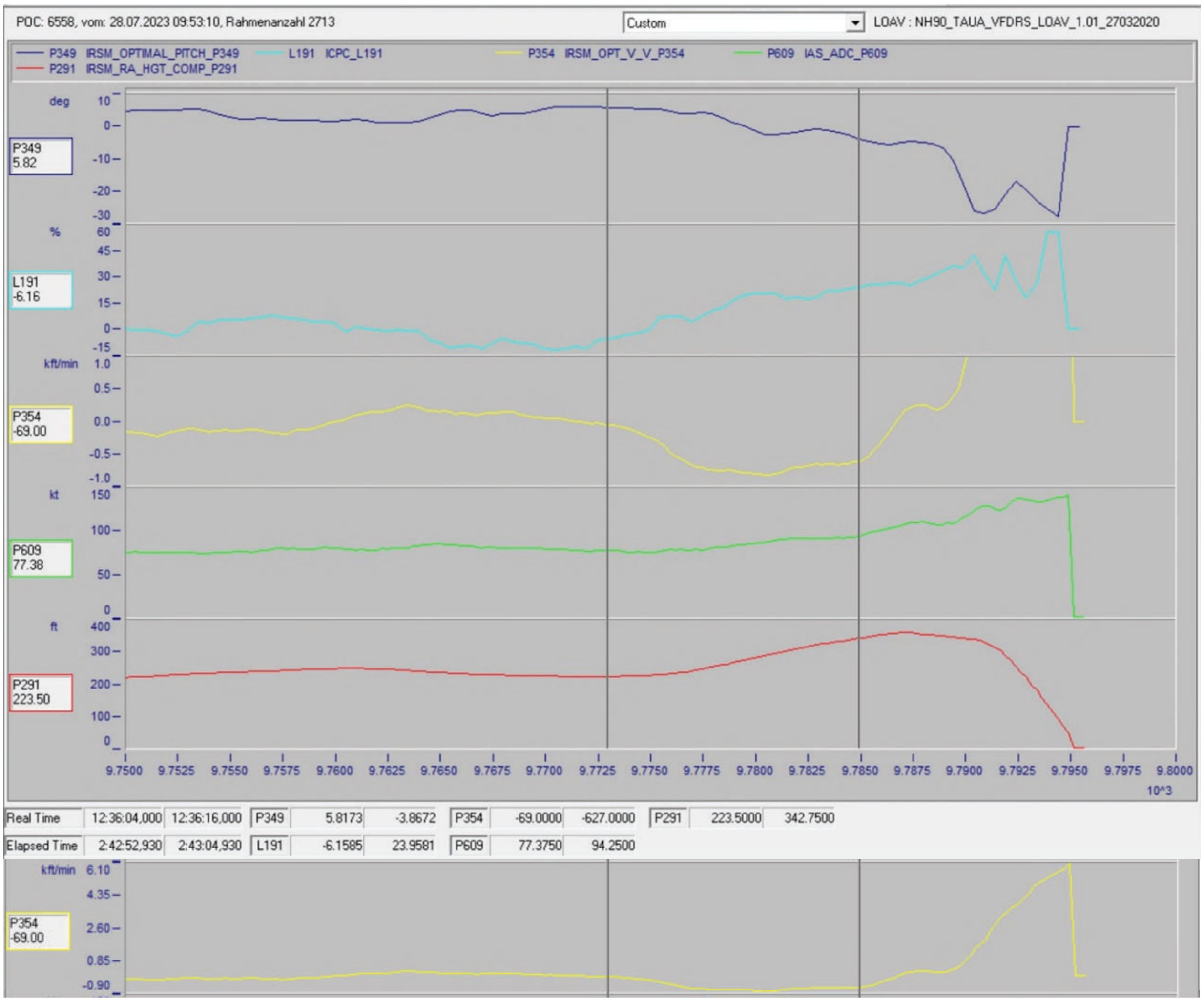

Figure 8: End of flight – Flight controls, pitch attitude, collective input, vertical speed, altitude and IAS

An increase of collective creates more lift force of the main rotor, which primarily would lead to a vertical acceleration and vertical speed. However, as the main rotor is installed together with the main gear box with a forward tilt angle of 5° and due to the tilting of the rotor plane in pitch and roll, the lift does only partially act in vertical direction. Another part of the lift force acts in forward direction to establish and increase the speed and in lateral direction for attitude changes and lateral flight. Hence the relation between collective input and vertical speed is not that close as for pitch and roll. Nevertheless, between RT 12:36:04 and 12:36:16 a clear correlation between the collective input from -6 to 24% and vertical speed (note that negative values indicate climb speed) from -70 to -630 ft/min can be seen in Figure 8. Additionally, the increase in airspeed from 77 to 94 kt due to increasing nose down inclination of the helicopter (+5,8 to -3.9°) is obvious.

[Airbus Amber]

After this the further increasing pitch-down attitude (-3.9 to -28°) leads, in spite of further collective increase of 30%, to a reversion from climb to descent and continuously increasing sink speed up to 6000 ft/min just before the impact (see Figure 8 last row).

The relation between control input, helicopter pitch and roll rate, attitude and speed indicates that the aircraft is following the control inputs and the control system is working properly. It can be concluded that control inputs, ACC commands and actuator movements are consistent and show no irregularities.

3.2.2 Engine Parameters

Figure 9 shows the rotor minimum RPM indication together with the rotor speed, the power turbine speed and torque of both engines for the end of the flight. Rotor and engine speed values and engine torque values are shown overlaid to demonstrate their consistency.

At the very end of the flight (last data point RT 12:36:26.00):

- RT 12:36:24.00-25.00[1] the collective was raised in one second from 17.8 to 56.1% [2]
- RT 12:36:24.00-25.75[1] leading to a torque increase from 500 to 620 Nm (mean of engine 1 & 2)
- RT 12:36:24.00-25.50 and a rotor speed decrease from 96.4 to 94.8% NR
- RT 12:36:25.50 which triggered the minimum RPM indication (RPM < 95%)

[1] last recorded value
[2] This value is limited to +50% by the flight control computers

This behavior is to be expected regarding the engine control characteristics.

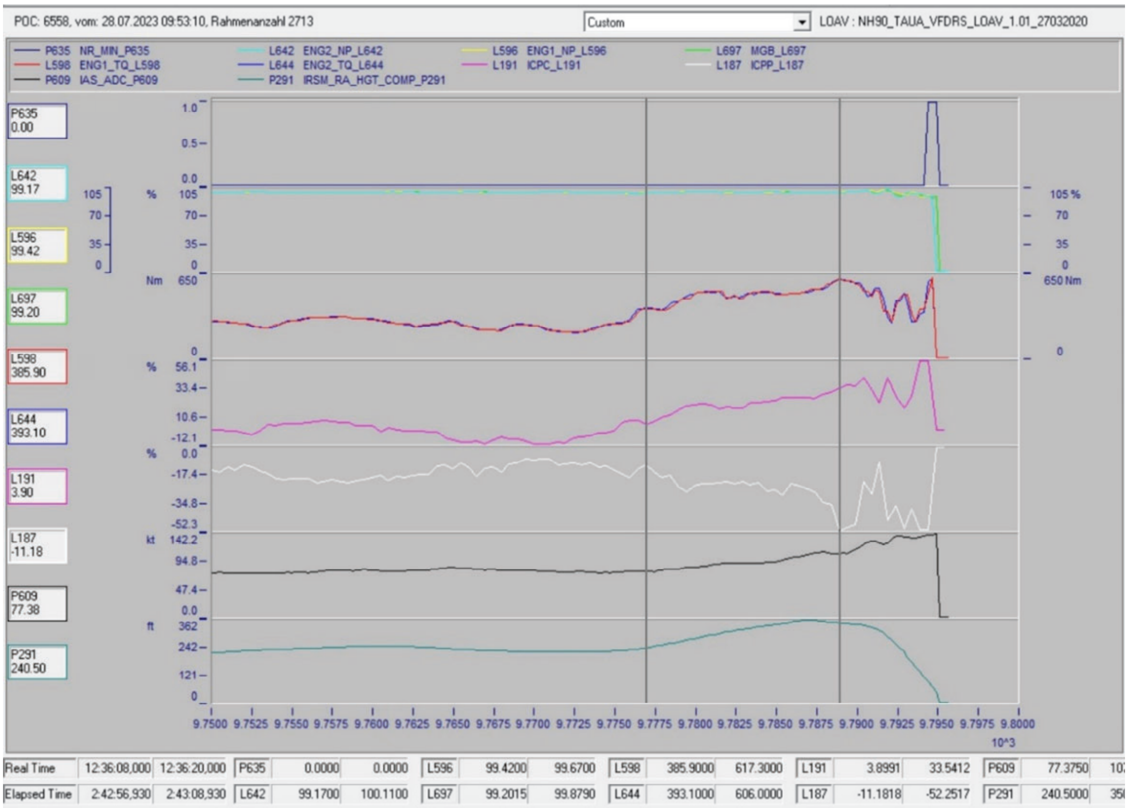

Figure 9: End of Flight - Engine Parameters

3.2.3 Alarm Indications

Figure 10 shows the z-acceleration, the engine minimum oil pressure indications and master alarm warnings during the last 19 seconds of the flight (RT 12:36:08 to 12:36:27). It can be seen that the oil pressure indications correlate with the occurrence of low vertical acceleration values (close to zero-g). The probable cause for the indication is the unusual oil distribution in the engine oil reservoir due to low g situation leading to a short time where the pumps were not fed sufficiently with oil (see Figure 11). The master alarm indications are a consequence of the oil pressure indications.

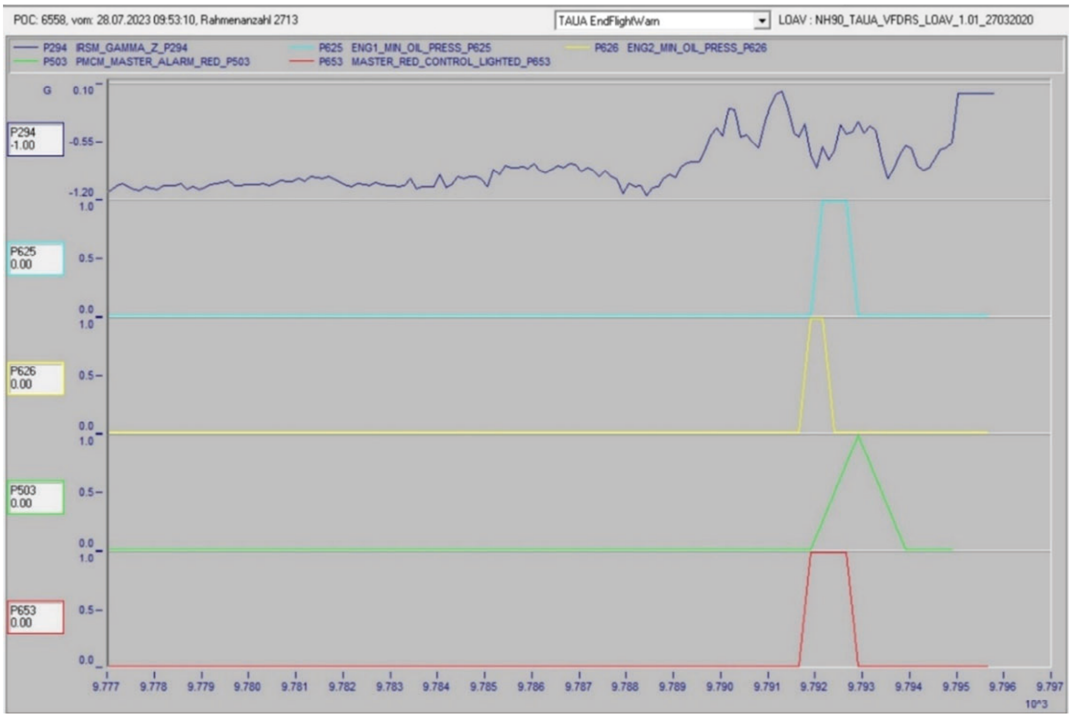

Figure 10: End of flight –Z-acceleration, oil pressure and alarm indications

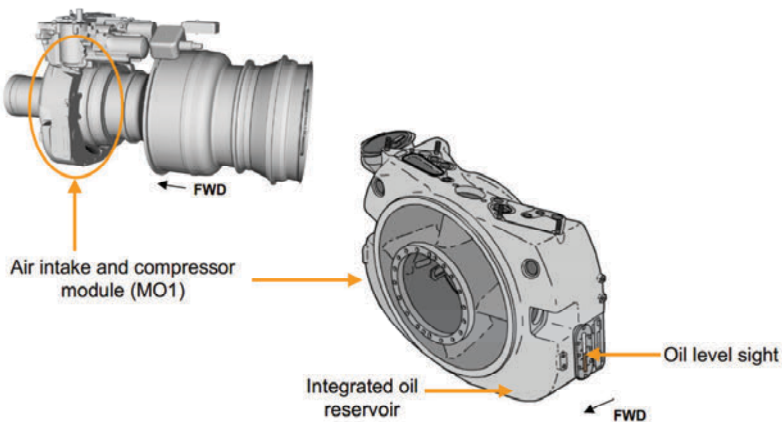

Figure 11: Engine oil reservoir

During the whole flight the engine control worked according to the power demand. Except the ones shown in Figure 10 no Master Caution or Warning appeared (no system abnormally determined).

3.3 Answers to Questions of DFSB

Can you determine the vertical acceleration at impact?
The recording of vertical acceleration ends with values less than nominal 1g condition. Therefore, the impact situation is not recorded and the actual acceleration resulting from the impact is not available. In addition, it has to be considered that

- The sampling rate of 8 Hz might not be sufficient to “catch” the maximum peak acceleration of the impact as this is a highly dynamic process
- due to the high forward speed the longitudinal acceleration during impact was also very high.

Is it possible to determine which set of controls is being used, ie left or right seat pilot?
The controls of the left and right seat are mechanically linked together, so they move always in the same way. There are sensors installed at both inceptors (left and right) which provide in essence the same signal to provide redundancy. From the inceptor position data recorded in the CSMU, it cannot be determined whether the right or left controls were used.

Does the data allow a determination of what was set on the Radar height hold?
Based on currently involved expertise this data is not recorded in the CSMU.

Is it possible to validate the integrity of the flight data being provided to the crew
All flight data are processed with redundancy and any discrepancies would raise an error message which will be displayed to the crew and recorded in the CSMU.

Regarding the collective inputs, from 12:36 is it possible to determine whether the pilot was using the 4 way trim or the trim release to raise the datum?
Usage of beep trims is not part of the data recorded in the CSMU.
However, there are parameters in all four control axes which indicate the hands/feet-on status. Figure 12 shows all control axes inputs together with the hands/feet-on detection. In addition, the first two rows contain the status of the stabilization modes “ATT” and “TAC”.
When TAC mode is selected by the pilot, the ATT mode becomes *active not selected*. On pilot request (button on the grip) the ATT mode is instantaneously selected

Through the whole flight as well as in the end phase there is a lot of manual control activity indicated by the hands-on parameters BPLPT/RL/CL/YW. It is very unlikely that the beep trim had been used in addition to that control activity.

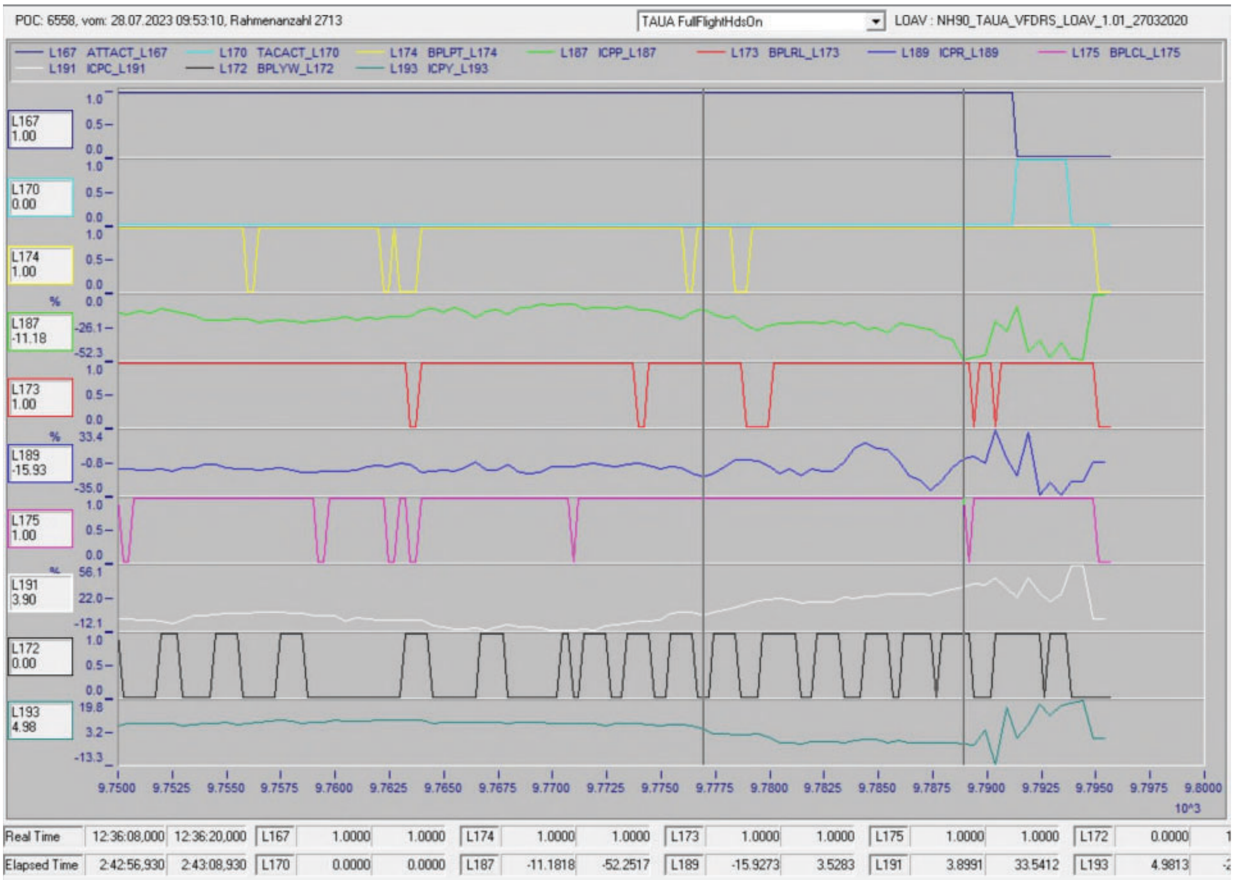

Figure 12: End of Flight – Stabilization Modes, Control Input and Hands on Detection

<u>Are there any flight critical systems whose status are not recorded on the VFDR?</u>
The flight data to be recorded contain the minimum requirements given in ED55 extended by further parameters. The status of the following systems is recorded:

- Flight control input and actuation output
- Engine parameters
- Helicopter flight data (alt, heading, speed, attitude,…)
- Rotor speed
- Caution and Warning indications

3.4 Summary

Based on the data analysis as shown above there were no technical abnormalities or failures of the helicopter and its systems detected which would have precluded a safe flight.

The operation of the helicopter appears normal and without specific events except the phase of the last 18 seconds. At RT 12:36:08 the more or less constant control input deviated first gradually for about 8 seconds from its stabilized position and then with increasing rate and – initially only in lateral control, later in all axes - oscillations of the input values.

It appears that, with the onset of a strong forward longitudinal control motion until the control stop and in parallel a left lateral control motion up to approximately 70% of the maximum range to the left, the helicopter was brought into an unusual attitude. This happened 9 seconds before the end of the flight at RT 12:36:17. The varying control inputs in all axes after this moment were properly executed by the helicopter but they were not adequate to prevent the collision with the surface.

3.5 Hypotheses

Even if the scope of available information is very limited some hypotheses for potential causes of the accident are presented. It has to be noted however, that they are affected by a significant degree of uncertainty.

The gradual change in control movements after RT 12:36:08 might have been caused by an inadvertent input during focusing on other task elements. Being alerted by the noticeable attitude change with increasing nose down pitch around RT 12:36:21, the remaining time of 5 seconds to gain full situational awareness about the helicopter flight state and to recover was not sufficient for the pilot. The oscillating control inputs during the last seconds of the flight might have been caused by counteracting inputs from pilot and copilot.

Another possible scenario explaining the observed facts is an incapacitation of the pilot at or shortly before RT 12:36:08. Due to the gradual change in the helicopter attitude and speed the detection by other crew members might have occurred in a very late stage around RT 12:36:21. The most pronounced inertial clue could have been the fast increase of nose down attitude. In case the copilot took over the controls, it might have not been possible to gain full situational awareness about the helicopter flight state and to recover in the remaining 5 seconds. In addition, the controls might have been partially restricted by the incapacitated pilot.

A third hypothesis can be made which is in line with the recorded data, based on the assumption of spatial disorientation. This might have been caused either due to the difficult visual conditions during the night and/or by entering inadvertently into IMC due to the altitude gain of about 140 ft until 12:36:18 in case the cloud base was below 400 ft.
A potential indication for a low cloud base could be the fact that earlier in the flight at 12:33-34 (see Figure 4) the altitude was rapidly changed from 350 to 250 ft. Assuming that 250 ft would be for a turn flight of the formation the target altitude for the lowest helicopter on position 2 (left) the highest one would be position 3 (right) which would then be the most exposed to entering into IMC.

[redacted] [redacted] Air Accident & Flight Safety Investigator Aviation Safety and Quality Airbus Helicopters	[redacted] Head of Accident & Flight Safety Investigation Aviation Safety and Quality Airbus Helicopters

- End of report –

ENCLOSURE 9

McGrath, BJ MRH90 Orientation Perceptual Study V1.0 22 Oct 24

28 July 2023
MRH-90 Taipan
173rd Special Operations Aviation Squadron, 6 AVN REGT
Night Formation Flight
Lindeman Island, Queensland

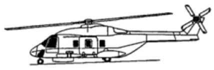

4 FATALITIES

An estimate of pilot perception of spatial orientation was calculated from flight data recorder aircraft data at the request of Defence Flight Safety Bureau (DFSB), Defence Aviation Safety Authority.

Modelling of a pilot's perceived spatial orientation represent a classic bioengineering problem and there exist many examples in the vestibular sciences literature that have been shown to successfully model many aspects of spatial orientation perception. Since 1996, the author of this report has responded to requests from civilian and military accident investigation organizations to provide perceptual modelling and analysis of mishaps using a spatial orientation perception mishap analysis tool originally developed by the US Navy [1]. This mishap analysis tool uses data processing, mathematical models, fuzzy logic, and animation techniques to produce 3-D animations of mishaps where pilot spatial orientation is suspected as a contributing factor and described in the following 4-step the process:

- Step 1: Gather Flight Data Recorder (FDR), pilot state, and environmental data
- Step 2: Input the angular and linear acceleration of the aircraft into two spatial orientation models to produce an initial estimate of pilot perceived orientation
- Step 3: Refine the initial orientation estimation with SME input into rule based fuzzy-logic system
- Step 4: 3D animation of pilot perceived orientation vs actual aircraft orientation and pilot position.

Estimated Perceived Pilot Orientation

For purposes of the analysis of the 2023 MRH-90 mishap, the flight is broken up into three phases (Figure 1):

- The first phase represents the phase of the flight that sets pre-conditions and consists of the left turn to a heading of 140 degrees [12:35:31 – 12:36:07]. [circle-star]
- The second phase represents the phase of the flight that contains the Top Event[2] and encompasses the climb [12:36:07 - 12:36:19]. [star-square], and
- The third phase represents the phase when the consequences are occurring and consists of the dive after the maximum altitude is reached [square-impact].

The critical phase of the flight was the climb in phase 2, and the Top Event occurs during this phase.

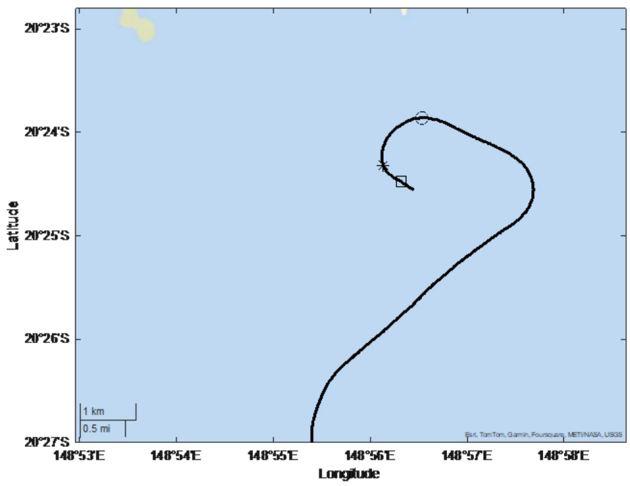

***Figure 1**: Flight Plan*

[1] McGrath, B. J., Rupert, A. H., and Guedry, F. E., "Analysis of Spatial Disorientation Mishaps in the US Navy," Spatial Disorientation in Military Vehicles: Causes, Consequences and Cures, RTO-MP-086, 2003, pp. 10-1 to 10-12.
[2] The Top Event is the central event in risk assessment sitting between causes and consequences and represents the point where control over a hazard is lost.

Top Event: *Phase 2: End of turn and climb [12:36:07 – 12:36:19 (~12 secs)].*

During Phase 2, the aircraft transitions from an altitude of ~220 ft to an altitude of ~362 ft (Figure 2).

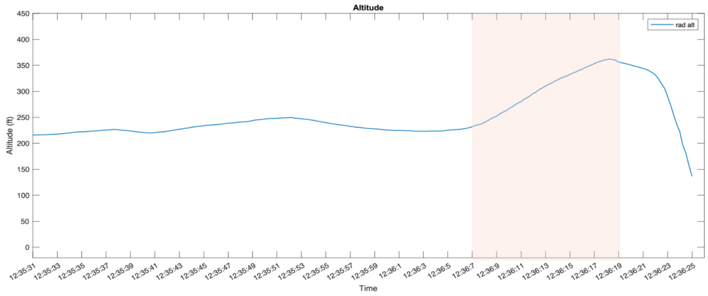

***Figure 2**: Aircraft Altitude – Phase 2 (Red Shaded Region)*

The following assumptions were used in the modelling analysis:

- No visible horizon
- Flying pilot (FP) and Non-Flying (NFP) are using Night Vision Systems (NVS)
- FP on the controls is maintaining formation flight by looking "outside" at BSMN82.

Figure 3 shows the actual aircraft pitch from Step 1 detailed above, the initial FP perceived pitch calculated from Step 2, and the more precise estimate of FP perceived pitch calculated in Step 3. During the climb, the actual aircraft pitch transitions from a nose up of ~+5 degrees to a nose down of ~-5 degrees crossing helicopter zero pitch at 12:36:11 (Figure 3, red solid line). The two mathematical models of pilot perceived orientation used in the analysis (Figure 3, blue dotted and dashed lines) are in good agreement and these results are then used to calculate the estimated FP perception of a nose up pitch of ~+5 degrees throughout this phase (Figure 3, blue solid line).

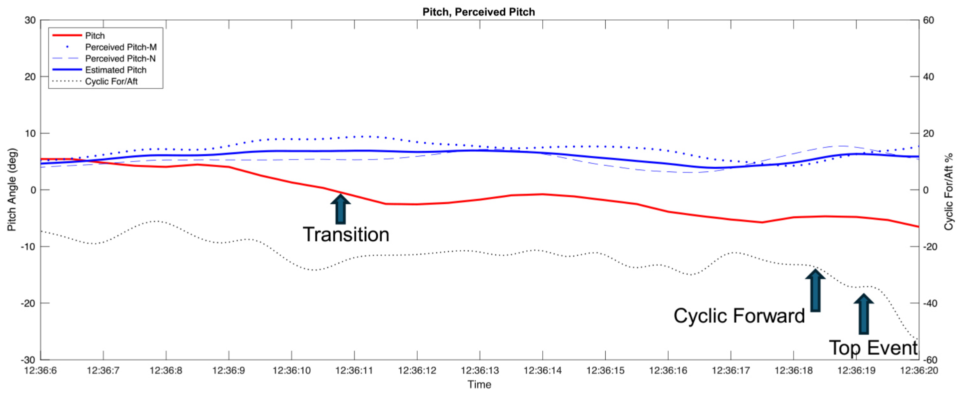

***Figure 3**: Aircraft Actual, Initial Perceived, and Estimated Perceived Pitch – Phase 2*

During the climb, the FP was likely deprived of meaningful visual orientation cues, prompting the brain to rely on the vestibular system and skin, muscle, and joint sensors to determine the body's orientation. As observed, these sensors failed to detect a reversal in pitch angle of the aircraft from approximately +5 degrees nose up to about -5 degrees nose down. Given the limited external visual cues, including the orientation of BSMN82, and high workload, it is highly probable that the FP struggled to accurately gauge the pitch angle. Consequently, conditions were disposed for the FP to perceive a pitch up attitude, as opposed to the actual aircraft pitch down attitude, leading to a loss of spatial orientation. This misperception of pitch resulted in two inappropriate pitch-down cyclic control inputs (Figure 3, black dotted line), the input at 12:36:19 being the top event ultimately causing an unrecoverable aircraft dive.

The undetected pitch attitude reversal, combined with unsafe control inputs and the absence of communication, strongly supports the occurrence of Type I spatial disorientation (unrecognised).

This mishap illustrates a tragic accident in which a series of events led to a physiologically normal misperception of pitch by the FP and more than likely the NFP, as both pilots were exposed to the same acceleration forces coupled with a lack of visual orientation information. Across the FVEY countries, we continue to lose skilled pilots and aircraft each year. Even the most dedicated and highly professional pilots are not immune to experiencing a loss of spatial orientation. Such loss of spatial orientation is a normal physiological response to acceleration forces in the absence of visual orientation cues.

I. Introduction

The safety of the aircraft and the ability to perform the aircraft's mission depends upon the pilot having an accurate awareness of the current situation, including the state of the aircraft, mission goals, external conditions, other aircraft, and other hostile factors. Without this situation awareness, the pilot will be unable to effectively perform the mission. Although loss of situation awareness is not restricted to the aviation environment, when it occurs during flight, the consequences are more severe, frequently resulting in loss of life and/or aircraft.

The first and critical step in acquiring and maintaining situation awareness is to perceive the status, attributes, and dynamics of elements in the environment (Figure 4, Level 1, shaded region).

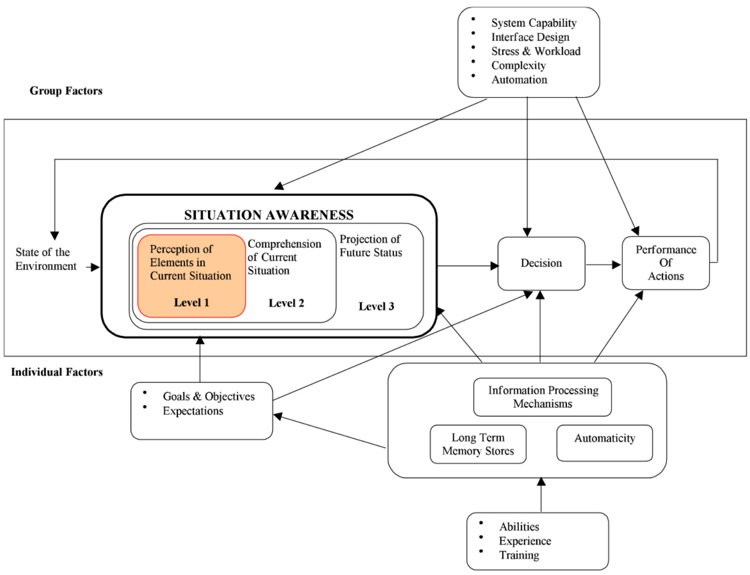

Figure 4: *Model of situation awareness[3].*

For aviation, a pilot perceives elements such as aircraft attitude, altitude, or motion relative to the earth or other significant objects.

FVEY AFIC INFORMATION PUBLICATION ASM 3009 Ed 1 v3 provides the following definition of spatial disorientation: …a term used to describe a variety of incidents occurring in flight where the aviator fails to sense correctly the position, motion or attitude of the aircraft or of him or herself within the fixed co-ordinate system provided by the surface of the earth and the gravitational vertical. In addition, errors in perception by the aviator of his or her position, motion or attitude with respect to his or her aircraft, or of his or her own aircraft relative to other aircraft, may also be embraced within a broader definition of spatial disorientation in flight.

As defined above, spatial disorientation leads to a loss of spatial orientation that in turn leads to an inaccurate percept of Level 1, resulting in the pilot experiencing a loss of situation awareness that can have severe and costly consequences.

In summary, a pilot who has an erroneous perception of aircraft orientation (spatial disorientation) always incurs a loss of situation awareness, but loss of situation awareness can occur for many different reasons in the absence of any spatial disorientation.

Mishaps due to the loss of orientation have occurred ever since the terrestrial human entered the dynamic aeronautical environment. As long as early aviators could maintain clear visual reference with respect to the ground or horizon, orientation did not pose a significant problem. However, "cloud flying" and other forms of flight in reduced visibility claimed many early aviators' lives[4]. The incidence of spatial disorientation resulting in a loss of situation awareness mishap declined when pilots began to receive the appropriate training in the correct use of aircraft instruments, including the attitude indicator and the

[3] Endsley MR. (1995). Toward a theory of situation awareness in dynamic systems. Hum Factors, 37(1):32- 64. 2Ocker WC, Crane CJ. (1932). Blind flight in theory and practice. San Antonio, TX: The Naylor Company. 3Stark HC. (1935). Instrument flying. Poughkeepsie NY. Howard C. Stark.
[4] Ocker WC, Crane CJ. (1932). Blind flight in theory and practice. San Antonio, TX: The Naylor Company.

turn indicator[5]. However, spatial disorientation mishaps have not been eliminated completely, because the attitude indicator is a foveal visual instrument, and only provides orientation awareness when the aviator repeatedly looks at the instrument for sufficient time to see and cognitively process the information. In today's military aviation missions, there is an added emphasis on high workload, night flying, formation, all weather capability, and low altitude missions, which are all factors that may increase loss of spatial orientation due to reduced ability to repeatedly look at the attitude indicator. For pilots to maintain spatial orientation in the dynamic aviation environment, they must centrally integrate enough sensory information and then develop/select an appropriate pattern of muscular response. In the normal earth-bound terrestrial environment, information is provided by three relatively independent and redundant sensory - motor systems: visual, vestibular, and somatosensory (skin-muscles-joint) sensory system. On Earth, these redundant systems are so reliable that when disorientation occurs it can usually be attributed to sensory- motor pathology. In aerospace flight all these systems function; however, both the vestibular and somatosensory systems can only detect the resultant gravito-inertial force which the Central Nervous System (CNS) (based on all previous experience) incorrectly interprets as the direction of down.

In addition, flying generates angular motion outside normal terrestrial frequencies, resulting in inaccurate information from the vestibular angular rate sensors. Thus, acquisition of orientation information is left to the visual system that can also experience inadequacies or illusions in the aerial environment. Most spatial disorientation accidents occur when periods of visual distraction from instrument scanning such as during intense concentration on night, formation, all weather capability, and low altitude missions or cockpit emergencies permit the perception of inaccurate skin-muscle-joint and vestibular stimuli.

Of the three sensory-motor systems, the vestibular system is dedicated to detecting motion of the head and body relative to the earth and generating reflexive motor activity that improves motion control while motion is in progress. The vestibular system does not detect objects in the environment but rather serves to provide an Earth reference to visual and auditory images of objects, slopes and paths as the head changes position and orientation relative to the environment. Vision, audition, smell and touch often serve to locate and detect motion of objects relative to the body. Vision, especially, can project the need for future change in the path of movement. The vestibular system signals only the current state of body motion and indicates the need for change only by signalling a current state of emergency, such as falling. Sensory messages from muscles and joints and tactile information are more closely allied to the vestibular system in detecting the direction of gravity, maintaining balance and aiding control of motion relative to the earth.

The definition of spatial disorientation corresponds to an inaccurate, or loss of, perception of the elements in the current situation (Figure 1, Situation Awareness Model, Level 1). The first and critical step in maintaining situation awareness is to maintain spatial orientation (Figure 1, Level 1, shaded region). Therefore, understanding and/or predicting a pilots' spatial orientation perception is a critical factor in preventing loss of situation awareness mishaps.

While there are many situations that contribute to spatial disorientation, the most common is when a pilot looks away from the aircraft's orientation instruments and the horizon. Most spatial disorientation mishaps are not due to radical maneuvers. When a pilot looks away from the horizon (loss of focal and peripheral visual cues) or looks away from the attitude indicator in instrument meteorological conditions (loss of focal visual cues), the Central Nervous System (CNS) computes spatial orientation with the remaining information at its disposal; vestibular and somatosensory. This vestibular and somatosensory information is redundant but frequently incorrect. In such circumstances, it is a physiologically normal response to experience spatial disorientation.

Aviators are instructed to use a strategy of visual dominance, where visual orientation cues - at the exclusion of all other sensory cues - must be used to avoid spatial disorientation [6]. When pilots have a clear view of the horizon, peripheral vision provides visual orientation cues through normal neural pathways. However, without a clear view of the horizon, visual orientation cues are obtained through focal vision of the attitude indicator, and because of training and experience are integrated cognitively to maintain spatial orientation. Pilots have learned to interpret the symbolic focal visual information on the attitude indicator and other flight instruments to develop a concept of where they are, what they are

---

[5] Stark HC. (1935). Instrument flying. Poughkeepsie NY. Howard C. Stark.
[6] Gillingham KK, Previc FH. Spatial orientation in flight. In RL DeHart (Ed.), Fundamentals of aerospace medicine. (2nd ed., pp. 309-398). 1996. Philadelphia: Lea & Febiger.

doing, and where they are going. As described by Langewiesche,[7] this complex talent must be developed through extensive training and maintained through practice; and it is the fragility of this concept that makes spatial disorientation such a hazard.

II. Spatial Disorientation Mishap Analysis System

Since 1996, the author of this report has responded to requests from civilian and military accident investigation organizations to provide perceptual modelling and analysis of mishaps using a spatial orientation perception mishap analysis system originally developed by the US Navy[1]. This mishap analysis tool uses data processing, mathematical models, fuzzy logic, and animation techniques to produce 3-D animations of mishaps to support mishap boards in their investigations, provide insight into the problem of spatial disorientation in aviation, and to train aviators to avoid spatial disorientation mishaps.

The mathematical models used in the Spatial Disorientation Mishap Analysis (SDMA) system are based on literature and additional data from centrifuge, aircraft experiments, and aircraft mishaps over the previous 40 years and have proven adequate to address many types of mishaps and are described in the next section. Further research and development continue to enhance the mishap analysis tool to provide an accurate description of a pilots' perception in all aviation environments.

In addition to mathematical models, the complete mishap analysis process has data input, fuzzy logic, and 3D output components, the architecture for which is shown in Figure 5 and described below:

> SDMA Step 1: Using data from flight data recorders; eyewitness accounts; videotapes; and ground, ship, and aircraft radar transcripts, estimates of the 3-D angular position and velocity, and 3-D linear acceleration of the mishap aircraft are processed using the mathematical analysis software package, MatLab® (The MathWorks, Inc.). Aircraft performance data, pilot state data, and environmental conditions are also obtained and/or estimated.
>
> SDMA Step 2: Angular and linear acceleration of the aircraft are input into spatial orientation models (Merfeld[2], and Grissett[3]) to produce an initial estimate of the pilot's perceived orientation.
>
> SDMA Step 3: To enhance the accuracy and validity of the initial orientation results, additional data from sources such as pilot control inputs and expert mission advice are integrated into a rule-based fuzzy logic expert system. This step generates a more precise estimation of the pilot's perceived orientation.
>
> The vestibular system responds in a reasonably consistent manner to acceleration inputs, and in most in-flight situations provides an incorrect perception of orientation – i.e., spatial disorientation. The problem occurs when this misperception is not overcome using correct visual information in the flight environment that includes factors such as distraction, expectation, and experience. It is these later factors that need to be captured in the fuzzy logic/expert system modelling and used to modify the sensory model spatial disorientation predictions to calculate an improved estimate of perceived pilot orientation.
>
> SDMA Step 4: The improved estimation of the pilot's perceived orientation, along with actual aircraft flight data and pilot position, are then used to develop a 3-D animation of the mishap under consideration. This animation permits visualization of a complex problem.

[7] Langewiesche W. A Flier's World. 1943. (Internet) http://www.skygod.com/quotes/.

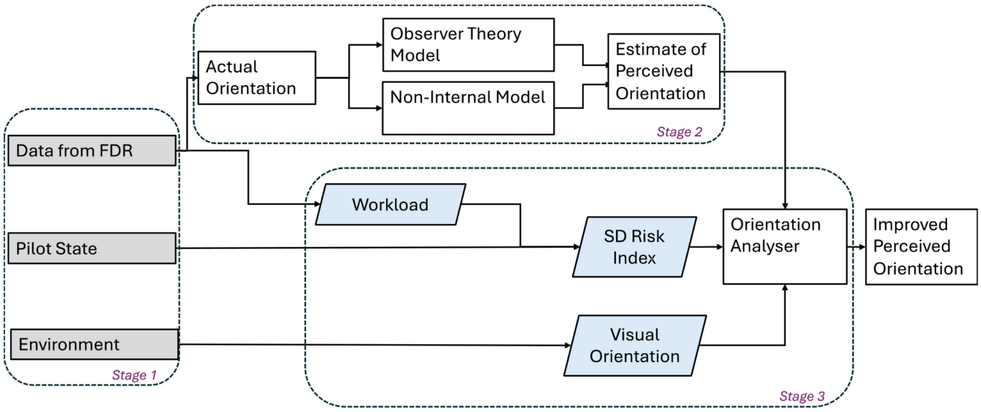

Figure 5: *Spatial Disorientation Mishap Analysis (SDMA) system architecture*

The SDMA system provides an intuitive tool that permits visualization of a complex problem. Previously, results from these analyses have been used in mishap board reports, Judge Advocate General (JAG) investigations, congressional hearings, and commercial television.

III Spatial Orientation Modelling

Modelling of a pilot's spatial orientation and predicting a pilots' perception of spatial orientation represent a classic bioengineering problem. There exist many examples in the vestibular sciences literature due to the importance of the vestibular system for orientation. These vestibular-based models can be grouped into two categories that are based on the underlying engineering formulation.

The first category of model is the "observer theory model" introduced by Young [8] and expanded by Oman[9]. These models are based on the hypothesis that the CNS includes internal models of sensory dynamics, body dynamics and physical relationships and only differ in their mathematical implementation (Figure 5). These models were developed to explain how the CNS integrates sensory information from disparate sensory modalities to estimate body motion and spatial orientation. Three types of internal models have emerged as the state-of-art models for human spatial orientation perception and include:

- An optimal estimator approach using Kalman filter techniques.
- A constant gain estimator.
- A sensory weighting technique. In this model, the central estimate of a physical variable is computed by a weighted averaging of multiple cues of available sensory information.

The observer theory models have been shown to successfully model many aspects of human spatial orientation perception and represent the majority of work in this field. The three types of models produce similar results however they differ in the following areas:

- The use of internal loops.
- The implementation of the gravito-inertial force resolution mechanism.
- The implementation of an idiotropic vector. An idiotropic vector is the tendency to perceive the vertical as oriented along the body axis.
- The use of visual inputs.

The constant gain estimator model developed by Merfeld and colleagues[10] implements a gravito-inertial force resolution mechanism where the estimate of gravity is constrained to have a constant norm. The other models (Kalman filter and Sensory weighting) do not. The Kalman Filter observer models [11] [12] [13]

[8] Young LR. (1970). On visual vestibular interactions. Proc. 5th Symposium of the role of the vestibular organs is space exploration. NASA SP 314:205-210.
[9] Oman CM. (1982). A heuristic mathematical model for the dynamics of sensory conflict and motion sickness. Acta Otolaryngol Suppl 392: 1–44.
[10] Merfeld DM, Young LR, Oman CM, Shelhamer MJ. (1993). A multidimensional model of the effect of gravity on the spatial orientation of the monkey. J Vestib Res 3(2):141-61.
[11] Borah, J., Young, L. R., and Curry, R. E., "Sensory Mechanism Modeling," AFHRL-TR-78-83, Air Force Human Resources Laboratory, Air Force Systems Command, Lowry Air Force Base, CO, 1978.
[12] Borah, J., Young, L. R., and Curry, R. E., "Optimal Estimator Model for Human Spatial Orientation. Representation of Three-Dimensional Space in the Vestibular, Oculomotor, and Visual System," Ann of the New York Academy of Sciences, V. 545, 1988
[13] Pommellet, P. E., "Suboptimal Estimator for the Spatial Orientation of a Pilot," Unpublished Masters Thesis, Massachusetts Institute of Technology, Cambridge, MA, 1990.

[14] [15] [16] [17] [18]use internal feedback loops that are defined by a gain followed by an integration term. This integration term originates from the formulation of the system model, because Gaussian noise is assumed to account for the uncertainties in the model regarding the variable to be estimated. The additional integration term leads to differences in optimal estimates compared to the sensory weighting model and observer model. The sensory weighting model by Zupan [19] includes an idiotropic vector that allows for the prediction of sinusoidal vertical and torsional components during yaw rotation about an Earth-horizontal axis.

The second category is the "non-internal model," which uses classical control theory to model the components of the vestibular system. Many authors have used this technique to describe eye movement responses of the vestibular system [20] [21] [22] [23]. None of these models explicitly include internal models of sensory dynamics, body dynamics, or physical relationships. Robinson[18] used a feedback loop to prolong the vestibular ocular reflex compared with the activity of the semicircular canal first-order afferent. Wearne[20] extended earlier models to implement the tendency of the eye movement rotation axis to shift toward alignment with gravity. These models were primarily designed to describe the vestibular ocular reflex responses with little emphasis on perception. Mayne[21] proposed a framework that explains how the information from the vestibular system is processed to give subjective orientation. This framework was the basis of a spatial orientation model implemented by Grissett [24].

The SDMA system uses a modified Merfeld[2] (observer model) and Grissett[3] (non-internal model) to produce an initial estimate of the pilot's perceived orientation.

IV. Fuzzy Logic

To enhance the accuracy and validity of the initial orientation results, additional data from sources such as pilot control inputs and expert mission advice are integrated into a rule-based fuzzy logic expert system to evaluate the effects of various environment and human factors on the pilot's performance and on risk of experiencing disorientation. To process the relevant inputs and estimate the outcome fuzzy logic is used to capture the imprecise nature of the human system.

The MATLAB® Fuzzy Logic Toolbox is used to create the fuzzy logic structure within the SDMA and the Toolbox provides a graphical interface to add or remove inputs, change the ranges of inputs, create the rules that establish the relationships between inputs and outputs, and assign relative importance to individual rules. For the purposes of this report, the higher-level aspects of the implementation such as the choice of inputs and outputs, division of these quantities into ranges, and the rules relating the inputs to the outputs are described below.

A fuzzy inference system is the framework where a set of inputs is evaluated using a set of rules to determine an output. The three inference systems in the SDMA system are:

- *Visual Orientation*: evaluates whether a pilot is receiving visual orientation information by considering the gaze location and the visibility of the horizon.
- *Workload*: evaluates pilot workload from various parameters including the pilot's actions and scan rate.
- *SD Risk Factor*: quantifies the effect of factors such as workload, fatigue, and flight experience to set the value of a multiplier used to increase the SD Risk Index.

[14] Bilien, V., "Modeling Human Spatial Orientation Perception in a Centrifuge Using Estimation Theory," S.M. thesis, Man- Vehicle Laboratory, Massachusetts Institute of Technology, Cambridge, MA, 1993.
[15] Kynor, D. B., "Disorientation Analysis and Prediction System," Final Report AFRL-HE-WP-TR-2002-0179, United States Air Force Research Laboratory, Wright-Patterson Air Force Base, OH, 2002.
[16] Selva, P., "Modeling of the Vestibular System and Nonlinear Models for Human Spatial Orientation Perception," Universit de Toulouse, Toulouse, 2009.
[17] Merfeld, D. M. and Zupan, L. H., "Neural Processing of Gravitoinertial Cues in Humans. III Modeling Tilt and Translation Response," Journal of Neurophysiology, Vol. 87, No. 2, 2002, pp. 819-833.
[18] Newman, M. C., "A Multisensory Observer Model for Human Spatial Orientation Perception," S. M. Thesis, Man-Vehicle Laboratory, Massachusetts Institute of Technology, Cambridge, MA, 02139.
[19] Zupan, L. H., Merfeld, D. M., Darlot, Christian: Using sensory weighting to model the influence of canal, otolith and visual cues on spatial orientation and eye movements. Biological Cybernetics 86(3): 209-230 (2002).
[20] Robinson DA. (1977). Vestibular and optokinetic symbiosis: an example of explaining by modeling. In: Baker R, Berthoz A, eds. Control of gaze by grain stem neurons, developments in neuroscience, Vol. 1. Amsterdam: Elsevier 49-58.
[21] Raphan T, Matsuo V, Cohen B. (1977). A velocity storage mechanism responsible for optokinetic nystagmus (OKN), optokinetic after-nystagmus (OKAN) and vestibular nystagmus. In: Baker R, Berthoz A, eds. Control of gaze by grain stem neurons, Amsterdam: Elsevier/North-Holland Biomedical Press, 37-47.
[22] Wearne S, Raphan T, Cohen B. (1999). Effects of tilt of the gravitoinertial acceleration vector on the angular vestibule- ocular reflex during centrifugation. J Neurophysiol 81: 2175–2190
[23] Mayne R. (1974). A systems concept of the vestibular organs. In: Kornhuber H (ed) Handbook of Sensory Physiology, vol VI., part 2: psychophysics, applied aspects and general interpretations. Springer, Berlin Heidelberg NY, pp 493–580
[24] Grissett, J. D., "Mathematical Model for Interaction of Canals and Otoliths in Perception of Orientation, Translation, and Rotation," NAMRL Special Report 93-5, Naval Aerospace Medical Research Laboratory, Pensacola, FL, 1993.

Visual Orientation

Aim. The aim of the Visual Orientation inference engine is to determine whether the pilot is receiving valid visual orientation information.

Inputs. In general, the inputs to this inference engine will be associated with: 1) an evaluation of the areas of interest containing the pilot's gaze, and 2) an assessment of the quality of visual information coming from these regions.

Outputs. The output from this inference engine is a parameter indicating the quality of visual orientation information that the pilot is receiving. This parameter determines when the pilot's perceived orientation, as determined by the CNS model, is reset to equal the actual aircraft orientation.

Method. The fuzzy logic structure involves two visual regions corresponding to: 1) attitude indicator, and 2) outside-cockpit view. The division of inputs for this example structure is provided in Figure 6

Attitude Indicator	
No	<0.25
Maybe	>0.25, <0.75
Yes	>0.75

Visibility	
Poor	< 0.5
Good	> 0.5

Outside View	
No	<0.25
Maybe	>0.25, <0.75
Yes	>0.75

Figure 6: *Division of Inputs into Categories for Resetting Pilot Orientation*

Using the division of inputs as provided in Figure 6, 6 rules to determine whether the pilot's perceived orientation should be reset to match that of the airplane is determined.

Rules. The output for each rule is an indication of whether reset should (1) or should not (0) be performed with an allowance for maybe (0.5) for certain inputs. The rules are summarized as follows:

Inputs that indicate the pilot orientation SHOULD be reset (1)

1. Yes *attitude indicator*
2. Yes *cockpit window* AND Good *visibility*

Inputs that indicate the pilot orientation SHOULD NOT be reset (0)

3. No *attitude indicator* AND No *cockpit window*
4. Yes *cockpit window* AND Poor *visibility*

Inputs that indicate the pilot orientation SHOULD MAYBE be reset (0.5)

5. *Maybe attitude indicator*
6. *Maybe cockpit window AND Marginal visibility*

Each rule is weighted equally in determining whether to reset the pilot orientation, except for the "maybe" rules that are given half the weight of the others. The weighted contribution from all factors are combined to determine whether the pilot's perceived orientation should be reset to be that of the airplane on a scale from 0 to 1 (no to yes). Since the output is a continuous function from 0 to 1, judgment must be made to determine whether factors less than unity should result in a reset of the pilot orientation. This is achieved by setting a cutoff value.

Workload

Aim. To evaluate the pilot's workload based on parameters available from the aircraft bus and expert mission advice. The workload estimate serves as an input to the SD Risk Factors inference engine.

Inputs. Seven (7) inputs are used to determine the level of pilot workload. The data from all these inputs are measurable quantities available from the aircraft data bus and validated against expert mission advice.

Outputs. A workload parameter that can range from 0 to 1 is the output.

Heading Change (deg/s)
Small <20
Medium >20, <40
Large >40

Aircraft Speed (%max)
Low <0.15
Medium>0.15, <0.95
High >0.95

Change in Speed (kt/s)
Small <0.5
Medium>0.5, <3
Large >3

Altitude Above Ground (ft)
Low <1000
Medium >1000, <5000
High >5000

Change in Altitude (ft/min)
Small <500
Medium >500, <1000
Large >1000

Pilot Control Actions
Low < 10%
Medium≥ 10%, ≤ 25%
High > 25%

G_z Load Stress
Large Negative <0.5
Medium Negative>0.5,<0.9
Low >0.9,<1.2
Medium Positive >1.2,<2.5
Large Positive >2.5

***Figure 7**. Division of Inputs into Categories Used for Workload Rules*

Rules. We have used the division of inputs as provided in Figure 6 to create 21 rules to estimate workload shown below. The workload output for each rule is divided into high (1), low (0), or medium (0.5) levels.

Inputs that indicate a high pilot workload (1)

1. Low *altitude*
2. Large *g-load stress*
3. High *pilot control actions*
4. High *aircraft speed*
5. Low *aircraft speed*
6. Large *aircraft speed change*
7. Large *altitude change*
8. Large *heading change*

Inputs that indicate a low pilot workload (0)

9. High *altitude*
10. Low *g-load stress*
11. Low *pilot control actions*
12. Medium *aircraft speed*
13. Small *aircraft speed change*
14. Small *altitude change*
15. Small *heading change*

Inputs that indicate a medium pilot workload (0.5)

16. *Medium altitude*
17. *Medium g-load stress*
18. *Medium pilot control actions*
19. *Medium aircraft speed change*
20. *Medium altitude change*
21. *Medium heading change*

We assign equal weights to each rule. Then, the weighted average contribution from all non-null rule evaluations is combined to determine a pilot workload estimate ranging from 0 to 1 (low to high workload).

SD Risk Factors

Aim. This inference engine sets the value of a multiplier used to increase the SD Risk Index to account for the deleterious effects of increased workload, fatigue, and flight experience.

Inputs. We use the following five inputs to determine the SD Risk Index: recent flight experience, hours awake, all flight experience, workload, and the workload integral.

Outputs. The output is a multiplier that increases the SD Risk Index to reflect the increased risks associated with high workload, fatigue, and flight experience.

Method. We use four inputs to determine SD Risk Index factor. Each input is divided into categories (membership functions) as shown in Figure 8.

Recent Flight Experience (hours within 12 months)	
Inexperienced	<100
Average	>100, <500
Highly experienced	>500

Hours Awake (hours)	
Low	<5.5
Average	>5.5, <14.5
High	>14.5

All Flight Experience (hours)	
Inexperienced	<500
Experienced	>500, <2000
Expert	>2000

Workload (no units)	
Low	<0.25
Medium	>0.25, <0.7
High	>0.7

Figure 8: *Division of Inputs into Categories for Pilot SD Risk Index Rules*

Rules. We have used the division of inputs as provided in Figure 8 to create 12 rules to estimate SD Risk Index:

Inputs that indicate decreased SD Risk (1)

1. Highly experienced *recent flight experience*
2. Low *hours awake*
3. Expert *all flight experience*
4. Low *workload*

Inputs that indicate increased SD Risk (0)

5. Inexperienced *recent flight experience*
6. High *hours awake*
7. Experienced *all flight experience*
8. High *workload*

Inputs that indicate average SD Risk (0.5)

9. Average *recent flight experience*
10. Average *hours awake*
11. Experienced *all flight experience*
12. Medium *workload*

Each rule is weighted equally in determining the effect on SD Risk Index *except* for the rules involving *All Flight Experience* (which receive half the weight as the other rules). The contribution from all non-null rules is combined by weight to determine SD Risk Index estimate ranging from 0 to 1.

III. Estimated Perceived Pilot Orientation –2023 MRH-90 Mishap

An estimate of pilot perception of spatial orientation of the 2023 MRH-90 mishap flight was calculated from flight data recorder aircraft data and expert mission advice using the SDMA system described above. For purposes of the analysis, the flight is broken up into 3 phases (Figures 9 and 10):

- The first phase represents the phase of the flight that sets pre-conditions and consists of the left turn to a heading of 140 degrees [12:35:31 – 12:36:07]. (Figure 9; circle-star), (Figure 10; green region)
- The second phase represents the phase of the flight that contains the Top Event[25] and encompasses the climb [12:36:07 - 12:36:19]. (Figure 9; star-square), (Figure 10; red region)
- The third phase represents the phase when the consequences are occurring and consists of the dive after the maximum altitude is reached (Figure 9; square-impact), (Figure 10; blue region).

The critical phase of the flight was the climb in phase 2, and the Top Event occurs during this phase.

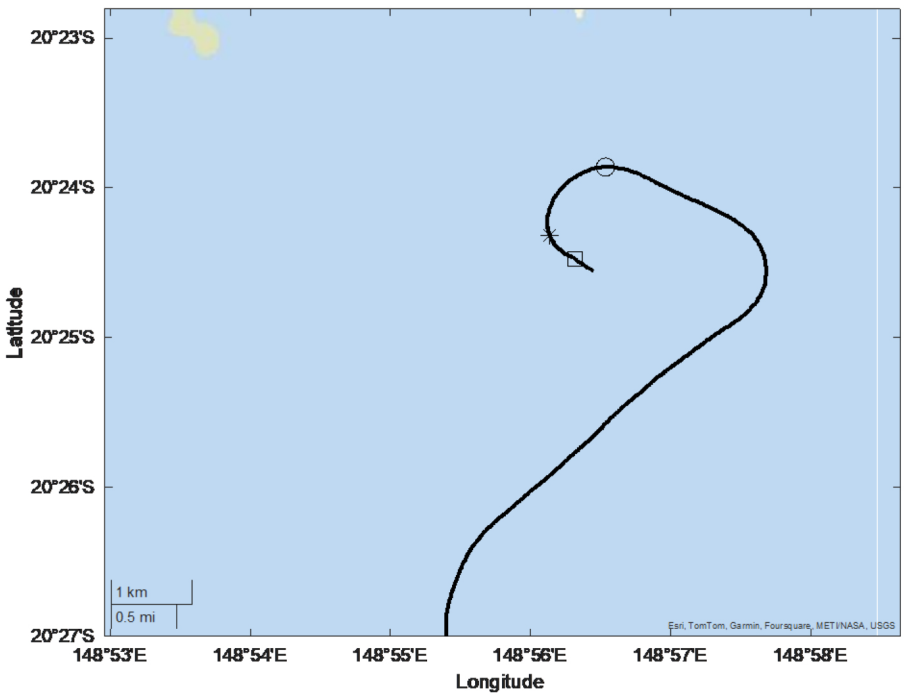

***Figure 9**: Flight Plan*

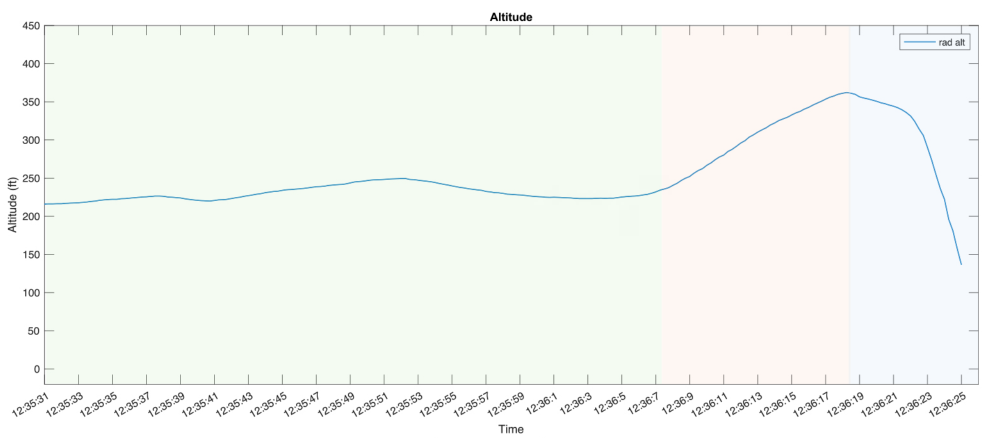

***Figure 10**: Aircraft Altitude*

[25] The Top Event is the central event in risk assessment sitting between causes and consequences and represents the point where control over a hazard is lost.

Phase 1: Left turn to a heading of 140 degrees [12:35:31 – 12:36:07].

BSMN83 makes a constant altitude of approximately 220 ft left turn (Figure 11).

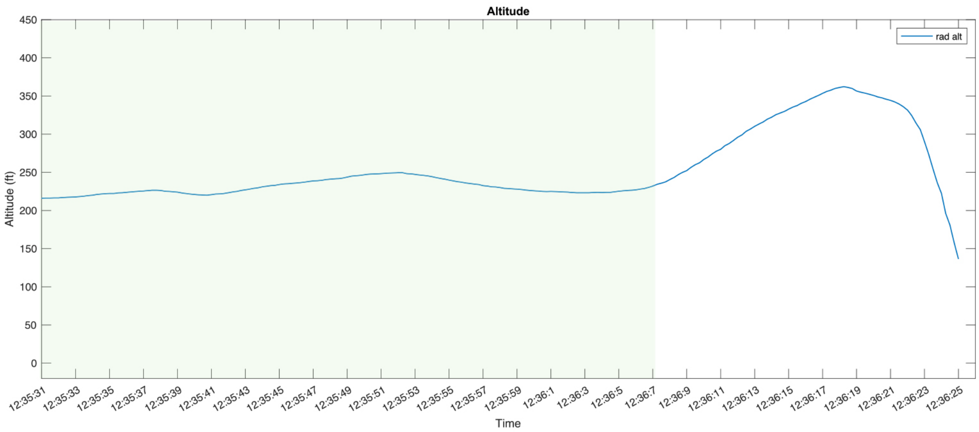

***Figure 11**: Mishap Aircraft Altitude – Phase 1*

Based on information provided by DFSB gathered from radio transcripts, pilot interviews from other aircrew in the flight formation, weather reports, and DSTG and DFSB simulator reconstruction flights, the following assumptions have been used in this phase to develop the SDMA inference systems outputs (Table 1):

- Reduced visible horizon.
- Flying pilot (FP) and Non-Flying (NFP) are using Night Vision Systems (NVS).
- FP on the controls is maintaining formation flight by looking "outside" at BSMN82.

Table 1: SDMA Inference Rules for Phase 1:

[green=selected, red = not selected]

Visual Orientation	*Pitch*	*Roll*
Inputs that indicate the pilot orientation SHOULD be reset (1)		
Yes attitude indicator	red	red
Yes cockpit window AND Good visibility	red	red
Inputs that indicate the pilot orientation SHOULD NOT be reset (0)		
No *attitude indicator* OR No *cockpit window*	green	red
Yes *cockpit window* AND Poor *visibility*	red	red
Inputs that indicate the pilot orientation SHOULD MAYBE be reset (0.5)		
Maybe attitude indicator	red	green
Yes cockpit window AND Marginal visibility	green	green

SD Risk	*Pitch*	*Roll*
Inputs that indicate decreased SD Risk (1)		
Experienced *recent flight experience*	green	green
Low *hours awake*	red	red
Expert *all flight experience*	green	green
Low *workload*	green	green
Inputs that indicate increased SD Risk (0)		
Inexperienced *recent flight experience*	red	red
High *hours awake*	green	green
Experienced *all flight experience*	red	red
High *workload*	red	red
Inputs that indicate average SD Risk (0.5)		
Average recent flight experience	red	red
Average hours awake	red	red
Experienced all flight experience	red	red
Medium *workload*	red	red

Workload	*Pitch*	*Roll*
Inputs that indicate a high pilot workload (1)		
Low *altitude*	green	green
Large *g-load stress*	red	red
High *pilot control actions*	red	red
High *aircraft speed*	red	red
Low *aircraft speed*	red	red
Large *aircraft speed change*	red	red
Large *altitude change*	red	red
Large *heading change*	red	red
Inputs that indicate a low pilot workload (0)		
High *altitude*	red	red
Low *g-load stress*	green	green
Low *pilot control actions*	red	red
Medium *aircraft speed*	green	green
Small *aircraft speed change*	green	green
Small *altitude change*	green	green
Small *heading change*	green	green
Inputs that indicate a medium pilot workload (0.5)		
Medium altitude	red	red
Medium g-load stress	red	red
Medium pilot control actions	green	green
Medium aircraft speed change	red	red
Medium altitude change	red	red
Medium heading change	red	red

Figure 12 shows the actual aircraft pitch from SDMA Step 1 detailed above, the initial FP perceived pitch calculated from SDMA Step 2, and the more precise estimate of FP perceived pitch calculated in

SDMA Step 3 during Phase 1. The actual aircraft pitch remains a constant nose up of approximately +5 degrees (Figure 12, red solid line). The results of the two mathematical models of pilot perceived pitch used in the analysis are in good agreement (Figure 12, blue dotted and dashed lines), and combined with Visual Orientation and SD Risk Index calculated in SDMA Step 3, the more precise estimate of FP perceived pitch is also a nose up pitch of approximately +5 degrees throughout this phase (Figure 16, blue solid line).

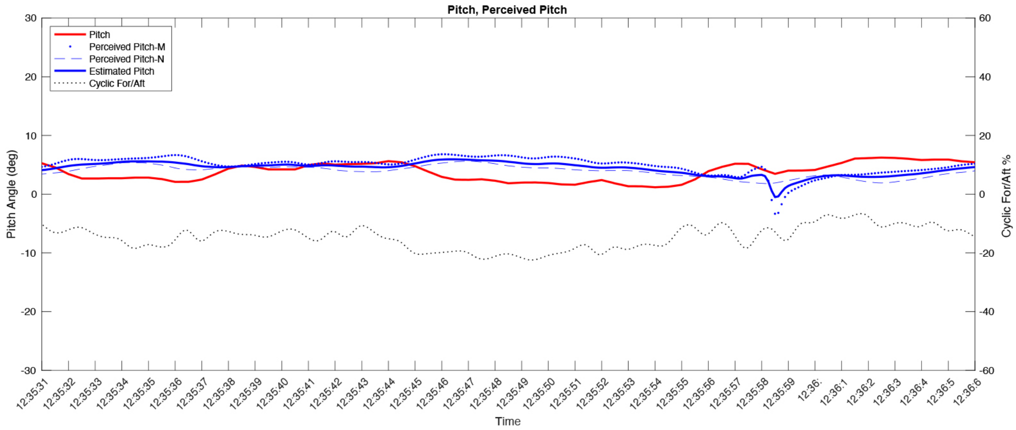

***Figure 12**: Mishap Aircraft Actual, Modelled Perceived, and Estimated Perceived **Pitch** – Phase 1*

Figure 13 shows the actual aircraft roll from SDMA Step 1 detailed above, the initial FP perceived roll calculated from Step 2, and the more precise estimate of FP perceived roll calculated in SDMA Step 3. During the left turn in phase 1, the actual aircraft maintains a roll left of approximately -10 to -20 degrees (Figure 13, red solid line). The mathematical model of pilot perceived roll used in the analysis predict a roll of approximately 0 degrees (Figure 12, blue dotted and dashed lines). Combined with Visual Orientation and SD Risk Index calculated in SDMA Step 3, the more precise estimate of FP perceived roll (Figure 18, blue solid line) conforms with the actual roll of the aircraft (Figure 18, red solid line).

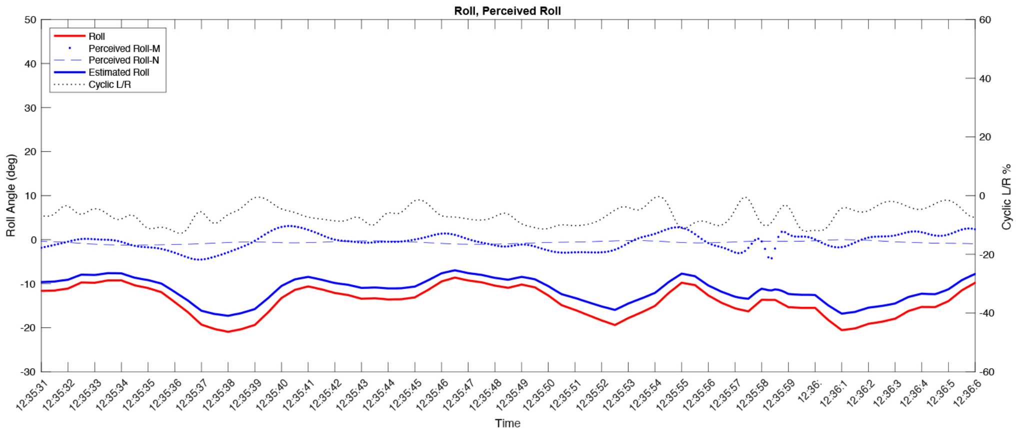

***Figure 13**: Mishap Aircraft Actual, Modelled Perceived, and Estimated Perceived **Roll** – Phase 1*

The analysis of pilot orientation during phase 1 is that the FP had a reasonable accurate perception of the aircraft orientation.

Phase 2: End of turn and climb [12:36:07 - 12:36:19].

BSMN83 makes a climb from approximately 220 ft to an altitude of 362 ft (Figure 14).

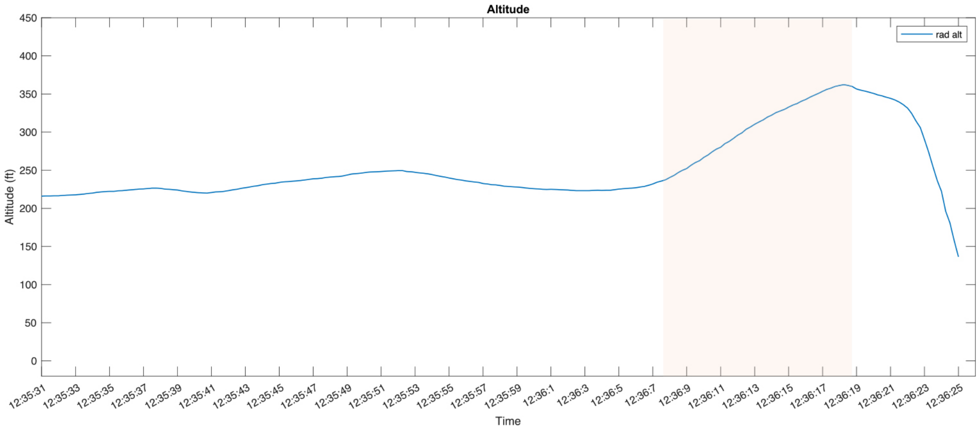

***Figure 14**: Mishap Aircraft Altitude – Phase 2*

Based on information provided by DFSB gathered from radio transcripts, pilot interviews from other aircrew in the flight formation, weather reports, and DSTG and DFSB simulator reconstruction flights, the following assumptions have been used in this phase to develop the SDMA inference systems outputs (Table 2):

- No visible horizon.
- Flying pilot (FP) and Non-Flying (NFP) are using Night Vision Systems (NVS)
- FP on the controls is maintaining formation flight by looking "outside" at BSMN82 and keeping BSMN82 in the centre of the visual scene.

Table 2: SDMA Inference Rules for Phase 2:

[green=selected, red = not selected]

Visual Orientation	*Pitch*	*Roll*
Inputs that indicate the pilot orientation SHOULD be reset (1)		
Yes *attitude indicator*		
Yes *cockpit window* AND Good *visibility*		
Inputs that indicate the pilot orientation SHOULD NOT be reset (0)		
No *attitude indicator* OR No *cockpit window*		
Yes *cockpit window* AND Poor *visibility*		
Inputs that indicate the pilot orientation SHOULD MAYBE be reset (0.5)		
Maybe attitude indicator		
Maybe cockpit window AND Marginal visibility		

SD Risk	*Pitch*	*Roll*
Inputs that indicate decreased SD Risk (1)		
Experienced *recent flight experience*		
Low *hours awake*		
Expert *all flight experience*		
Low *workload*		
Inputs that indicate increased SD Risk (0)		
Inexperienced *recent flight experience*		
High *hours awake*		
Experienced *all flight experience*		
High *workload*		
Inputs that indicate average SD Risk (0.5)		
Average *recent flight experience*		
Average *hours awake*		
Experienced *all flight experience*		
Medium *workload*		

Workload	*Pitch*	*Roll*
Inputs that indicate a high pilot workload (1)		
Low *altitude*		
Large *g-load stress*		
High *pilot control actions*		
High *aircraft speed*		
Low *aircraft speed*		
Large *aircraft speed change*		
Large *altitude change*		
Large *heading change*		
Inputs that indicate a low pilot workload (0)		
High *altitude*		
Low *g-load*		
Low *pilot control actions*		
Medium *aircraft speed*		
Small *aircraft speed change*		
Small *altitude change*		
Small *heading change*		
Inputs that indicate a medium pilot workload (0.5)		
Medium altitude		
Medium g-load		
Medium pilot control actions		
Medium aircraft speed change		
Medium altitude change		
Medium heading change		

Note increasing workload during the climb in phase 2.

Figure 15 shows the actual aircraft pitch from SDMA Step 1 detailed above, the initial FP perceived pitch calculated from SDMA Step 2, and the more precise estimate of FP perceived pitch calculated in SDMA Step 3. During the climb, the actual aircraft pitch transitions from a nose up of approximately +5 degrees to a nose down of approximately -5 degrees crossing helicopter zero pitch at 12:36:11 (Figure 15, red solid line, Figure 16). As seen in Figure 15, the results of the two mathematical models of pilot perceived pitch used in the analysis are in good agreement (Figure 15, blue dotted and dashed lines), and combined with Visual Orientation and SD Risk Index calculated in SDMA Step 3, the more precise estimate of FP perceived pitch is a nose up pitch of approximately +5 degrees throughout this phase (Figure 15, blue solid line).

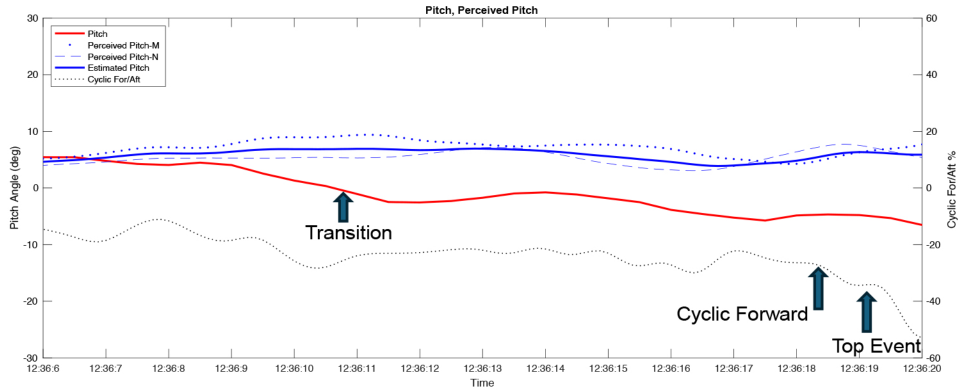

***Figure 15**: Aircraft Actual, Initial Perceived, and Estimated Perceived Pitch – Phase 2*

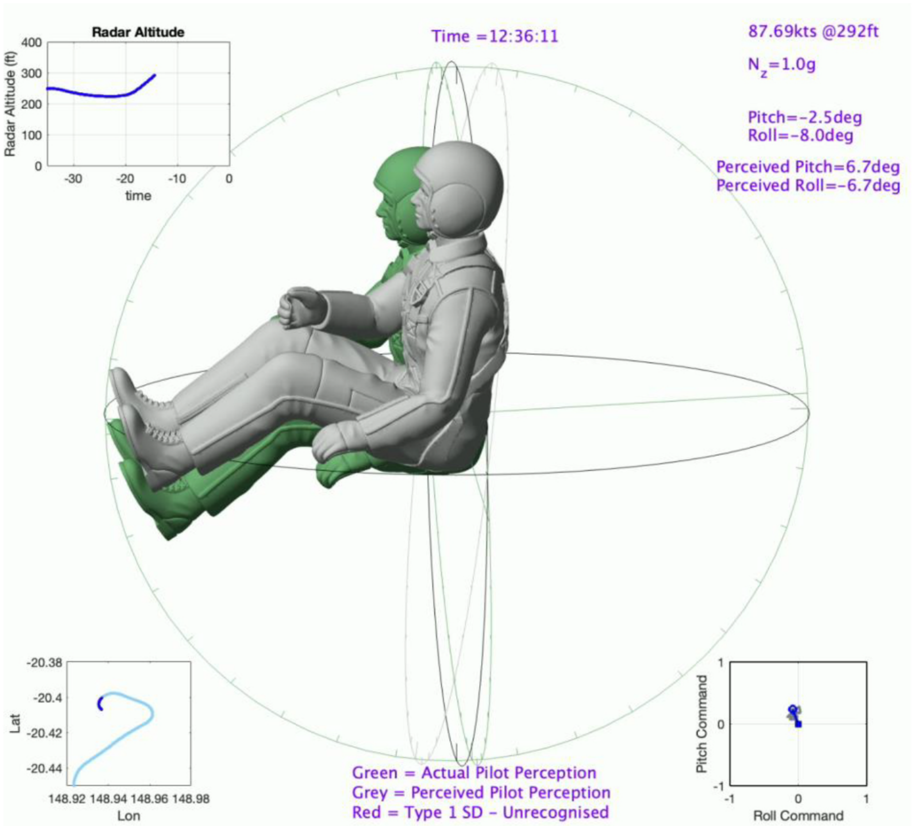

***Figure 16**: Pilot Actual and Estimated Pilot Perceived Orientation at 12:36:11*

The average threshold for detection of pitch rotation with an approximately 10 second stimulus is 2.0 – 3.3 degree/sec [26]. However, this average threshold range was measured in the laboratory. Anecdotal evidence from other mishaps investigated suggests that the threshold value is higher in a vibrating, high workload environment. During phase 2, the pitch rate was below threshold (Figure 17). Therefore, it is concluded that the FP would perceive an under-estimate of aircraft pitch attitude from their vestibular angular sensors.

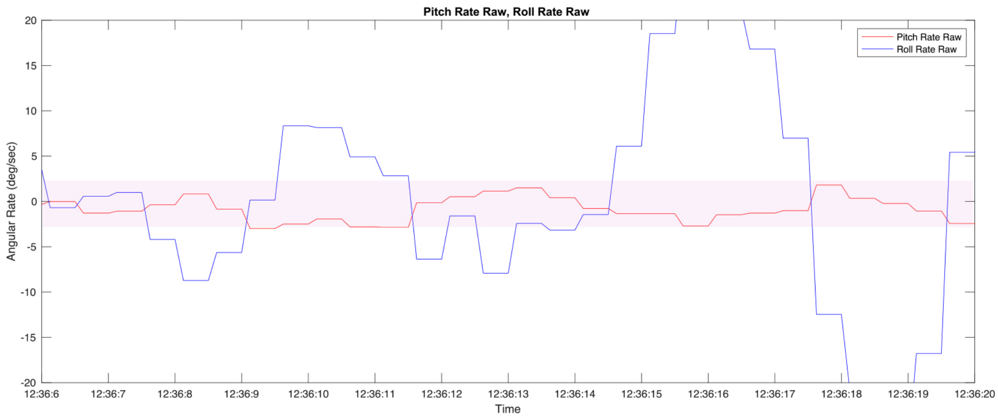

***Figure 17**: Mishap Aircraft Pitch and Role Rate with Threshold – Phase 2*

Figure 18 shows the actual aircraft roll from SDMA Step 1 detailed above, the initial FP perceived roll calculated from Step 2, and the more precise estimate of FP perceived roll calculated in SDMA Step 3.

During the climb, the actual aircraft maintains a roll left of approximately -10 degrees for the first 8 seconds and then the FP at 12:36:14 initiates a roll right manoeuvre to a roll right of approximately +20 degrees and then roll back to approximately level at 12:36:19 (Figure 18, red solid line). Combined with Visual Orientation and SD Risk Index calculated in SDMA Step 3, the more precise estimate of FP perceived roll (Figure 18, blue solid line) conforms with the actual roll of the aircraft (Figure 18, red solid line).

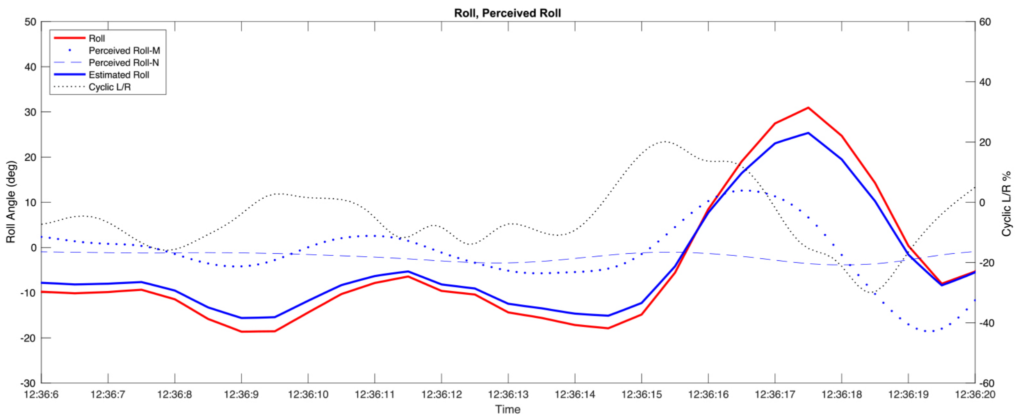

***Figure 18**: Mishap Aircraft Actual, Modelled Perceived, and Estimated Perceived **Roll** – Phase 2*

The average threshold for detection of roll rotation with an approximately 10 second stimulus is 2.0 – 3.3 degree/sec [27] and during this phase the roll rate was above the threshold (Figure 17), providing further evidence that the FP was correctly perceiving both the direction and the approximate magnitude of the aircraft roll.

[26] Benson AJ, Hutt EC, Brown SF. Thresholds for the perception of whole body angular movement about a vertical axis. Aviat Space Environ Med 60: 205–213, 1989

[27] Benson AJ, Hutt EC, Brown SF. Thresholds for the perception of whole body angular movement about a vertical axis. Aviat Space Environ Med 60: 205–213, 1989

During the climb in Phase 2, the FP was likely deprived of meaningful outside visual orientation cues, and it is highly probable that it would have been difficult for the FP to obtain a good estimate of the pitch angle attitude from the BSMN82 orientation.

Pilot performance has been shown to degrade when pilots need to integrate both external information (far-domain) and symbology information (near-domain). Research[28] shows that combining these two information sources can lead to interference in scanning patterns and distraction from external threats or obstacles[29]. In addition, high cognitive workload in the aviation environment often results in a narrowing of the visual attentional focus, where individuals concentrate on primary task (i.e. BSMN82 location) while secondary tasks (i.e. NVS pitch symbology) receive less attention[30]. This is known as "cognitive tunnelling". High workload may also be accompanied by reduced scan frequency[31], increased fixation duration[32], and less predictable scan patterns[33].

Research has shown HMD symbology can capture the pilot's attention, resulting in fixation on the display and reduced attention to external cues. This problem is exacerbated during critical manoeuvres, where quick transitions between near field and far domain views are required. This cognitive tunnelling limits the pilot's ability to maintain optimal scanning patterns for external awareness[34] [35]. Note that HMD performance research has primarily focussed on the transition from near domain symbology to far domain external views. Nevertheless, as the visual and cognitive processes are the same, it is appropriate to consider these research findings in the context of this mishap analysis where fixation on the far domain external view at the expense of comprehension of the near domain symbology is assumed.

Research also suggests that younger pilots tend to rely more on symbology, while older pilots perform better with scene information[36]. This indicates that individual differences can play a role in how efficiently pilots switch between symbology and external cues, with experience influencing adaptation to HMD systems.

Furthermore, the shift between different visual reference frames (far domain external views and near domain symbology) may degrade the pilot's awareness of spatial orientation, especially during dynamic tasks or in degraded visibility conditions[37] .

Given the high workload, limited external visual cues, cognitive tunnelling, and reduced scan frequency, it is highly probable that the FP struggled to accurately gauge the pitch angle using visual cues, thus prompting the brain to rely on the vestibular system and skin, muscle, and joint sensors to determine the body's pitch orientation. As modelled above, these sensors failed to detect a reversal in pitch angle of the aircraft from approximately +5 degrees nose up to about -5 degrees nose down. Consequently, the conditions were disposed for the FP to perceive a pitch up attitude, as opposed to the actual aircraft pitch down attitude, leading to a loss of spatial orientation. This misperception of pitch resulted in two

---

28 Overall, this research has been conducted with HUDs. Nevertheless, since they superimpose the ND on the FD, it is clearly appropriate to extrapolate from the HUD to the HMD (Yeh et al., 2003).

29 McAnulty, D. M., Hamilton, D. B., & Leedom, D. K. (1994). Individual Differences in Pilots' Perception of Simulated Night Vision Goggle Scene Imagery and Superimposed Flight Symbology. *Proceedings of the Human Factors and Ergonomics Society Annual Meeting*, *38*(15), 977-977

30 Wickens, C.D., Helton, W.S., Hollands, J.G., & Banbury, S. (2021). Engineering Psychology and Human Performance (5th ed.). Routledge. 2021.

31 Crundall, D., Underwood, G., & Chapman, P. (1999). Driving experience and the functional field of view. Perception, 28(9), 1075-1087.

32 Van Orden, K. F., Limbert, W., Makeig, S., & Jung, T. P. (2001). Eye activity correlates of workload during a visuospatial memory task. Human factors, 43(1), 111-121.

33 Di Stasi, L. L., Antolí, A., & Cañas, J. J. (2011). Main sequence: an index for detecting mental workload variation in complex tasks. Applied ergonomics, 42(6), 807-813.

34 Brewer, M. T. (2000). An Investigation of the Non-Distributed Flight Reference (NDFR) Ownship Status Symbology. https://apps.dtic.mil/sti/citations/ADA381862

35 Lorenz B, Tobben H, Schmerwitz S "Human performance evaluation of a pathway HMD", Proc. SPIE 5802, Enhanced and Synthetic Vision 2005, (25 May 2005)

36 McAnulty, D. M., Hamilton, D. B., & Leedom, D. K. (1994). Individual Differences in Pilots' Perception of Simulated Night Vision Goggle Scene Imagery and Superimposed Flight Symbology. *Proceedings of the Human Factors and Ergonomics Society Annual Meeting*, *38*(15), 977-977

37 Liggett, K. K., & Gallimore, J. J. (2001). The OKCR and Pilot Performance during Transitions between Meteorological Conditions Using HMD Attitude Symbology. *Proceedings of the Human Factors and Ergonomics Society Annual Meeting*, *45*(2), 115-119

inappropriate pitch-down cyclic control inputs (Figure 15, black dotted line), the input at 12:36:19 being the top event ultimately causing an unrecoverable aircraft dive (Figure 19).

The undetected pitch attitude reversal, combined with unsafe control inputs and the absence of communication, strongly supports the occurrence of Type I spatial disorientation (unrecognised).

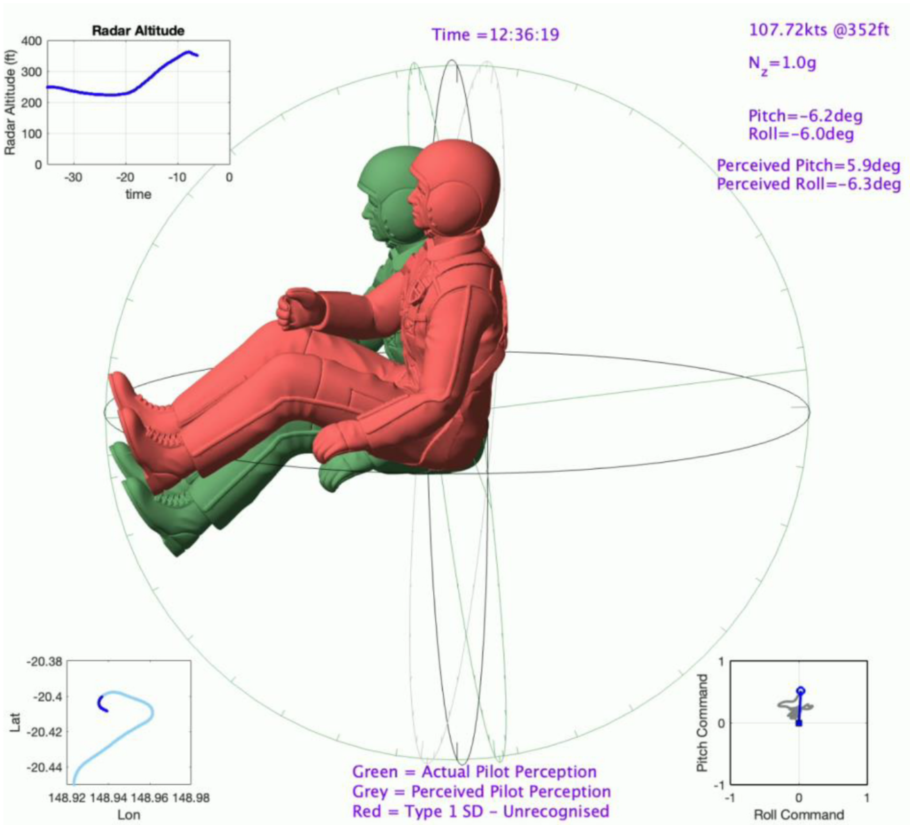

Figure 19: *Pilot Actual and Estimated Pilot Perceived Orientation at 12:36:19 - Type I spatial disorientation (unrecognised).*

Phase 3: Max Altitude to Impact (12:36:19 -> Impact)

During this phase, BSMN83 moves from an altitude of approximately 362 ft to impact (Figure 20).

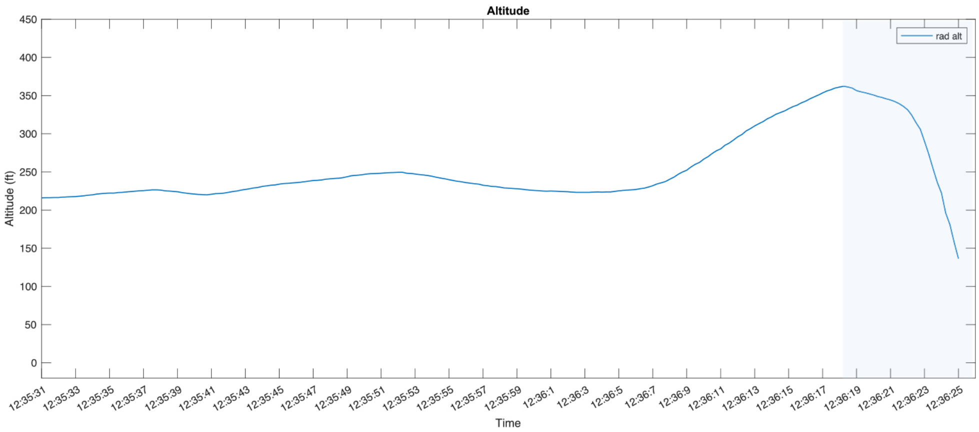

***Figure 20**: Mishap Aircraft Altitude – Phase 3*

Based on information provided by DFSB gathered from radio transcripts, pilot interviews from other aircrew in the flight formation, weather reports, and DSTG and DFSB simulator reconstruction flights, the following assumptions have been used in this phase to develop the SDMA inference systems outputs (Table 3):

- Reduced visible horizon.
- Flying pilot (FP) and Non-Flying (NFP) are using Night Vision Systems (NVS).
- FP on the controls is still looking “outside” trying to maintain visibility of BSMN82.

Table 3: SDMA Inference Rules for Phase 3:

[green=selected, red = not selected]

Visual Orientation	*Pitch*	*Roll*
Inputs that indicate the pilot orientation SHOULD be reset (1)		
Yes *attitude indicator*		
Yes *cockpit window* AND Good *visibility*		
Inputs that indicate the pilot orientation SHOULD NOT be reset (0)		
No *attitude indicator* OR No *cockpit window*		
Yes *cockpit window* AND Poor *visibility*		
Inputs that indicate the pilot orientation SHOULD MAYBE be reset (0.5)		
Maybe attitude indicator		
Maybe cockpit window AND Marginal visibility		

SD Risk	*Pitch*	*Roll*
Inputs that indicate decreased SD Risk (1)		
Experienced *recent flight experience*		
Low *hours awake*		
Expert *all flight experience*		
Low *workload*		
Inputs that indicate increased SD Risk (0)		
Inexperienced *recent flight experience*		
High *hours awake*		
Experienced *all flight experience*		
High *workload*		
Inputs that indicate average SD Risk (0.5)		
Average *recent flight experience*		
Average *hours awake*		
Experienced *all flight experience*		
Medium *workload*		

Workload	*Pitch*	*Roll*
Inputs that indicate a high pilot workload (1)		
Low *altitude*		
Large *g-load stress*		
High *pilot control actions*		
High *aircraft speed*		
Low *aircraft speed*		
Large *aircraft speed change*		
Large *altitude change*		
Large *heading change*		
Inputs that indicate a low pilot workload (0)		
High *altitude*		
Low *g-load*		
Low *pilot control actions*		
Medium *aircraft speed*		
Small *aircraft speed change*		
Small *altitude change*		
Small *heading change*		
Inputs that indicate a medium pilot workload (0.5)		
Medium altitude		
Medium g-load		
Medium pilot control actions		
Medium aircraft speed change		
Medium altitude change		
Medium heading change		

This phase would be characterized by extreme aircraft attitudes (> 20 nose down pitch, Figure 21) and excessive vertical velocity (> 3000 ft/min). Visual orientation cues would still be absent, vestibular orientation cues would still have a reversed pitch attitude, and the delay in transitioning from the Type I spatial disorientation (unrecognised) condition that occurred in phase 2 would preclude changing the outcome of the event.

Figure 21 shows the actual aircraft pitch from SDMA Step 1 detailed above, the initial FP perceived pitch calculated from SDMA Step 2, and the more precise estimate of FP perceived pitch calculated in SDMA Step 3. During the descent, the actual aircraft pitch transitions from a nose down of approximately -5 degrees to a nose down of over -20 degrees (Figure 21, red solid line).

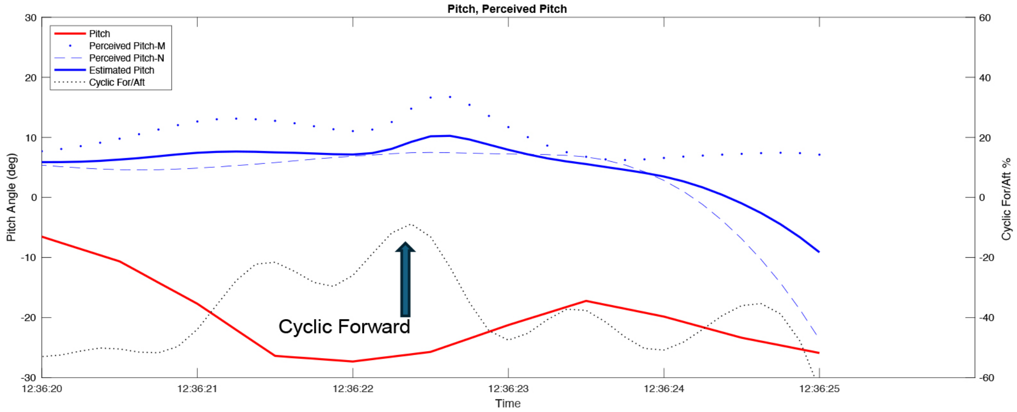

***Figure 21**: Mishap Aircraft Actual, Modelled Perceived, and Estimated Perceived **Pitch** – Phase 3*

The actual BSMN83 pitch down attitude would cause aircraft velocity to increase corresponding to a downward acceleration. This acceleration force when combined with gravity would result in an increasing positive pitch perception experienced by the FP, even though the aircraft is pitched down significantly (Figure 21)[38 39]. Of special note, at 12:36:22.5, the FP pushes the stick forward again, despite the aircraft being pitched down more than -20 degrees. The orientation model estimate, combined with this unsafe control input, strongly supports the Type I spatial disorientation (unrecognised) from phase 2 was still present during this phase (Figure 22).

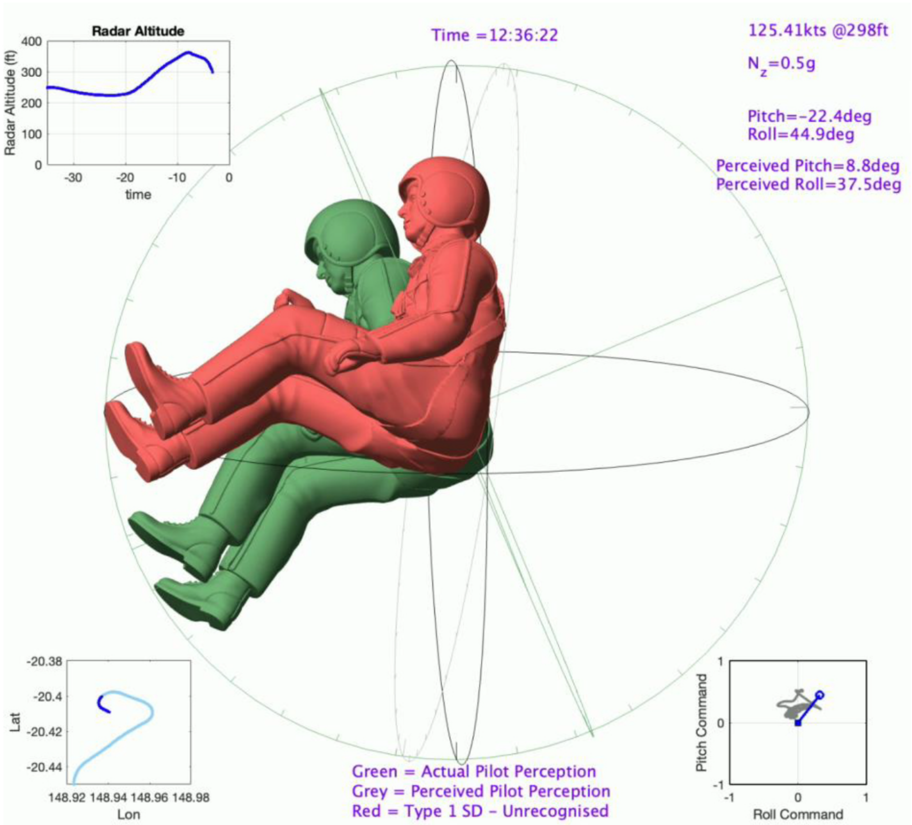

***Figure 22**: Pilot Actual and Estimated Pilot Perceived Orientation at 12:36:22 - Type I spatial disorientation*

[38] Iraq, CH-53 mishap 1996

[39] Hawaii UH-60 mishap

Furthermore, when Type I spatial disorientation (unrecognised) is identified and the pilot attempts to transition to an orientated state, research[40] has shown that when aircrew are disorientated, and attempt to transition to instruments, it can take time to recognise the disoriented state and recover correct orientation. Kraus[41] in an in-flight study looked at reports of spatial disorientation when the pilot was making a transition from outside to inside. Kraus showed that the average time for a pilot to transition from outside VFR to inside IFR in a two (2) aircraft formation was estimated to be 14 seconds.

Figure 23 shows the actual aircraft roll from SDMA Step 1 detailed above, the initial FP perceived roll calculated from Step 2, and the more precise estimate of FP perceived roll calculated in SDMA Step 3.

During the descent, the actual aircraft rolls right to approximately +50 degrees before reducing to a roll right of approximately +10 degrees prior to impact (Figure 23, red solid line). Combined with Visual Orientation and SD Risk Index calculated in SDMA Step 3, the more precise estimate of FP perceived roll (Figure 23, blue solid line) conforms with the actual roll of the aircraft (Figure 23, red solid line).

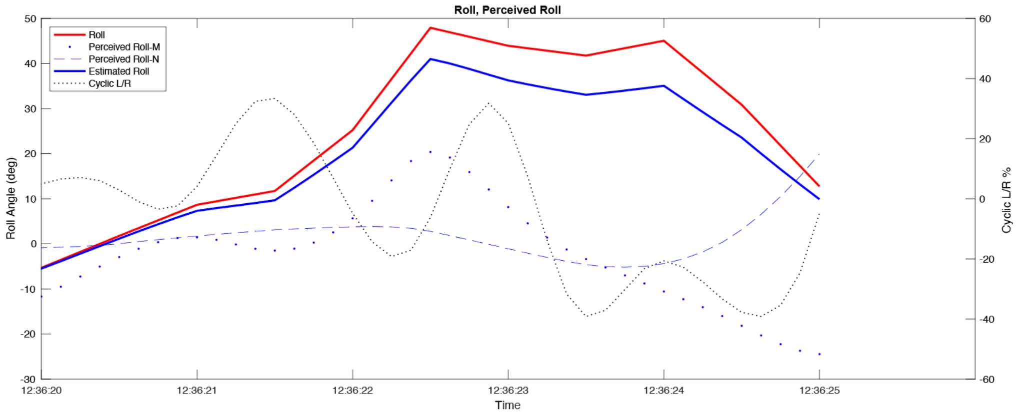

***Figure 23**: Mishap Aircraft Actual, Modelled Perceived, and Estimated Perceived **Roll** – Phase 3*

[40] Cheung, Bob. (2004). Nonvisual spatial orientation mechanisms. Spatial Disorientation in Aviation. 37-94.

[41] Kraus, R. N. 1959. Disorientation in flight, an evaluation of the etiological factors. Aerospace Medicine. 30,:664-673

Discussion

The foregoing analysis of the BSMN83 FP supports the occurrence of Type I spatial disorientation (unrecognised) during the climb phase from 220 to 362 ft. This loss of spatial orientation leads to control of the aircraft based on false perception of orientation. The first and critical step in maintaining situation awareness is to maintain spatial orientation (Figure 1, Level 1, shaded region). The resulting loss of situation awareness yields an inappropriate and unsafe control input leading to a mishap. This sequence of events - pilot is unaware of error in perception that leads to control based on false precept, leading to inappropriate control and aircraft mishap – and is shown as the grey shaded boxes in Figure 24.

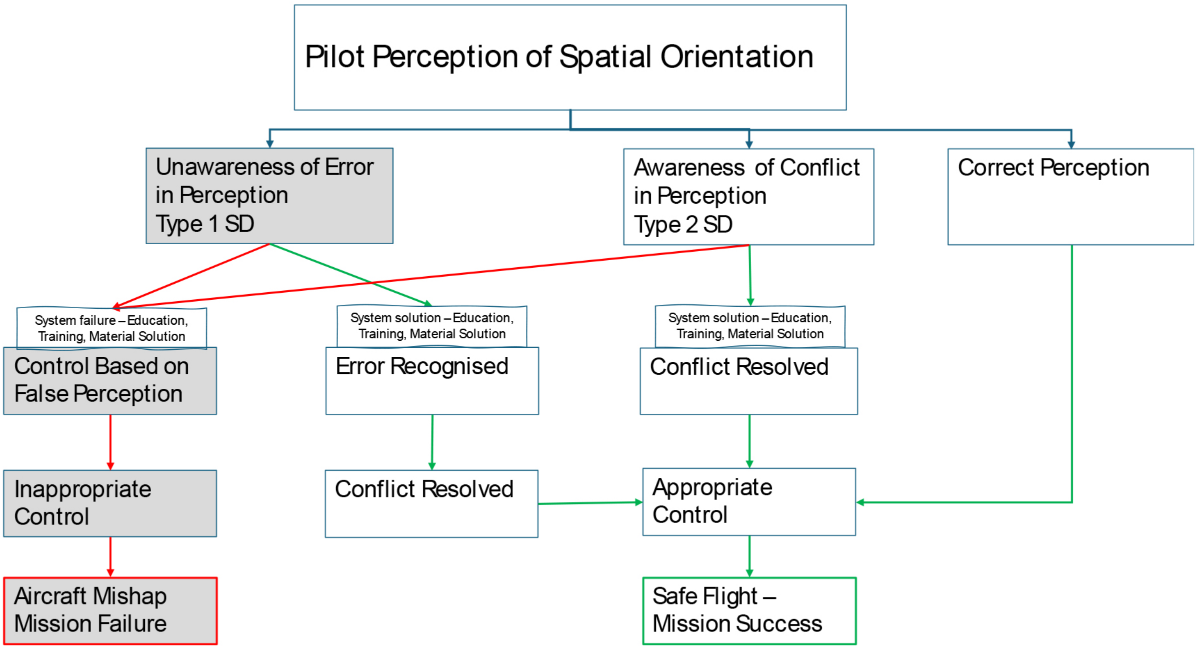

***Figure 24**: Illustration of how Type I and Type II spatial disorientation can influence the pilot's control of the aircraft (Modified from Benson[42])*

The MRH-90 mishap presented in this report is not a rare type of helicopter mishap. In a review of all US Navy and Marine Corps Class A rotary-wing mishaps for the period FY 1997-2002 [43], 29% were classified spatial disorientation mishaps and spatial disorientation mishaps were more deadly than other mishaps, with 71% of spatial disorientation mishaps claiming lives versus 43% of non- spatial disorientation mishaps. The influence of night vision devices appears to be an important factor in aviation mishaps, with 64% of all spatial disorientation mishaps occurring at night. More importantly, there has been little change in these statistics over the past 20+ years [44] [45].

The "typical" picture of rotary-wing spatial disorientation mishap is less one of a classical vestibular or visual illusion giving a pilot vertigo (classic spatial disorientation), but more one of an aircrew in a high workload environment, flying a systems intensive aircraft using NVSs in formation, failing to detect a dangerous flight path[46] (loss of spatial orientation leading to a loss of situation awareness). This is confirmed by the high proportion of spatial disorientation Type 1 accidents in rotary wing operations. The role of poor visual cues was highlighted by the relationship between spatial disorientation and night flight, and by the high percentage of accidents in which NVSs were considered to have played a part.

In the preceding perceptual analysis, the key assumption is that the pilot was NOT allocating attention to the primary flight display located heads down and was relying on the heads-up attitude symbology of the NVS. There are a multitude of contributory factors related to the high workload of a night formation flight in poor weather, and these factors are superimposed on a strong sensation of erroneous pitch created by several physical forces acting in concert. This assists in explaining why neither pilot directed sufficient attention to the primary flight display. It is often asked why the non-flying pilot does not

[42] Benson AJ. Spatial Disorientation – A Perspective Spatial Disorientation in Military Vehicles: Causes, Consequences and Cures, RTO-MP-086, 2003
[43] McGrath, B. J., & Rupert, A. H. (2004). Spatial disorientation in naval aviation rotary wing mishaps [Abstract]. Aviat Space Environ. April Supp, 57.
[44] Gibb R, Ercoline B, Scharff L (2011) Spatial disorientation: decades of pilot fatalities. Aviat Space Environ Med 82:717–724.
[45] Parker (2024) US Army Helicopter Mishap Summary. International Combat Safety Symposium, May 2024
[46] Durnford, Simon J. et al. "Spatial Disorientation: A Survey of U.S. Army Helicopter Accidents 1987-1992." (1995).

recognise the situation. Both pilots are exposed to the same set of physical forces and will have a similar perception provided they are not visual referring to the instruments. There are minor variations between individuals and minor deviations from the model may be expected based on differences in orientation of the head during manoeuvre, but overall, both crewmembers will have a similar perception of roll and pitch and experience the delays in transitioning from the disorientated state to an orientated state.[47]

Despite extensive efforts in spatial orientation research, education, training, and material solutions, spatial disorientation mishaps, especially Type 1 unrecognised, continues to have a significant impact on rotary wing operations, resulting in considerable crew and aircraft losses.

Current spatial orientation education primarily consists of didactic lectures emphasizing the anatomy and physiology of sensory systems but a more focussed on Type 2 recognised visual and vestibular illusions.

Significant training resources have been allocated to simulating various visual and vestibular illusions that pilots may experience in flight; however, spatial disorientation mishaps still occur. Pilots learn about spatial disorientation and how to manage the situation during instrument flying training with the ability to recover from unusual attitude of primary importance in preventing spatial disorientation mishaps, but experience gained during training and operational flight is limited, especially for Type 1 unrecognised situations.

To improve Type 1 unrecognised spatial disorientation education and training, pilots should be equipped with the skills to anticipate and assess the risk of spatial disorientation during mission planning. They should also be made aware of the physical and mental performance decrements that occur during sensory conflicts and inadequacies. Additionally, instructions should be provided on strategies to recover from spatial disorientation when a loss of orientation occurs. Special attention should be given to the characteristics of missions that are known to contribute to Type 1 unrecognised situations.

With the heavy demands placed on the pilot's visual sensory system in the modern cockpit, research has focused on material solutions that use other sensory systems for the presentation of orientation information to the pilot. The development of 3D audio displays and/or haptic (sense of touch) displays allows spatial orientation information to be provided to the pilot like how this information is naturally received on earth. Using 3D audio displays and/or haptic has been shown to enhance the accurate perception of aircraft orientation, situational awareness, and operational effectiveness. Despite these promising research results, none of these material solutions have reached operational status.

Across the FVEY countries, we continue to lose fine pilots and aircraft every year. Even the most dedicated, highly professional pilots are not immune to experiencing a loss of spatial orientation leading to a loss of situation awareness. It is a normal physiological response by all pilots to the acceleration forces that occurs in the absence of visual orientation inputs.

<u>Conclusion</u>

Based on the information provided, the analysis of the FP perception of BSMN83 aircraft attitude indicates that the conditions were present to create the situation in which the FP, and more than likely the NFP, in the absence of true visual orientation cues, experienced a misperception of pitch. Due in part to the compelling nature of this loss of spatial orientation and the task saturation associated with night formation flight, the FP did not perceive the true attitude of the aircraft. Indeed, based on the model prediction of the pilots' perception of pitch up as opposed to the actual aircraft being pitched down, the FP initiated control inputs that resulted in further aircraft pitch down deviations causing impact with the water.

The undetected pitch attitude reversal, combined with unsafe control inputs and the absence of communication, strongly supports the occurrence of Type I spatial disorientation (unrecognised).

Due to the low-level altitude, it is probable that the time needed to regain orientation by transitioning to instruments was insufficient to allow for appropriate control to prevent impact.

This mishap represents a tragic accident in which a series of events led to a physiologically normal misperception of pitch orientation by the pilot in control of the aircraft. Such loss of spatial orientation is a normal physiological response to acceleration forces in the absence of visual orientation cues.

[47] Tormes, F., & Guedry, F. (1974). Disorientation phenomena in naval helicopter pilots. Aviat Space Environ Med, 46, 387-393

Signed

Braden McGrath 22October 2024

Braden McGrath, PhD
FIEAust CPEng EngExec APEC Engineer IntPE(Aus)

About the Author:
Dr. Braden McGrath is an Enterprise Professor at University of Canberra. With a foundation in military medical research and development, Braden throughout the past 30 years in Australia and the United States has established a reputation as an interdisciplinary technology executive able to solve highly complex, human-focused system problems.

Braden is a Chartered Engineer in the Engineers Australia Colleges of Biomedical Engineering and Leadership and Management; a Fellow of Engineers Australia; a QinetiQ Fellow; and a member of the Society of Flight Test Engineers. Braden holds a Ph.D. in Aeronautical Engineering from the University of Sydney and a Master's in Aeronautics and Astronautics from Massachusetts Institute of Technology (MIT).

During his civilian career with the US Navy, Braden developed a Spatial Disorientation (SD) mishap analysis tool to support mishap investigations, to provide insight into the problem of SD in naval aviation, and to train aviators to avoid SD mishaps. The SD mishap analysis system provides an intuitive tool that permits visualization of a complex problem. Braden continues to be engaged by US and Australian governments to analyse the human factors considerations of aircraft mishaps using this SD mishap analysis tool. Braden was also a flight test engineer and successfully completed research, DT, and OE flight tests on T-34, UH-60, MH-53E, and Canadian NRC 206 aircraft, and CV-22 simulator. Not only did the flights involve substantial flying, 1000's of hours was spent in simulators prior to the actual flight developing plans, CONOPS, data integration and test pilot training. Braden has demonstrated a commitment to the safe execution of high-risk flight.

Selected Spatial Orientation Modelling Publications, Conference Proceedings, and Presentations:

- Rupert AH, McGrath BJ, Brill JC, Mortimer BJ. "Spatial Orientation Modeling: Expanding the Helicopter Envelope," 2023 IEEE Aerospace Conference, Big Sky, MT, USA, 2023
- McGrath BJ, Mortimer BJ, French J Drakunov S. "Mathematical Multi-Sensory Model of Spatial Orientation" Invited Paper. Proceedings, American Institute of Aeronautics and Astronautics conference on Guidance, Navigation and Control, San Diego, CA, USA, 4 - 8 January 2016
- Lawson, BD., McGrath, BJ., Newman, MC., & Rupert, AH. "Requirements for developing the model of spatial orientation into an applied cockpit warning system." Proceedings of the 18th International Symposium on Aviation Psychology, Dayton, OH, USA, 4-7 May 2015.
- McGrath BJ, Newman MC, Lawson BD, Rupert AH. "An Algorithm to Improve Ground-Based Spatial Disorientation Training". Proceedings, American Institute of Aeronautics and Astronautics conference on Guidance, Navigation and Control, Kissimmee, Florida, USA, 5 - 9 January 2015
- Newman, MC., Lawson, BD., Rupert, AH., Thompson, LB., McGrath, BJ. The orientation modeling system (OMS): Description of the user interface. Fort Rucker, AL: U.S. Army Aeromedical Research Laboratory Technical Report No. 2014-09. Sept 2014.
- Newman MC, Lawson BD, McGrath BJ, Rupert AH. "Perceptual Modeling as a Tool to Prevent Aircraft Upset Associated with Spatial Disorientation" Proceedings, American Institute of Aeronautics and Astronautics conference on Guidance, Navigation and Control, National Harbor, Maryland, USA, 13-17 January 2014
- Newman MC, Lawson BD, Rupert AH, McGrath BJ. "The role of perceptual modeling in the understanding of spatial disorientation during flight and ground-based simulator training". Proceedings, American Institute of Aeronautics and Astronautics on Guidance, Navigation and Control, Minneapolis, MN, 15 August 2012
- Beaton, KH, McGrath, BJ, Rupert, AH, & McGrath, EA. (2007). Using spatial disorientation training to create a normative database for screening dynamic visual and vestibular abnormalities in military aviation [Abstract]. Aviation, Space, and Environmental Medicine, 78, 295-296.
- McGrath, B., & Rupert, A. (2006). Visualization of spatial disorientation mishaps in the US Navy: Case study [Abstract]. Aviation, Space, and Environmental Medicine, 77, 281-282.
- McGrath, B. J., Gierber, G., & Rupert, A. H. (2005). Spatial disorientation in naval aviation [Abstract]. Aviation, Space, and Environmental Medicine, 76(3), 240.
- McGrath, B. J., & Rupert, A. H., (2004). Spatial disorientation in naval aviation rotary wing mishaps [Abstract]. Aviation, Space, and Environmental Medicine, April Supp, 57.
- Dietz, A., Kynor, D., Berg, J., Audette, W., Hill, R., McGrath, BJ, & Robinow, D. (2004). Disorientation analysis and prediction system: Implementation and validation [Abstract]. Aviation, Space, and Environmental Medicine, April Supp, 132.
- McGrath BJ, Gierber G, Rupert AH. "Can We Prevent SD?" Approach, US Navy Safety Center, May-June 2004
- McGrath BJ, Guedry FE, Rupert AH. "Analysis of Spatial Disorientation Mishaps in the US Navy." Proceedings for NATO Symposium on Spatial disorientation in military vehicles: Causes, consequences and cures. April 2002, A Coruna, Spain
- McGrath BJ, Guedry FE, Oman CM, and Rupert AH. "Vestibulo-ocular response of human subjects seated in a pivoting support system during 3 Gz Centrifuge Stimulation", Journal of Vestibular Research, 5:331-334, 1995.
- Guedry FE, Rupert AH, McGrath BJ, Oman CM. "The Dynamics of Spatial Orientation During Complex and Changing Linear and Angular Acceleration". Journal of Vestibular Research, Vol 2, 259-283,1992.

ENCLOSURE 11

DFSB Supplementary Report 01/2024 Snapshot Survey Spatial Disorientation Survey Results 02 Oct 24

ENCLOSURE 11 TO
BP44206784

SNAPSHOT SURVEY

Spatial Disorientation Survey Results

Defence Flight Safety Bureau – Supplementary Report 01/2024

Authors
Dr Gerard J. Fogarty PhD

Mr Andrew Ee

Mr Ryan Cooper

Approval
Ryan Cooper
Deputy Director
Reporting, Intelligence and Research

Sponsor

Reporting, Intelligence and Research within the Defence Flight Safety Bureau (DFSB) of the Defence Aviation Safety Authority, Australia. Requests and enquiries should be addressed to dasa.registry@defence.gov.au.

CONTENTS

EXECUTIVE SUMMARY

The report provides an in-depth analysis of Spatial Disorientation (SD) items administered as a part of the 2024 Snapshot survey.

The Air Standard Coordination Committee (AIR STD 61/117/07) provides the following standardised definition of SD:

> *Spatial Disorientation is used to describe a variety of incidents occurring in flight where the pilot fails to sense correctly the position, motion, or attitude of the aircraft or of [themselves] within the fixed co-ordinate system provided by the surface of the earth and the gravitational vertical.*

In 2024, the Defence Flight Safety Bureau took the opportunity to gather information on SD experiences, including their frequency, severity and the effectiveness of SD training. It did so through the annual *Snapshot* survey, which collects data on a wide range of safety issues across the ADF aviation community. The section of *Snapshot* addressing SD events used a definition drawn from the *USAF Spatial Disorientation Survey* (Matthews et al., 2002) and a more recent (2022) survey administered by the RAAF Institute of Aviation Medicine.

> *The incorrect perception of one's linear and angular position and motion relative to the plane of the earth's surface or another aircraft that affected your performance, situation awareness or workload - however slight that effect may be*.

The key findings are summarised below:

- Overall. A significant proportion (86%) of respondents reported experiencing at least one of the 17 possible SD types or situations listed in the survey during the last three years on their primary aircraft type. 37% of respondents reported experiencing more than five of the SD event types.

- Top Three. The most frequently encountered SD types or situations were the Leans (53%), Loss of SA (52%), and Sloping Clouds or Terrain (44%).

- Recency and Severity of Latest SD Experience. 30% of respondents reported experiencing SD in the six month prior to the survey, and 43% of respondents had experienced SD in the previous 12 months. The majority of respondents rated the severity of their most recent SD event as ‘minor’ (flight safety not at risk). Only 2% of ‘most recent’ SD events were rated as ‘significant’ (flight safety not at risk but could have been jeopardised under different conditions) and no respondents rated their latest SD event as ‘severe’ (flight safety was at risk).

- Severity of Worst SD Experience. A noteworthy proportion of respondents (15%) rated their worst SD experience in the past 3 years as ‘significant’. A further 2% (18 respondents) rated their worst SD experience as ‘severe’. There were large differences based on respondents’ aircraft category. For example, the majority of ‘severe’ SD experiences were among the Rotary Wing (8 respondents) and Air Combat (7 respondents) categories.

  Difference between Aircraft Categories. There were differences in the most common types and frequency of SD between aircraft categories. There were also differences among the aircraft types within each category. The top three SD types or situations for each aircraft category were:

Heritage. Sloping Clouds or Terrain (36%), Loss of SA (36%), and Blending of Earth and Sky (27%).

Surveillance. Blackhole Approach (59%), the Leans (46%), Sloping Clouds or Terrain (39%).

Air Combat. The Leans (82%), Loss of SA (59%) and Blackhole Approach (47%) / NVD Related Illusions (47%).

Training. The Leans (65%), Loss of SA (57%) and Sloping Clouds or Terrain (55%).

Air Mobility. Blackhole Approach (65%), Sloping Clouds or Terrain (50%) and the Leans (46%) / Loss of SA (46%).

Rotary. NVD Related Illusions (61%), Undetected Drift (58%), and Loss of SA (55%).

- Type of SD Training. Most of the respondents (93%) reported completing some form of SD training, with the lecture format featuring strongly. Many respondents completed multiple forms of SD training. We were not able to explore the timing and sequencing of training.

- Effectiveness of SD Training. All aircraft types gave favourable ratings to training. Overall, approximately 72% found the training effective and a further 18% as helpful to some extent. The lowest (marginally) ratings came from the Rotary Wing and Air Mobility categories. Approximately 2% reported the training as Very Ineffective, 4% as Ineffective, 18% as Moderately Effective, 41% as Effective, and 31% as Very Effective.

- Implications This report provides Defence Aviation with a thorough understanding of SD experiences, including their frequency, severity and the effectiveness of SD training. This brief look at SD phenomena in Defence Aviation context indicates that all aircrew are susceptible to SD experiences. The data indicate that SD is an ongoing and significant hazard to military aviation. The report includes recommendations of the types of training that are likely to be effective in reducing SD-related safety events. The report closes with emphasising the need for SD preventative and recovery controls to extend beyond classroom-based training. This includes actions to anticipate, avoid and communicate SD risk factors within operational environments.

SECTION 1: INTRODUCTION

1. Spatial Orientation refers to 'the ability to develop an internal representation of an exterior space, including one's own position in that space' (Hunt, 2011, p. 167). In the literature on human intelligence, it belongs to the group of visual-spatial abilities. Earl Hunt, the author just quoted, is one of the few researchers who has studied spatial orientation. He summed up the state of play in these words:

> *Spatial orientation serves as a shining example of a cognitive skill that is socially important, for which there are wide individual differences.....but that has been almost ignored in research on intelligence' (p. 169).*

2. The reason for this neglect is that it is more difficult to study than other visual-spatial abilities (e.g. spatial memory) that researchers can explore quite easily in a standard laboratory. A search of the recent literature reveals that there has not been a lot of progress since Hunt wrote those words. Spatial Orientation is a construct that we still do not fully understand.

3. Spatial Disorientation (SD) in an aviation setting refers to a situation where pilots (and possibly other aircrew) have developed an incorrect perception of how they are oriented in relation to the ground and other aircraft. The sensory systems that provide information about our spatial orientation have become unreliable, usually because of confusing environmental circumstances. SD is a major cause of fatal aviation accidents. Much of what we know about the incidence of SD comes from aircraft mishap data. Matthews et al. (2002) estimated that between 1991 and 2000, 20-30% of US aviation accidents were due to SD, with a fatality rate three times that of non-SD accidents.

4. Matthews and his colleagues acknowledged the importance of mishap data in drawing attention to what was clearly a major human factors issue in aviation. To address this problem in a proactive fashion, they developed the *USAF Spatial Disorientation Survey* to learn more about the frequency with which pilots experience SDs and the effect SDs have on performance. Variations of this survey, along with newer surveys developed by other researchers have contributed to a growing body of knowledge on types of SDs, their causes, training methods, and preventive techniques (e.g., Poisson & Miller, 2014; Newman, 2007). There is no shortage of papers on the different types of SD, their prevalence, and their effects. The RAAF Institute of Aviation Medicine has conducted investigations of SD, paying particular attention to training methods that may help to prevent or overcome SDs.

5. In 2024, the Defence Flight Safety Bureau took the opportunity to gather information on the incidence of SDs, their severity, and the effectiveness of SD training. It was able to do that as part of the Annual Snapshot survey, which collects data on a wide range of safety issues across the ADF Defence aviation community.

6. This report summarises the findings of the Snapshot data relating to SDs.

SECTION 2: METHODOLOGY

7. The section of Snapshot addressing SD events used definitions drawn from the USAF Spatial Disorientation Survey (Matthews et al., 2002) and a more recent (2022) survey administered by the RAAF Institute of Aviation Medicine.

8. The introductory text to this section was as follows:

> *In this section, we are gathering information from aircrew who have experienced Spatial Disorientation (SD) events. This information will help us develop a more thorough understanding of the frequency and types of SD being experienced and may be used to inform appropriate countermeasures to reduce its impact.*

9. SD was defined as:

> *The incorrect perception of one's linear and angular position and motion relative to the plane of the earth's surface or another aircraft that affected your performance, situation awareness or workload - however slight that effect may be*.

10. All respondents were asked to rate the effectiveness of the SD training they had completed. Respondents then indicated whether they had undertaken Defence related flying duties **in the last three years**. To improve the prospects of accurate recall and hence reliable data, this item filtered out respondents who had no recent flying experience.

11. Respondents then indicated how frequently they had experienced a list of 17 SDs using a response scale with five options: Never (1), Rarely (2), Seldom (3), Occasionally (4), Frequently (5). To assist respondents, a description of each of the SDs was available. Appendix A shows the SD types and associated descriptors.

12. Respondents were also asked to rate the severity of their most recent SD experience and the severity of their worst SD experience. Respondents were advised to answer the SD frequency and severity questions based on their experience **over the past three years on their primary aircraft type.**

To Note: All percentages may not equal to 100% in tables due to rounding.

SECTION 3: RESULTS BY AIRCRAFT CATEGORY

13. The survey captured data from Snapshot aircrew respondents that indicated having undertaken Defence flying related duties in the last 3 years. Respondents were categories based on the selection of their primary aircraft type. Respondent that did not select a primary aircraft type were excluded from the analysis.

14. A total of 831 respondents met the above criterion representing 25 Defence Aviation aircraft types that were assigned to seven aircraft categories: Heritage (N = 11), Surveillance (N = 56), Air Combat (N = 145), Training (N = 132), Air Mobility (N = 124), Rotary Wing (N = 337), Other (N = 16).

15. Preliminary analyses of the SD results revealed that for all 17 SDs the 'never' and 'rarely' response categories captured the vast majority of responses. For example, the percentage who selected 'Frequently' was never above 2% for any of the 17 SDs. Given this lopsided outcome, for subsequent analyses the response categories were collapsed to form a dichotomy where the 'Never' responses were scored as '0' and the 'Rarely' ,'Seldom', 'Occasionally', 'Frequently' responses were scored as '1'.

Experience of SD Types

16. Table 1 displays the results for each of the 17 SD types listed in the survey by aircraft category.

Table 1. Percentage Experiencing SDs by Aircraft Category

SD Type	Total	Pilots only	Heritage	Pilots only	Surveillance	Pilots only	Air Combat	Pilots only	Training	Pilots only	Air Mobility	Pilots only	Rotary	Pilots only	Other	Pilots only
N (Overall)	821	649	11	11	56	54	145	115	132	129	124	124	337	203	16	14
Leans	53%	56%	18%	18%	46%	48%	82%	83%	65%	64%	46%	46%	42%	49%	19%	21%
White out	12%	12%	0%	0%	11%	11%	10%	9%	8%	8%	15%	15%	14%	16%	7%	8%
Blending	40%	43%	27%	27%	32%	33%	36%	37%	44%	45%	39%	39%	44%	54%	7%	8%
Sloping	44%	49%	36%	36%	39%	41%	46%	50%	55%	55%	50%	50%	40%	48%	27%	23%
Coriolis	24%	25%	9%	9%	13%	13%	38%	39%	36%	37%	19%	19%	19%	20%	13%	8%
Blackhole	43%	50%	9%	9%	59%	61%	47%	52%	48%	49%	65%	65%	32%	43%	13%	8%
Takeoff	26%	30%	18%	18%	30%	31%	43%	47%	36%	37%	35%	35%	12%	12%	13%	15%
Pitchdown	14%	16%	18%	18%	21%	22%	19%	20%	18%	19%	19%	19%	8%	8%	7%	8%
G-excess	15%	16%	18%	18%	5%	6%	37%	38%	23%	23%	11%	11%	5%	5%	7%	8%
Autokinesis	29%	30%	9%	9%	29%	30%	21%	20%	30%	30%	30%	30%	34%	37%	13%	15%
Misleading	34%	36%	18%	18%	31%	32%	30%	31%	29%	29%	33%	33%	39%	49%	20%	23%
Loss of SA	52%	54%	36%	36%	31%	32%	59%	61%	57%	57%	46%	46%	55%	59%	40%	38%
Giant Hand	6%	6%	0%	0%	5%	6%	3%	4%	9%	9%	6%	6%	6%	7%	0%	0%
Elevator	8%	8%	0%	0%	5%	6%	5%	5%	8%	8%	6%	6%	12%	12%	0%	0%
NVD	40%	38%	0%	0%	4%	4%	47%	47%	5%	5%	35%	35%	61%	68%	7%	8%
Drift	30%	30%	9%	9%	9%	9%	11%	11%	10%	10%	13%	13%	58%	73%	13%	7%
Vertigo	11%	10%	9%	9%	5%	6%	4%	4%	11%	11%	5%	5%	18%	19%	0%	0%

NB: Results 1 standard deviation above the SD type average are highlighted orange.

17. Noteworthy results in this table include:

a. The Leans were more likely in aircraft belonging to the Air Combat and Training categories.

b. Whiteout, Pitchdown, G-Excess Illusion, Giant Hand illusion, Elevator Illusion, and Vertigo Flickering experiences were uncommon.

c. Blending of Earth and Sky SD experiences were common in all categories barring 'Other'

d. Sloping Clouds or Terrain SD experiences occurred in most aircraft categories.

e. Coriolis Illusion experiences were most common in the Air Combat and Training category

f. Blackhole Approach SD experiences were most common in the Air Mobility and Surveillance categories but affected other categories too.

g. Takeoff/Acceleration Pitch Up SD experiences were more likely in aircraft belonging to the Air Combat, Training, Surveillance and Air Mobility categories.

h. Autokinesis SD and Misleading Altitude Cues SD experiences occurred in most aircraft categories.

i. Loss of Situation Awareness SD experiences was one of the higher occurrences rates.

j. Night Vision Device (NVD) Related Illusions SD experiences were most common in the Rotary Wing category but they also occurred in the Air Combat and Air Mobility categories.

k. Undetected Drift SD experiences were uncommon across all categories but were most prevalent in Rotary Wing.

18. Table 1 also shows that, with the exception of the Rotary Wing category, aircrew reported experiencing SDs at almost the same rate as pilots. With that finding in mind, there is no further attempt in this report to separate the pilot responses.

Number of SD Types by Respondent

19. The number of SD types reported per respondent is shown in Table 2. Most respondents experienced 0-5 different SD types or situations. 36% of Air Combat respondents selected 6-10 different SD types or situations.

Table 2. Number of Different SD Events Experienced

	Category	Total N	Heritage	Surveillance	Air Combat	Training	Air Mobility	Rotary Wing	Other
	N In Category	823	11	56	145	132	124	339	16
Number of SD experienced	0	118	6	13	11	16	17	48	7
	%	14%	55%	23%	8%	12%	14%	14%	44%
	1-5	405	3	28	68	73	65	160	8
	%	49%	27%	50%	47%	55%	52%	47%	50%
	6-10	221	1	11	52	30	25	101	1
	%	27%	9%	20%	36%	23%	20%	30%	6%
	11-14	56	1	3	9	10	13	20	0
	%	7%	9%	5%	6%	8%	10%	6%	0%
	15-17	25	0	1	5	3	5	11	0
	%	3%	0%	2%	3%	2%	4%	3%	0%

Recency of Latest SD Experience

20. Respondents indicated the time elapsed since their most recent SD experience. Table 3 presents these SD recency data summarised across aircraft groups. The table includes those who did not experience any SDs (NA row).

Table 3. Most Recent SD Episode by Aircraft Category

Time Since Last Experience

Category	Total N	Heritage	Surveillance	Air Combat	Training	Air Mobility	Rotary Wing	Other
N In Category	**823**	**11**	**56**	**145**	**132**	**124**	**339**	**16**
< 1 week	16	0	2	1	3	3	7	0
%	2%	0%	4%	1%	2%	2%	2%	0%
< 1 month	62	1	1	12	13	7	28	0
%	8%	9%	2%	8%	10%	6%	8%	0%
< 6 months	161	0	4	47	30	18	61	1
%	20%	0%	7%	32%	23%	15%	18%	6%
< 1 year	111	0	11	22	15	24	38	1
%	14%	0%	20%	15%	11%	19%	11%	6%
≥ 1 year	279	2	18	46	44	46	117	6
%	34%	18%	32%	32%	33%	37%	35%	38%
NA	194	8	20	17	27	26	88	8
%	24%	73%	36%	12%	21%	21%	26%	50%

21. Figure 1 displays the data in Table 2, omitting the NA category.

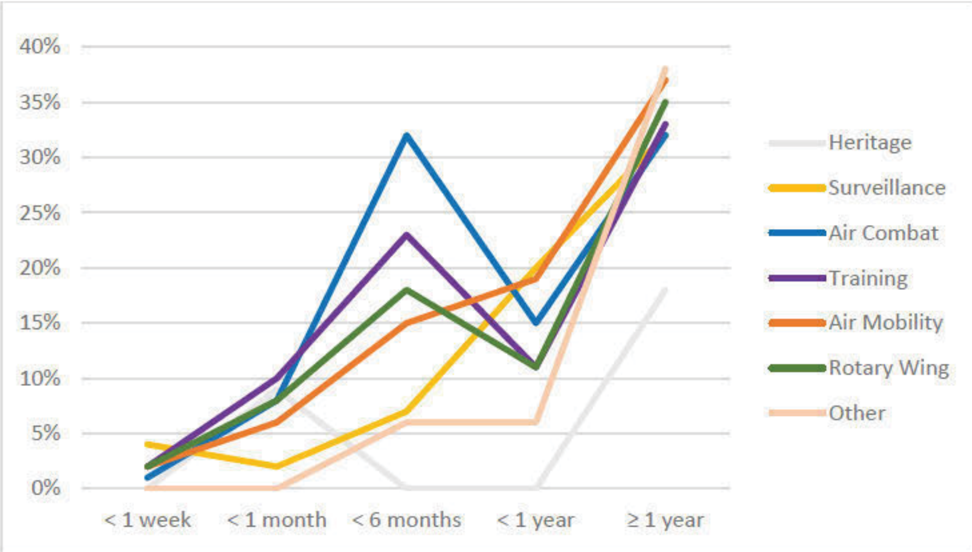

Figure 1. Recency of SD Episodes by Aircraft Category

22. Table 3 and Figure 1 show that for most of these respondents the event was some time ago; that is, longer than a month and possibly over a year ago.

Severity of Latest SD Event

23. Respondents were asked to rate the severity of their most recent SD event. The four response options were:

a. Minor - flight safety not at risk.
b. Significant - Flight safety not at risk but could have been jeopardised under different conditions.
c. Severe - Flight safety was at risk.
d. NA - no SD event reported.

Table 4. Severity of Latest SD Event by Aircraft Category

	Category	Total N	Heritage	Surveillance	Air Combat	Training	Air Mobility	Rotary Wing	Other
	N in Category	821	11	56	145	132	124	337	16
Most recent SD	Minor	607	3	32	126	105	98	237	6
	%	74%	27%	57%	87%	80%	79%	70%	38%
	Significant	18	0	2	3	3	1	9	0
	%	2%	0%	4%	2%	2%	1%	3%	0%
	Severe	0	0	0	0	0	0	0	0
	%	0%	0%	0%	0%	0%	0%	0%	0%
	NA	196	8	22	16	24	25	91	10
	%	24%	73%	39%	11%	18%	20%	27%	63%

24. The most notable feature of Table 4 is the low percentages who reported significant (2%) and severe risk (0%). The length of time since the last SD experience (see Table 2) may have diminished the sense of risk.

Severity of Worst Event

25. Respondents were asked to rate the severity of their worst SD event in the past three years. The four response options were the same as those for the recency item:

a. Minor – flight safety not at risk.
b. Significant - Flight safety not at risk but could have been jeopardised under different conditions.
c. Severe - Flight safety was at risk.
d. NA - no SD event reported.

Table 5. Severity of Worst SD Event by Aircraft Category

	Category	Total N	Heritage	Surveillance	Air Combat	Training	Air Mobility	Rotary Wing	Other
	N in Category	**825**	**11**	**56**	**147**	**132**	**124**	**339**	**16**
Worst SD experience	Minor	497	2	31	106	88	88	176	6
	%	60%	18%	55%	72%	67%	71%	52%	38%
	Significant	124	0	3	20	22	11	67	1
	%	15%	0%	5%	14%	17%	9%	20%	6%
	Severe	18	1	1	7	1	0	8	0
	%	2%	9%	2%	5%	1%	0%	2%	0%
	NA	186	8	21	14	21	25	88	9
	%	23%	73%	38%	9%	16%	20%	26%	56%

* All respondents that rated their worst SD experience as 'severe' were categorised into their appropriate category regardless if they did not state an aircraft. Respondents that did not state an aircraft were categorised by using Snapshot survey demographic data.

26. When reporting their <u>worst</u> experience, as opposed to their <u>most recent</u>, respondents made more use of the 'Significant' and 'Severe' options. 15% of respondents rated their worst SD event in the past 3 years as 'significant'. A further 2% (18 respondents) rated their worst SD event as 'severe'. There were large differences based on respondents' aircraft category with the majority of 'severe' SD experiences were among the Rotary Wing (8 respondents) and Air Combat (7 respondents) categories.

SD Training Methods

27. The data in Table 6a show the main methods of training for the different aircraft categories. The percentages refer to the number in the category. For example, 261 respondents from the Rotary Wing category (N = 337) attended lectures, which represents 80% of their number.

Table 6a. SD Training Methods by Aircraft Category.

SD Training Method	Category	Total N	Heritage	Surveillance	Air Combat	Training	Air Mobility	Rotary Wing	Other
	N in Category	**821**	**11**	**56**	**145**	**132**	**124**	**337**	**16**
	None	56	3	3	5	10	6	27	2
	%	7%	27%	5%	3%	8%	5%	8%	13%
	Lecture	648	7	42	122	104	100	261	12
	%	79%	64%	75%	79%	79%	81%	80%	75%
	Ground Demo	430	6	36	93	75	81	127	12
	%	52%	55%	64%	60%	57%	65%	39%	75%
	Flight Demo	429	7	24	67	71	46	202	12
	%	52%	64%	43%	44%	54%	37%	62%	75%
	Simulation	505	7	41	108	89	90	160	10
	%	62%	64%	73%	70%	67%	73%	49%	63%

28. Table 6a does not show how many respondents undertook multiple forms of training but it is possible to extract this information from the survey database. The breakdown in this sample was approximately 30% for one method only, 25% for two methods, 35% for three methods, and 34% for all four methods. Table 6b displays this information for the different aircraft categories.

Table 6b. SD Training Methods by Aircraft Category

SD Training Method	Category	Total N	Heritage	Surveillance	Air Combat	Training	Air Mobility	Rotary Wing	Other
	N in Category	821	11	56	145	132	124	337	16
	None	52	3	3	5	10	6	27	2
	%	7%	27%	5%	3%	8%	5%	8%	13%
	1 Method	172	1	13	25	26	27	78	2
	%	21%	9%	23%	17%	20%	22%	23%	13%
	2 Methods	163	0	5	27	18	22	91	0
	%	20%	0%	9%	19%	14%	18%	27%	0%
	3 Methods	226	2	20	39	39	37	85	4
	%	28%	18%	36%	27%	30%	30%	25%	25%
	4 Methods	208	5	15	49	40	33	58	8
	%	25%	45%	27%	34%	30%	27%	17%	50%

29. It is not easy to draw conclusions from this table other than that Rotary Wing aircrew were least likely to undertake multiple forms of training. The survey did not explore issues relating to the timing and sequencing of the different forms of training.

Effectiveness of SD Training

30. Respondents rated the effectiveness of the SD training they had completed. The results are in Table 7.

Table 7. Ratings of the Effectiveness of SD Training by Aircraft Category

Rating of Effectiveness	Category	Total N	Heritage	Surveillance	Air Combat	Training	Air Mobility	Rotary Wing	Other
	N Responses	819	11	56	144	131	125	336	16
	Very Ineffective	12	0	1	0	2	0	9	0
	%	2%	0%	2%	0%	2%	0%	3%	0%
	Ineffective	29	0	2	1	2	3	21	0
	%	4%	0%	4%	1%	2%	2%	6%	0%
	Somewhat Effective	147	0	7	11	25	31	73	0
	%	18%	0%	13%	8%	19%	25%	22%	0%
	Effective	332	2	20	56	50	57	142	5
	%	41%	18%	36%	39%	38%	46%	42%	31%
	Very Effective	255	6	24	71	44	28	73	9
	%	31%	55%	43%	49%	34%	22%	22%	56%
	NA	44	3	2	5	8	6	18	2
	%	5%	27%	4%	3%	6%	5%	6%	13%

31. Most respondents rated their overall training as effective. The trend is clearest when graphed. Figure 2 shows the results.

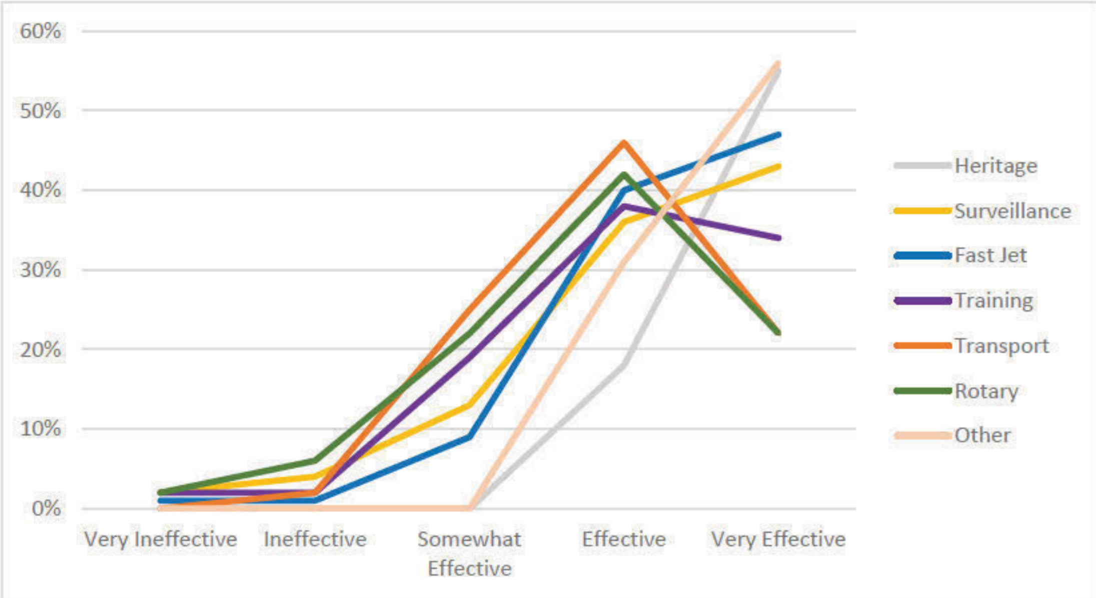

Figure 2. Ratings of Training Effectiveness by Aircraft Category

SECTION 4: RESULTS BY AIRCRAFT TYPE

32. This section explores similar breakdowns across aircraft types.

Table 8. Percentages Reporting SD by Aircraft Type

Spatial Disorientation Type	Overall	Pilot Overall	Super Hornet	F-35A	Hawk 127	EA-18G Growler	B737-BBJ	Hercules C130 (J)	C17 Globemaster	C-27J Spartan	Falcon 7X	KC-30A	P-8A Poseidon	E-7A Wedgetail	Orion (AP3C)	Kingair B350	PC21	AW139	CH-47F Chinook	E EC-135 T2+	Seahawk MH-60R	MRH-90 Taipan	ARH Tiger	Black Hawk
N Total	821	649	34	47	33	31	10	30	28	23	9	24	25	24	7	20	112	9	42	76	101	57	38	16
Leans	53%	56%	91%	79%	73%	87%	30%	50%	46%	48%	44%	46%	44%	46%	57%	65%	65%	11%	37%	51%	46%	36%	42%	31%
Whiteout	12%	12%	6%	15%	3%	13%	0%	20%	21%	13%	11%	13%	4%	17%	14%	5%	8%	11%	12%	11%	12%	21%	13%	25%
Blending	40%	43%	26%	32%	42%	45%	0%	52%	54%	48%	22%	21%	32%	38%	14%	45%	44%	33%	45%	34%	37%	66%	58%	31%
Sloping	44%	49%	47%	45%	52%	39%	40%	60%	64%	52%	22%	33%	32%	50%	29%	65%	54%	33%	50%	39%	32%	48%	45%	25%
Coriolis	24%	25%	38%	38%	42%	30%	0%	28%	18%	30%	0%	13%	4%	21%	14%	25%	38%	22%	7%	17%	20%	25%	24%	19%
Blackhole	43%	50%	44%	51%	33%	57%	50%	70%	68%	57%	56%	71%	60%	63%	43%	50%	48%	22%	15%	32%	34%	38%	45%	19%
Take off	26%	30%	38%	55%	38%	35%	10%	40%	25%	57%	56%	25%	20%	42%	29%	35%	37%	22%	0%	13%	12%	22%	8%	6%
Pitchdown	14%	16%	21%	21%	18%	16%	20%	23%	11%	25%	22%	13%	16%	29%	14%	15%	19%	11%	0%	8%	9%	14%	5%	13%
G Excess	15%	16%	44%	47%	18%	32%	0%	20%	11%	8%	0%	13%	4%	4%	14%	15%	24%	11%	2%	3%	3%	11%	8%	6%
Autokinesis	29%	30%	35%	15%	12%	23%	10%	37%	25%	42%	33%	21%	28%	25%	43%	30%	29%	22%	33%	30%	27%	49%	39%	38%
Misleading	34%	36%	35%	28%	27%	29%	0%	50%	39%	42%	11%	17%	28%	38%	14%	35%	28%	44%	24%	47%	35%	49%	37%	38%
Loss of SA	52%	54%	56%	70%	48%	58%	50%	50%	54%	50%	33%	29%	16%	42%	43%	50%	58%	22%	50%	58%	61%	56%	45%	44%
Giant Hand	6%	6%	3%	2%	0%	6%	10%	10%	7%	8%	0%	0%	8%	0%	14%	5%	10%	11%	2%	5%	3%	12%	8%	13%
Elevator	8%	8%	3%	4%	3%	10%	0%	7%	11%	8%	0%	4%	8%	0%	14%	5%	8%	11%	5%	8%	11%	21%	16%	13%
NVD	40%	38%	35%	57%	39%	52%	0%	57%	39%	67%	0%	0%	4%	4%	0%	5%	4%	44%	50%	62%	58%	68%	71%	50%
Drift	30%	30%	9%	11%	12%	13%	0%	30%	4%	21%	0%	4%	8%	13%	0%	10%	10%	56%	64%	57%	47%	72%	66%	44%
Vertigo	11%	10%	3%	4%	3%	6%	0%	7%	4%	8%	0%	4%	4%	4%	14%	10%	11%	11%	26%	8%	14%	23%	29%	19%

NB. There is no data in this table for Hot Air Balloon (N =2) because of low numbers. See the category tables.

Table 9. Percentage of Pilots Reporting SDs by Aircraft Type

Spatial Disorientation Type

Pilot Only	Overall	Pilot Overall	Super Hornet	F-35A	Hawk 127	EA-18G Growler	B737-BBJ	Hercules C130 (J)	C17 Globemaster	C-27J Spartan	Falcon 7X	KC-30A	P-8A Poseidon	E-7A Wedgetail	Orion (AP3C)	Kingair B350	PC21	AW139	CH-47F Chinook	E EC-135 T2+	Seahawk MH-60R	MRH-90 Taipan	ARH Tiger	Black Hawk
N Total	821	649	34	47	33	31	10	30	28	23	9	24	25	24	7	20	112	9	42	76	101	57	38	16
Leans	53%	56%	95%	79%	77%	94%	30%	50%	46%	48%	44%	46%	44%	50%	57%	59%	65%	0%	55%	60%	67%	31%	42%	13%
Whiteout	12%	12%	0%	15%	3%	12%	0%	20%	21%	13%	11%	13%	4%	18%	14%	6%	8%	0%	15%	15%	17%	21%	13%	25%
Blending	40%	43%	26%	32%	45%	47%	0%	52%	54%	48%	22%	21%	32%	41%	14%	53%	44%	33%	48%	43%	57%	69%	58%	38%
Sloping	44%	49%	53%	45%	55%	53%	40%	60%	64%	52%	22%	33%	32%	55%	29%	65%	54%	67%	52%	49%	48%	51%	45%	25%
Coriolis	24%	25%	42%	38%	45%	29%	0%	28%	18%	30%	0%	13%	4%	23%	14%	29%	38%	33%	5%	17%	21%	24%	24%	25%
Blackhole	43%	50%	58%	51%	35%	81%	50%	70%	68%	57%	56%	71%	60%	68%	43%	53%	48%	33%	15%	46%	50%	46%	45%	25%
Take off	26%	30%	42%	55%	39%	47%	10%	40%	25%	57%	56%	25%	20%	45%	29%	41%	37%	0%	0%	13%	10%	24%	8%	13%
Pitchdown	14%	16%	16%	21%	19%	24%	20%	23%	11%	26%	22%	13%	16%	32%	14%	18%	19%	0%	0%	6%	7%	15%	5%	25%
G Excess	15%	16%	42%	48%	16%	47%	0%	20%	11%	9%	0%	13%	4%	5%	14%	18%	24%	0%	0%	4%	2%	11%	8%	13%
Autokinesis	29%	30%	42%	15%	13%	24%	10%	38%	25%	43%	33%	21%	29%	27%	43%	35%	29%	33%	25%	34%	33%	54%	39%	13%
Misleading	34%	36%	37%	28%	29%	35%	0%	50%	39%	43%	11%	17%	29%	41%	14%	35%	28%	67%	35%	58%	45%	59%	37%	50%
Loss of SA	52%	54%	58%	70%	52%	53%	50%	50%	54%	52%	33%	29%	17%	45%	43%	53%	58%	33%	60%	66%	69%	59%	45%	43%
Giant Hand	6%	6%	5%	2%	0%	12%	10%	10%	7%	9%	0%	0%	8%	0%	14%	6%	10%	0%	0%	8%	2%	13%	8%	14%
Elevator	8%	8%	5%	4%	3%	12%	0%	7%	11%	9%	0%	4%	8%	0%	14%	6%	8%	0%	0%	6%	14%	21%	16%	14%
NVD	40%	38%	37%	57%	42%	41%	0%	57%	39%	70%	0%	0%	4%	5%	0%	6%	4%	33%	40%	79%	69%	72%	71%	38%
Drift	30%	30%	5%	11%	13%	18%	0%	30%	4%	21%	0%	4%	8%	14%	0%	12%	10%	100%	86%	74%	71%	82%	66%	13%
Vertigo	11%	10%	0%	4%	3%	12%	0%	7%	4%	8%	0%	4%	4%	5%	14%	12%	11%	0%	29%	11%	17%	21%	29%	13%

18

Table 10. Count of SD Severity and Training

		Overall	Super Hornet	F-35A	Hawk 127	EA-18G Growler	B737-BBJ	Hercules C130 (J)	C17 Globemaster	C-27J Spartan	Falcon 7X	KC-30A	Orion (AP3C)	E-7A Wedgetail	P-8A Poseidon	Kingair B350	PC21	AW139	CH-47F Chinook	EC-135 T2+	MH-60R Seahawk	MRH-90 Taipan	Tiger ARH	UH-60M Black Hawk
	N Total	823	34	47	33	31	10	30	28	23	9	24	7	24	25	20	112	9	42	76	101	57	38	16
Time Since Last Experience	< 1 week	16	0	1	0	0	0	0	2	0	0	1	0	1	1	0	3	1	1	2	3	0	0	0
	< 1 month	62	3	5	3	1	0	1	1	3	1	1	0	1	0	3	10	0	2	11	9	1	4	1
	< 6 months	161	11	23	6	7	0	6	3	6	2	1	0	1	3	2	28	1	6	23	16	0	13	2
	< 1 year	111	5	7	6	4	3	6	3	3	2	7	2	6	3	3	12	0	3	8	15	9	2	1
	≥ 1 year	279	11	8	13	14	4	12	14	7	1	8	4	5	9	6	38	3	15	16	31	36	11	5
	NA	194	4	3	5	5	3	5	5	4	3	6	1	10	9	6	21	4	15	16	27	11	8	7
Severity of Most Recent Experience	Minor – No risk	607	31	43	26	26	6	26	21	19	7	19	4	13	15	16	89	3	28	57	72	42	27	8
	Potential risk	18	0	1	2	0	0	0	1	0	0	0	1	1	0	0	3	1	0	4	0	3	1	0
	Severe risk	0	0	0	0	0	0	0	0	0	0	0	0	0	0	0	0	0	0	0	0	0	0	0
	NA	196	3	3	5	5	4	4	6	4	2	5	2	10	10	4	20	5	14	15	29	11	9	8
Severity of Worst Experience	Minor – No risk	497	27	35	20	24	5	22	19	17	6	19	4	12	15	13	75	3	20	44	52	32	17	8
	Potential risk	124	3	7	7	3	1	4	3	2	1	0	0	3	0	3	19	1	7	17	16	13	13	0
	Severe risk	14	1	2	2	0	0	0	0	0	0	0	1	0	0	0	1	0	1	0	3	0	2	0
	NA	186	3	3	4	4	4	4	6	4	2	5	7	9	10	4	17	5	13	15	30	9	8	8
SD Training Method	None	56	0	0	3	2	0	2	0	3	1	0	1	2	0	3	7	1	1	6	15	4	0	0
	Lecture	648	33	37	26	26	9	24	24	16	7	20	5	16	21	15	89	8	38	53	72	44	32	14
	Ground Demo	430	21	33	22	17	5	21	19	16	5	15	6	13	17	9	66	4	12	31	38	23	15	4
	Flight Demo	429	17	27	13	10	3	12	13	4	5	9	4	5	15	12	59	4	33	37	43	40	30	15
	Simulation	505	28	38	23	19	8	20	24	15	8	15	5	16	20	13	76	3	18	47	50	24	15	3
Effectiveness of SD Training	Very Ineffective	12	0	0	0	0	0	0	0	0	0	0	0	0	1	0	2	1	1	2	1	1	1	2
	Ineffective	29	0	0	0	1	1	0	0	0	0	2	0	1	1	0	2	1	3	4	4	6	2	1
	Somewhat Effective	147	2	5	1	3	3	7	7	5	0	9	0	7	0	6	19	2	7	25	20	12	2	5
	Effective	332	17	12	11	16	3	13	16	12	4	9	3	10	7	4	46	5	20	31	40	22	19	5
	Very Effective	255	14	30	18	9	3	8	5	4	4	4	3	5	16	7	37	0	10	11	23	12	14	3
	NA	44	0	0	3	2	0	2	0	3	1	0	1	1	0	3	5	0	1	3	11	3	0	0

19

SECTION 5: PREVENTIVE STEPS

Individual Differences

33. Some useful findings have emerged from what was a small section of the Snapshot survey. They confirm, if any confirmation was needed, that SD experiences are an unpleasant fact in aviation. The literature is also very clear on this point: Any pilot or aircrew member can experience an SD at any time. The triggers are located in the environment, not in the pilot, although there are individual differences in a pilot's reactions to these triggers.

34. To pursue the question of individual differences further, we summed scores on the 17 SDs to form an overall score representing how often each respondent had experienced SDs. This score was weakly correlated with Snapshot fatigue scores ($r = 0.17$, $P < .01$), psychological distress scores ($r = 0.12$, $P < .01$), and job stressor scores ($r = 0.15$, $p < .01$). Together, these variables explained slightly less than 5% of the variance in the total SD score. This outcome is consistent with the view that SDs are a natural phenomenon.

Training

35. The literature is also very clear on the importance of training. This issue was explored by checking whether there was any association between training and experiencing different types of SD. We found that Loss of Situation Awareness was more likely where the training was ineffective but, from a statistical point of view, it was a weak effect and needs further support.

36. The trend was more evident in the Rotary Wing group where 24% of those who rated training as ineffective reported a Loss of Situation Awareness SD compared with 12% of those who rated training effective. This result was significant at the .05 level. Other SDs where there appeared to be a minor benefit of training were Elevator Illusion, Undetected Drift, and Vertigo Flickering. However, we cannot learn much from such small numbers without replication. The high training ratings also made it difficult to detect training effects in this sample.

37. The comments above reflect the limitations of the survey rather than the importance of training, which we believe to be a very high priority. The high ratings for the effectiveness of training suggest that the current program addresses this priority but we make the following observations based on the findings from the Snapshot survey and the literature on SD.

a. The first type of training should aim at educating pilots on the causes and symptoms of SD. The list of known SDs is not long and there are coherent and consistent descriptions of the various types in the literature. Such training would promote heightened awareness of SD producing conditions and early recognition of signs that individuals may be succumbing to these conditions.

b. The second type of training involves simulator-based experiences to mimic actual SD conditions, also called Scenario-Based Training (SBT) and Upset Prevention and Recovery Training (UPRT). It could involve exposure to complex flight scenarios that simulate the conditions leading to SD, such as flying in degraded weather/visual cues, experiencing equipment failures, or managing high workloads. The focus of such training would be on maintaining, or re-establishing, spatial orientation in difficult circumstances. Such training in controlled conditions would assist individuals to recognise SD phenomena quickly and either maintain or recover spatial orientation.

c. The third type of training concerns the external aids that pilots can call upon to help them overcome the threats posed by SD situations, what is often called Augmentation Training where external aids supplement the skills acquired by the individual. The aim would be to reinforce the principles of Instrument Flight Rules (IFR) Training, fundamental to which is the practice of relying on instruments rather than their senses when SD situations are encountered and recognised.

d. At a more general level, Non-Technical Skills (NTS) training can assist pilots deal with unpredictable events, such as SD. NTS refers to those human performance skills that promote reliable and effective task performance in complex work systems. To be effective, NTS training must move beyond the classroom to focus on skills-based performance. NTS skills-based performance focuses on competencies such as maintaining situation awareness, decision-making, communication and the management of available resources and involves active practice, assessment and feedback on NTS performance.

e. There is a need for training to cover situations where pilots have not recognised SD situations, or have recognised them but succumbed. Confusion, narrowed attentional focus, and high stress levels are common in such situations – but recovery may still be possible, even in what may be dire circumstances. Stress Exposure Training can be helpful here.

f. Continuation training is important. SD Training cannot be a one off activity when, as we have seen in this survey, there may be a year or more between SD events.

Beyond Training

38. Anticipate, avoid and communicate. Given the unpredictable nature of flying conditions and the link between conditions and the likelihood of experiencing SDs, assessing SD risk factors should form part of mission planning and pre-mission briefings. Similarly, when flying conditions change, there is a need to be proactive and avoid SD with increased vigilance, enhanced crew coordination and increased instrument crosschecks. In crewed environments, the importance of communicating early when encountering conditions that may lead to SD or experiencing difficulty maintaining situation awareness cannot be overstated.

39. The Australian Transport Safety Bureau (ATSB) Transport Safety Report - An Overview of Spatial Disorientation as a Factor in Aviation Accidents and Incidents (2007) remains a useful and comprehensive resource. The report provides an explanation of the various types of SD in the aviation environment, and suggests strategies for managing the risk associated with SD events.

REFERENCES

Hunt, E. (2011). *Human Intelligence*. Cambridge University Press.

Matthews, R. S. J., Previc, F., & Bunting, A. (2002). *USAF Spatial Disorientation Survey*. Paper presented at the Spatial Disorientation in Military Vehicles: Causes, Consequences, and Cures, a symposium organised by the NATO Human Factors and Medicine Panel, La Caoruna, Spain, 15-17 April 2002. Published in RTO-MP-086.

Newman, D. G. (2007). *An overview of spatial disorientation as a factor in aviation accidents and incidents* (Vol. 2007). Canberra City: Australian Air Mobility Safety Bureau.

Possson, R. J. & Miller, M. E. (2014). Spatial disorientation mishap trends in the US Air Force 1993-2013. *Aviation, Space, and Environmental Medicine*, *85* (9), 919-924.

Appendix A

17 Spatial Disorientation (SD) Types

SD Type	Description
Leans	A false banking sensation usually in a turn.
Whiteout	Disorientation with a lack of horizon due to atmospheric whiteout or blowing sand, dust, or snow.
Blending of Earth and Sky	Trouble keeping orientation due to poor or no distinct horizon.
Sloping Clouds or Terrain	Falsely flying by orienting on a sloping cloud or terrain horizon.
Coriolis Illusion	Sensation of rolling and/or pitching after abrupt head movements.
Black Hole Approach	An approach to a dark area short of the runway. A night-time aviation landing illusion that occurs when only the runway is visible to the pilot.
Takeoff/Acceleration Pitch Up	A false sensation or pitching up on take-off or accelerating in flight.
Rapid Deceleration Pitch Down	A false nose-down pitch sensation with abrupt deceleration (speed brakes).
G-excess Illusion	False or exaggerated sensation of body tilt (eg penetration or procedure turn).
Autokinesis	The apparent motion of a single light.
Misleading Altitude Cues	Misleading altitude cues from ground texture (eg over flat water, small trees etc).
Loss of situation awareness	Disorientation due to loss of visual cues.
Giant Hand Illusion	False banking sensation of a giant hand pushing down on the airframe.
Elevator Illusion	False sensation of upward or downward motion as in an elevator.
Night Vision Device related Illusions	Disorientation due to use of night vision devices.
Undetected Drift	
Vertigo Flickering	Vertigo caused by flickering light - strobe light or sunlight through rotor disc/prop.

NOTES

OFFICIAL

NOTES

NOTES

INTENTIONALLY BLANK

DEFENCE FLIGHT
DFSB
SAFETY BUREAU